# Chapter 4
# FROM MASSIVE TO MASSLESS MODELS

*Our bodies are given life from the midst of nothingness. Existing where there is nothing is the meaning of the phrase, "Form is emptiness." That all things are provided for by nothingness is the meaning of the phrase, "Emptiness is form." One should not think that these are two separate things.*

From 'The Book of the Samurai, Hagakure'

In the last chapter we saw that integrability of 1+1 dimensional quantum field theories leads to severe restrictions on the scattering processes allowing to determine the scattering matrix exactly via the bootstrap principle. The question which then comes to mind is, how natural is the concept of integrability? In particular, can one understand the set of infinite conserved charges in terms of a higher symmetry? The answer to these questions was first put forward in the work by Zamolodchikov [15], who suggested to view integrability as relict of broken conformal symmetry and to interpret integrable models as *perturbed conformal field theories*.

Conformal field theories (CFT) are characterized by scale invariance, i.e. they describe massless relativistic particles or (in Euclidean space) statistical mechanics systems at a critical point. As was shown in the seminal paper by Belavin, Polyakov and Zamolodchikov [16] conformal symmetry becomes extremely powerful in two-dimensions*. There an infinite number of conserved currents arises due to the chiral splitting of the theory into an holomorphic and an anti-holomorphic part (see below for an explanation). Upon a perturbation by a relevant operator of the conformal theory this splitting is in general lost and the system dragged away from the critical point exhibits a finite correlation length, i.e. it becomes massive. However, in [15] an argument was provided that an infinite set of the original conserved currents, even though they get deformed, might survive the breaking of conformal invariance.

To be more precise, consider an action functional in Euclidean space of the form

$$S = S_{\rm CFT} - \lambda \int d^2x\, \Phi(x,t) \quad \text{with} \quad \Delta_\Phi = \bar{\Delta}_\Phi < 1\ . \tag{4.1}$$

Here $S_{\rm CFT}$ is the action of the unperturbed conformal field theory, $\lambda \sim m^{2-d_\Phi}$ is a coupling constant of the perturbation term proportional to the overall mass scale $m$ and $\Phi$ is assumed to be a relevant spinless field operator, i.e. in the conformal limit

*There exist earlier considerations of field theories in 1+1 dimensions which focus on the aspect of conformal invariance, e.g. [82]. However, the key feature, i.e. the role played by the Virasoro algebra, which lead to a more universal formulation and allowed to find their solution was first realized and exploited in [16].

$\lambda = 0$ it has anomalous scaling dimension $d_\Phi = 2\Delta_\Phi$ with conformal weight $\Delta_\Phi < 1$. See below for an explanation of the various quantities. Now introducing complex coordinates $z = x^0 + ix^1, \bar{z} = x^0 - ix^1$ the theory at the conformal point $\lambda = 0$ exhibits the characteristic chiral splitting, i.e. there are infinitely many currents $J, \bar{J}$ which depend either on $z$ or $\bar{z}$ only,

$$\lambda = 0 : \quad \bar{\partial} J = 0 \quad \text{and} \quad \partial \bar{J} = 0 \, .$$

In the perturbed theory this splitting is in general lost and $J, \bar{J}$ acquire an additional $\bar{z}, z$-dependence, respectively. In fact, up to first order in the coupling constant the change of the above conversation law changes to [15]

$$\lambda \neq 0 : \quad \bar{\partial} J(z, \bar{z}) = \lambda \oint_z \frac{d\zeta}{2\pi i} \, \Phi(\zeta, \bar{z}) J(z) + ...$$

Now, if there exist another current, say $\bar{J}'$, such that the r.h.s. in the above equation can be expressed as the derivative $-\partial \bar{J}'$, one obtains a conservation law for the perturbed theory, $\bar{\partial} J + \partial \bar{J}' = 0$. Under the assumption that this holds true for infinitely many cases and if the perturbed theory is purely massive one then ends up with an integrable quantum field theory whose S-matrix should be tractable by the bootstrap approach.

In this chapter we will adopt this point of view and regard the quantum field theories implicitly defined by the construction of the exact S-matrices in Chapter 3 as perturbed conformal field theories. In fact, one can reverse the picture and recover to each massive quantum field theory the corresponding conformal one by taking the high-energy limit, where the masses become negligible and the system loses its scale dependence. To perform the high-energy limit and to regain the conformal field content from the massive one is in general a highly non-trivial task, which requires renormalization group techniques and a profound insight into the structure of the field theory under consideration.

In case of factorizable S-matrices, however, there is an alternative method originating in the early work of Yang and Yang [22], the *thermodynamic Bethe ansatz* (TBA). First formulated in the context of the non-relativistic Bose gas it was extended about ten years ago to systems of particles which interact in a relativistic manner through a factorizable scattering matrix [23]. Nowadays it is established as one of the most important techniques in exploring the close relationship between conformal and integrable field theories. Provided the two-particle scattering amplitude of the massive quantum field theory is known the TBA allows to calculate the most characteristic quantities of the underlying UV conformal model, as for instance the effective central charge or conformal anomaly (see below for its definition). The latter information is often sufficient to determine the field content at the critical point and once the perturbing operator has been identified the integrable field theory can formally be described in terms of a classical Lagrangian. If on the other hand the conformal field theory is a priori known the TBA provides a consistency check for the S-matrix and allows to remove the CDD ambiguities inherent to the bootstrap construction (compare 3.1.2).

Both applications of the TBA will play a role in this chapter. To keep the discussion self-contained some basic notions of conformal field theory are introduced in the first section. Afterwards the thermodynamic Bethe Ansatz in context of integrable relativistic field theories is presented. Central issue is the derivation of a set of non-linear integral equations whose solutions describe the thermodynamics of the system and allow to compute the effective central charge. In general, the integral equations can only be solved numerically by an iterative method and we will therefore comment on existence and uniqueness of the solution as well as on the convergence properties of the numerical procedure. However, the numerics can be supplemented by various analytical approximation schemes which allow to derive explicit formulas for the most important conformal data, such as the effective central charge or the scaling dimension of the perturbing operator.

In a second step these approximation schemes are applied to affine Toda field theories. Exploiting the Lie algebraic structure revealed in the last chapter universal formulas are presented which describe the high energy behaviour to lowest order for all ATFT models at once. These approximate solutions are then checked for explicit examples, the Sinh-Gordon model and the $(G_2^{(1)}, D_4^{(3)})$-ATFT, against the numerical data. The results will prove to be an additional consistency check for the ATFT S-matrix constructed in Chapter 3.

In case of the colour valued S-matrices constructed in 3.3 emphasis will be given first to the so-called Homogeneous Sine-Gordon models [47], which form a particular subclass of the $\mathfrak{g}|\tilde{\mathfrak{g}}$-theories with $\mathfrak{g} = A_n$ and $\tilde{\mathfrak{g}}$ arbitrary but simply-laced. By means of a semi-classical analysis these kind of integrable models have been proposed as perturbations of WZNW coset models. In the TBA analysis several of the semi-classical considerations like the breaking of parity invariance and the existence of unstable bound states will be probed for consistency. Especially, the $\tilde{\mathfrak{g}} = A_2 \equiv su(3)$ model is investigated in detail numerically and analytically for several examples. In general, the S-matrix will be shown to give rise to the correct central charge providing strong evidence for the conjecture.

The TBA analysis of the Homogeneous Sine-Gordon models is then extended to all possible $\mathfrak{g}|\tilde{\mathfrak{g}}$-theories by means of the underlying Lie algebraic structure. The central charge calculation is performed and a general formula derived depending only on the rank and on the Coxeter number of the associated Lie algebras.

## 4.1 Basic notions of conformal field theory

The first considerations of conformally invariant quantum field theories took place in the sixties, however, the subject started to flourish after the recognition that local field theories which are scale invariant are also conformally invariant [17]. This motivated to use the notion of conformal invariance in the study of statistical mechanics system at criticality. The breakthrough in the understanding of these theories was the appearance of the already mentioned pioneering paper by Belavin, Polyakov and Zamolodchikov [16] in 1986. Today conformal field theory is an established branch of research, which has recently experienced new interest due to its applications in string theory. By now there are numerous review articles and text books on the subject

(see e.g. [83]), whence in the following only a survey of the most important results is given. Emphasis lies on assembling the relevant notions for the subsequent discussion.

*4.1.1 Conformal coordinate transformations and Witt algebra*

Conformal symmetry is defined as the invariance under **conformal coordinate transformations**. The latter are defined as such transformations $x^\mu \to y^\mu(x)$ which leave the metric tensor $g_{\mu\nu}$ invariant up to a positive scaling factor, i.e.

$$g'_{\mu\nu}(y) = \Omega(x) g_{\mu\nu}(x) \; . \tag{4.2}$$

In particular, the angle between two vectors is preserved. For an infinitesimal conformal coordinate transformation $x^\mu \to x^\mu + \epsilon^\mu(x)$ the above requirement can be translated into the so-called **conformal Killing equation** which for two dimensions reads

$$\partial_\mu \epsilon_\nu + \partial_\mu \epsilon_\nu = (\partial_\rho \epsilon^\rho)\, g_{\mu\nu} \tag{4.3}$$

The $\epsilon^\mu$'s can be interpreted as the components of a conformal Killing vector field, i.e. they determine the tangent vector to a conformal coordinate transformation. *Now, the crucial feature of two dimensions is that the Killing equation specializes for Euclidean space $g_{\mu\nu} = \delta_{\mu\nu}$ to the Cauchy-Riemann equations familiar from complex analysis.* This motivates to introduce complex coordinates via the relations

$$\begin{aligned} z &= x^0 + i x^1 & \bar{z} &= x^0 - i x^1 \\ \partial &= \frac{1}{2}\left(\partial_0 - i\partial_1\right) & \bar{\partial} &= \frac{1}{2}\left(\partial_0 + i\partial_1\right) \; . \end{aligned} \tag{4.4}$$

The infinitesimal transformations $\epsilon = \epsilon^0 + i\epsilon^1, \bar{\epsilon} = \epsilon^0 - i\epsilon^1$ solving (4.3) are now simply those which are holomorphic or anti-holomorphic, $\bar{\partial}\epsilon = 0$ and $\partial\bar{\epsilon} = 0$. Mathematically this implies that they admit for a Laurent expansion

$$\epsilon(z) = \sum_{n=-\infty}^{\infty} c_n z^{n+1} \qquad \text{and} \qquad \bar{\epsilon}(\bar{z}) = \sum_{n=-\infty}^{\infty} c'_n \bar{z}^{n+1}$$

showing that the infinitesimal conformal symmetry transformations are locally generated by

$$l_n = -z^{n+1}\partial \qquad \text{and} \qquad \bar{l}_n = -\bar{z}^{n+1}\bar{\partial} \; .$$

These local generators form similar like the generators of the Poincare group or the rotation group a Lie algebra. As one immediately deduces from their definition they are subject to the commutation relations

$$\begin{aligned} [l_m, l_n] &= (m-n) l_{m+n} \; , \\ [\bar{l}_m, \bar{l}_n] &= (m-n) \bar{l}_{m+n} \; , \\ [l_m, \bar{l}_n] &= 0 \; . \end{aligned} \tag{4.5}$$

In the literature the associated Lie algebra is known under the name **Witt algebra**. Note that in comparison to other space-time symmetries *local* conformal transformations give rise to an infinite set of symmetry generators what makes conformal

invariance to an extremely powerful concept. However, it should be pointed out that only a finite subalgebra $\{l_{-1}, l_0, l_1\}$ can be "lifted" to *global* conformal transformations, i.e. mappings which are defined everywhere and are invertible. Explicitly,

$$z \to \frac{a\,z+b}{c\,z+d}\,, \qquad ab-cd=1\,, \tag{4.6}$$

where $a, b, c, d$ are complex numbers. These coordinate transformations form a group via composition and are known as **projective** or **Möbius group**. Interpreting the constraint on the complex constants in (4.6) as determinant it is easy to see that the projective transformation can be parametrized by the complex $2\times 2$ matrices with unit determinant modulo the negative unit matrix, i.e. $SL(2,\mathbb{C})/\mathbb{Z}_2$. The same holds true for the anti-holomorphic part of the Witt algebra.

As is straightforward to verify the Möbius group contains for special choices of the parameters translations, rotations and dilatations. In particular, the generators which correspond to dilatations and rotations on the real surface are

$$l_0+\bar{l}_0 \qquad \text{and} \qquad i(l_0-\bar{l}_0)\,,$$

respectively. As we will see below in conformally invariant field theories the set of relevant operators will be assumed to be eigenstates to these generators.

### *4.1.2 The energy-momentum tensor and the Virasoro algebra*

Conformal invariance in terms of a field theory is equivalent to the vanishing of the variation of the classical action functional under an infinitesimal conformal transformation $x^\mu \to x^\mu + \epsilon^\mu(x)$,

$$\delta S = \frac{1}{2}\int d^2x\, T^{\mu\nu}\,(\partial_\mu\epsilon_\nu + \partial_\mu\epsilon_\nu) = \frac{1}{2}\int d^2x\, T^{\mu}_{\ \mu}\cdot\partial_\nu\epsilon^\nu\,. \tag{4.7}$$

Here $T^{\mu\nu}=T^{\nu\mu}$ is the canonical **energy-momentum tensor**, which can always be made symmetric and we have used the determining relation (4.3) for the Killing field $\epsilon^\mu$ in the second step. Thus, conformal invariance is guaranteed if the trace of the energy-momentum tensor is zero $T^{\mu}_{\ \mu}=0$, which in turn is the requirement that the theory is scale invariant. Together with translation and rotation invariance, $\partial_\mu T^{\mu\nu}=0$, this constraint on the energy-momentum tensor can be transformed into complex coordinates (4.4),

$$\bar\partial T = 0 \qquad \text{and} \qquad \partial\bar{T}=0\,, \tag{4.8}$$

where $T\equiv T_{zz}=\frac{1}{4}(T_{00}-T_{11}-2iT_{10})$, $\bar{T}\equiv T_{\bar{z}\bar{z}}=\frac{1}{4}(T_{00}-T_{11}+2iT_{10})$ are the only non-vanishing complex components. Thus, the energy-momentum tensor splits into a holomorphic and an anti-holomorphic part, a property which is assumed to hold also true when the field theory is quantized. Similar as above, Laurent expanding the components $T,\bar{T}$ gives then rise to the *quantum* generators of the conformal space-time symmetry,

$$T(z)=\sum_{n\in\mathbb{Z}}\frac{L_n}{z^{n+2}}\,, \qquad L_{-n}:=\frac{1}{2\pi i}\oint_{\mathbb{S}^1}\frac{dz}{z^{n+1}}\,T(z)\,. \tag{4.9}$$

An analogous relation is assumed for the anti-holomorphic part. However, in contrast to the classical generators of conformal transformations the coefficients in the Laurent expansion of the energy-momentum tensor are assumed to obey commutation relations different from (4.5)

$$\begin{aligned} [L_n, L_m] &= (n-m)L_{m+n} + \frac{c}{12}\, n(n^2-1)\delta_{m+n,0} \\ [\bar{L}_n, \bar{L}_m] &= (n-m)\bar{L}_{m+n} + \frac{c}{12}\, n(n^2-1)\delta_{m+n,0} \\ [L_n, \bar{L}_m] &= 0\,. \end{aligned} \tag{4.10}$$

Each set of the generators $\{L_n\}, \{\bar{L}_n\}$ constitutes a copy of the so-called **Virasoro algebra** which differs from the Witt algebra (4.5) by the appearance of the term containing the **central charge** $c$ [84]. As we will see below this additional term can be understood as a soft breaking of conformal invariance when macroscopic length scales are introduced into the system. One therefore refers to the central charge also as **conformal anomaly**. Notice that the central term is absent for the subalgebra $\{L_{-1}, L_0, L_1\} \cong sl(2,\mathbb{C})$ belonging to the global conformal mappings.

Mathematically, the transition from the Witt to the Virasoro algebra can be understood analogous to the Wigner-Bargmann theorem. Because of the phase-freedom inherent to quantum theory classical symmetry groups are reflected by projective representations on the quantum level, i.e. the quantum symmetry operations form a representation of the classical group up to a phase factor. In terms of the corresponding Lie algebra this amounts to the allowance of central extensions. In fact, the Virasoro algebra is just such a central extension of the Witt algebra.

### *4.1.3 Primary fields and highest weight representations*

After having introduced the quantum generators of conformal transformations it remains to construct a field theory invariant under their action. The crucial step is the introduction of so-called **primary fields** $\phi$, which form the fundamental building constituents of the field content and transform like covariant tensors under a change of variables

$$\phi(z,\bar{z}) \to \phi'(w,\bar{w}) = \left(\frac{\partial w}{\partial z}\right)^{-\Delta} \left(\frac{\partial \bar{w}}{\partial \bar{z}}\right)^{-\bar{\Delta}} \phi(z,\bar{z})\,. \tag{4.11}$$

The real exponents $(\Delta, \bar{\Delta})$ are called **conformal weights** of the primary field $\phi$. Their linear combinations

$$d = \Delta + \bar{\Delta} \qquad \text{and} \qquad s = \Delta - \bar{\Delta} \tag{4.12}$$

determine the transformation behaviour of $\phi$ under dilatations and rotations and are known as **anomalous scaling dimension** and **spin**, respectively. Clearly, the covariance property (4.11) is only well defined for *global* conformal transformations, but it might be restated in terms of local generators and in this manner allows for a generalization to *local* conformal transformations,

$$[L_n, \phi(z,\bar{z})] = z^{n+1}\partial\phi(z,\bar{z}) + \Delta(n+1)z^n\phi(z,\bar{z})\,, \quad n \in \mathbb{Z}\,. \tag{4.13}$$

We shall take the above identity as defining relation for primary fields. A similar relation is assumed to hold for the anti-holomorphic part. However, since both parts commute we will henceforth only concentrate on the holomorphic part and assume analogous algebraic relations to hold for the anti-holomorphic one.

### Conformal families

The primary fields are the central objects of a conformal field theory since their linear combinations and derivatives generate the whole field content of the algebra. In fact, introducing the operators

$$L_{-n}(z) = \oint \frac{d\zeta}{2\pi i} \frac{T(\zeta)}{(\zeta - z)^{n+1}} \tag{4.14}$$

one can assign to each primary field a **conformal family** $[\phi]$ obtained by successive actions of $L_n(z)$ on it

$$[\phi] := \{L_{n_1}(z)...L_{n_N}(z)\phi(z,\bar{z}) : n_1 \leq ... \leq n_N < 0\} \ . \tag{4.15}$$

The elements in $[\phi]$ are called **secondary fields** or **descendants**. Notice the close connection between the operators (4.14) and the Virasoro generators (4.10) by means of the limit $\lim_{z\to 0} L_n(z) = L_n$. In fact, by exploiting this relation one can easily show that each conformal family defines a highest weight representation of the Virasoro algebra.

### Verma modules

We introduce the Hilbert space of states by defining the **vacuum vector** of the theory through the relation

$$L_n \left|0\right\rangle = 0 \ , \quad n \geq 0 \ . \tag{4.16}$$

This in particular ensures the invariance of the vacuum sector under global conformal transformations. To each primary field $\phi$ with conformal weight $\Delta$ there exists a highest weight vector $\left|\Delta\right\rangle := \phi(0)\left|0\right\rangle$ which by use of (4.13) can be seen to satisfy

$$L_0 \left|\Delta\right\rangle = \Delta \left|\Delta\right\rangle \qquad \text{and} \qquad L_n \left|\Delta\right\rangle = 0 \ , \quad n > 0 \ . \tag{4.17}$$

The remaining Virasoro generators with indices $n < 0$ now produce a huge state space upon acting on the highest weight vector,

$$V_{c,\Delta} = \{L_{n_1} \cdots L_{n_k} \left|\Delta\right\rangle : n_i \leq 0, \ k \in \quad \} \ . \tag{4.18}$$

The space $V_{c,\Delta}$ is called a **Verma module** and is invariant under the action of the Virasoro algebra. Clearly, from the defining relation of the highest weight vector and the intimate relation between the operators (4.14) and the Virasoro generators one deduces that Verma modules and conformal families $[\phi]$ are in one-to-one correspondence. Thus, the concept of a primary field allows to classify all possible CFT's, namely via the highest weight representations of the Virasoro algebra.

### Singular vectors

According to the above definitions the total state space may now be obtained by summing over all tensor products $V_{c,\Delta} \otimes \bar{V}_{c,\bar{\Delta}}$, where the second factor represents the anti-holomorphic part and $\Delta, \bar{\Delta}$ run over all conformal weights occurring in the theory. However, in general the Verma modules will be reducible, i.e. it contains a subspace invariant under the action of the Virasoro algebra. The latter are generated from so-called **singular** or **null vectors** which are itself highest weight states. To see this more clearly, notice first that all elements in a Verma module are eigenvectors of $L_0$. In fact, exploiting the commutation relations (4.10) one deduces that

$$L_0 \, L_{n_1} \cdots L_{n_k} \, |\Delta\rangle = (\Delta + \ell) \cdot L_{n_1} \cdots L_{n_k} \, |\Delta\rangle \ , \quad \ell = -\sum_{i=1}^{k} n_i \ .$$

Here all $n_i < 0$ and the integer $\ell$ is called the **level.** (It is off course not related to the order of the Dynkin diagram automorphism defined in Chapter 2 and 3). The states of a given level are in general degenerate, in particular, they may contain a vector $|\upsilon\rangle$ satisfying $L_n \, |\upsilon\rangle = 0$, for all $n > 0$. Thus, each singular vector defines another highest weight representation $V_{c,\Delta+\ell}$, which lies inside the original one $V_{c,\Delta}$. Moreover, if one defines an inner product on $V_{c,\Delta}$ such that the Hermitian conjugate of a Virasoro generator is given by $L_n^* = L_{-n}$ one infers that singular vectors and all their descendants have vanishing norm and are orthogonal to all other elements in the Verma module. The physical state space is obtained by "dividing" out all the possible null subspaces generated from singular vectors $|\upsilon\rangle$ which can occur at different levels. The resulting quotient space $V'_{c,\Delta}$ forms then an irreducible representation and the physical subspace has the structure

$$\mathcal{H} = \bigoplus\nolimits_{\Delta,\bar{\Delta}} m_{\Delta,\bar{\Delta}} \, V'_{c,\Delta} \otimes \bar{V}'_{c,\bar{\Delta}} \tag{4.19}$$

where $m_{\Delta,\bar{\Delta}}$ is the multiplicity that the conformal weights $\Delta, \bar{\Delta}$ occur. The linear structure of a Verma module is in general very intricate and complex and can be encoded in so-called **Virasoro characters,** which appear as natural mathematical objects,

$$\chi_{c,\Delta}(q) = \mathrm{Tr} \, q^{L_0 - c/24} = \sum_{\ell=0}^{\infty} \dim(\ell) q^{\Delta+\ell-c/24} \ . \tag{4.20}$$

Here $\dim(\ell)$ is the number of linear independent vectors at level $\ell$. The characters form important mathematical tools to elucidate the structure of a conformal field theory, see [83] for further details. We comment on a possible connection between results from the TBA analysis of integrable models and Virasoro characters in a subsequent section.

### The Kac determinant

Another quantity to determine the number of linear independent vectors of a Verma module $V_{c,\Delta}$ at a given level $\ell$ is the Gram matrix $M^{(\ell)}(c, \Delta)$ formed by all the inner

products of the basis states

$$\langle\Delta|L_{m_1}\cdots L_{m_l}L_{-n_1}\cdots L_{-n_k}|\Delta\rangle \ , \quad n_i, m_i \geq 0, \ \sum_{i=1}^{k} n_i = \sum_{i=1}^{l} m_i = \ell \ .$$

Now, if the determinant $\det M^{(\ell)}(c,\Delta)$ vanishes one can conclude that there are linear dependent or null vectors at level $\ell$. Moreover, if the determinant is negative there must be states with negative norm present and the representation is not unitary. Remarkably, $\det M^{(\ell)}(c,\Delta)$ can be brought into the following universal form found by Kac and proven by Feigin and Fuchs [85],

$$\det M^{(\ell)}(c,\Delta) = a_\ell \prod_{rs\leq\ell} (\Delta - \Delta_{r,s})^{P(\ell-rs)} \tag{4.21}$$

with the product running over all positive integers $r, s$ whose product is smaller than or equal to the level. The constant $a_\ell$ does not depend on the central charge or conformal weight and $P(\ell - rs)$ denotes the number of partitions of the integer $\ell - rs$. The roots $\Delta_{r,s}$ of the determinant can be parametrized as

$$\Delta_{r,s}(m) = \frac{[(m+1)r - ms]^2 - 1}{4m(m+1)} \quad \text{with} \quad m = -\frac{1}{2} \pm \frac{1}{2}\sqrt{\frac{25-c}{1-c}} \ . \tag{4.22}$$

Note that the auxiliary quantity has two branches and is in general complex. One can now use this explicit formula to infer certain restriction on the allowed central charges and conformal weights when the representation of the Virasoro algebra ought to be unitary. Explicitly, one can show that all representations with $c \geq 1, \Delta \geq 0$ are unitary, while for $c \geq 25$ one deduces that $-1 < m < 0$ and therefore $\Delta_{r,s}(m) \leq 0$ implying that the associated representations are non-unitary. The structure becomes especially restrictive for $0 < c < 1$, where only a discrete set of possible unitary theories exist,

$$c = 1 - \frac{6}{m(m+1)} \quad \text{with} \quad m = 3, 4, \ldots , \ 1 \leq r < m, \ 1 \leq s \leq r \ . \tag{4.23}$$

The associated conformal weights are given by the parametrization (4.22). The set of the above conformal models is known as the **minimal unitary series** in the literature. They belong to the class of theories possessing only a *finite* number of primary fields associated with the allowed conformal weights $\Delta_{r,s}(m)$ and are the best studied CFT's, for further details see [83].

### *4.1.4 Ward identities and elementary correlation functions*

After having analyzed the implications of conformal invariance on the physical state space and the field content we now turn to more elementary constraints on the measurable quantities of the theory, the correlation or $n$-point functions. In general, **Ward identities** for correlation functions reflect symmetries possessed by a quantum field theory and can be thought of as an infinitesimal version of covariance under a symmetry operation. Implementation of covariance under global conformal transformations with generators $\{L_{-1}, L_0, L_1\}$ leads to the identities

$$\langle [L_n, \Phi_1(z_1,\bar{z}_1)\cdots\Phi_n(z_n,\bar{z}_n)]\rangle = 0 \ , \quad n = -1, 0, 1 \ ,$$

where the bracket indicates the vacuum expectation value of radially[†] ordered fields, i.e. $|z_1| < ... < |z_n|$. Again an analogous relation holds for the anti-holomorphic generators $\{\bar{L}_{-1}, \bar{L}_0, \bar{L}_1\}$. In case of primary fields the above Ward identities take the more explicit form

$$\begin{aligned} \sum_i \partial_{z_i} \langle \phi_1 \cdots \phi_n \rangle &= 0 \\ \sum_i \left( z_i \partial_{z_i} + \Delta_i \right) \langle \phi_1 \cdots \phi_n \rangle &= 0 \\ \sum_i \left( z_i^2 \partial_{z_i} + 2 z_i \Delta_i \right) \langle \phi_1 \cdots \phi_n \rangle &= 0 \end{aligned}$$

where we have used the defining relation (4.13). These three equations reflect invariance under translations, rotations and dilatations as well as special conformal transformations and constitute the minimal requirement on each conformal model. However, they are already sufficient to determine the explicit form of the two and three-point functions,

$$\langle \phi_1(z_1, \bar{z}_1) \phi_2(z_2, \bar{z}_2) \rangle = \frac{C_{12}}{|z_{12}|^{2d}} \tag{4.24}$$

$$\langle \phi_1(z_1, \bar{z}_1) \phi_2(z_2, \bar{z}_2) \phi_3(z_3, \bar{z}_3) \rangle = \frac{C_{123}}{|z_{12}|^{d_1+d_2-d_3} |z_{13}|^{d_1+d_3-d_2} |z_{23}|^{d_2+d_3-d_1}} \tag{4.25}$$

where $z_{ij} := z_i - z_j$ and the coefficient $C_{12}$ of the two-point function vanishes unless $d_1 = d_2$. Thus, two and three point functions are completely determined by the coefficients $C_{ij}, C_{ijk}$. (Note that the three point coefficient and the three-point coupling in context of ATFT are different quantities. In particular, the *fusion* of two primary fields in the sense of the OPE discussed below is in general not linked to the *fusing* of quantum particles encountered before in context of ATFT.) The latter carries further important information about the structure of the field content via the operator product expansion and the algebra hypothesis, which are additional ingredients to each CFT besides conformal invariance.

### *4.1.5 Operator product expansion*

From the explicit expressions (4.24) and (4.25) we infer that the correlation functions possess singularities when the arguments of two fields approach each other, $z_{ij} \to 0$. This holds true for all $n$-point functions and has its origin in the infinite quantum fluctuations when a quantum field is taken at a precise position. The singular behaviour of a correlation function can be extracted by a short-distance expansion of operator products in a sum of terms involving only single operators. Exploiting the decomposition (4.9) and the transformation properties (4.13) one deduces for example the following **operator product expansion** (OPE) for the energy-momentum tensor and a primary field,

$$T(z)\phi(w, \bar{w}) = \frac{\Delta\, \phi(w, \bar{w})}{(z-w)^2} + \frac{\partial_w \phi(w, \bar{w})}{z-w} + \text{ regular terms} \tag{4.26}$$

[†]Note that radial ordering in Euclidean space is the equivalent of time-ordering in Minkowski space.

where the regular terms vanish as $z \to w$. In fact, the above OPE is equivalent to (4.13) and can be used as alternative definition of primary fields. *Note that the OPE is always understood to be well defined only within correlation functions, i.e. in a weak sense.* Similar one might now derive the OPE for the components of the energy-momentum tensor by exploiting the commutation relations (4.10) yielding

$$T(z)T(w) = \frac{c/2}{(z-w)^4} + \frac{2T(w)}{(z-w)^2} + \frac{\partial_w T(w)}{z-w} + \text{regular terms} \,. \tag{4.27}$$

In comparison with (4.26) this shows that when the term involving the central charge would be absent $T$ could be interpreted as a primary field with conformal weight $(\Delta = 2, \bar{\Delta} = 0)$. In fact, $T$ is a so-called **quasi-primary field**, i.e. it transforms covariantly under global conformal mappings.

Now turning to the OPE of two primary fields one of the central assumptions in context of CFT is the **operator algebra hypothesis** [16] which states that the set of field forms a closed associative algebra such that

$$\phi_i(z,\bar{z})\phi_j(w,\bar{w}) = \sum_k \sum_{\varphi \in [\phi_k]} C_{ijk}^{\varphi} (z-w)^{\Delta_k + \ell - \Delta_i - \Delta_j} (\bar{z}-\bar{w})^{\bar{\Delta}_k + \bar{\ell} - \bar{\Delta}_i - \bar{\Delta}_j} \varphi(w,\bar{w}) + \ldots$$

Here the first sum runs over all primary fields $\phi_k$ and the second about the descendants $\varphi \in [\phi_k]$ with $\ell, \bar{\ell}$ being its level w.r.t. the two copies of Virasoro algebras. By use of conformal invariance the coefficients determining the expansion can be shown to be of the form $C_{ijk}^{\varphi} = C_{ijk}\beta_{ijk}^{\varphi}\bar{\beta}_{ijk}^{\varphi}$, where the $C_{ijk}$'s are identical to the ones occurring in the three-point function (4.25) and the $\beta$-functions can be calculated from the conformal weights and central charge. In principle, the above OPE allows to calculate all correlation functions provided the structure constants $C_{ijk}^{\varphi}$ and the conformal weights $\Delta_i, \bar{\Delta}_i$ are known. From the correlation functions the whole field theory can then be reconstructed. Thus, we can summarize the central objects of interest in conformal field theory as follows,

- the central charge $c$ of the representation of the Virasoro algebra
- the conformal weights $\Delta, \bar{\Delta}$ of the primary fields
- the OPE coefficients $C_{ijk}$ for primary fields
- the correlation functions.

### *4.1.6 The central charge as Casimir energy*

We conclude this short survey of CFT by presenting an interpretation of the central charge as Casimir energy which will play a central role throughout the rest of this chapter.

From the OPE of the energy-momentum tensor we already pointed out that it deviates from the one of primary fields. In fact, the term involving the central charge

leads to the following transformation behaviour under a local conformal mapping [83],

$$T(z) \to T(w) = \left(\frac{\partial w}{\partial z}\right)^{-2} T(z) + \frac{c}{12}\, s(z;w) \ ,$$
$$s(z;w) := \frac{z'z''' - \frac{3}{2}(z'')^2}{(z')^2} \ .$$

Here $s(z;w)$ is known as the Schwarzian derivative. Notice that it vanishes for global conformal transformations. Consider the mapping from the plane onto an infinite cylinder with circumference $R$ then the general formula above yields

$$z \to w = \frac{R}{2\pi} \ln z \ , \quad T_{\rm cyl}(w) = \left(\frac{2\pi}{R}\right)^2 \left(z^2 T(z) - \frac{c}{24}\right) \ .$$

Thus, setting the vacuum energy density $\langle T(z)\rangle$ on the plane to zero, we infer that due to the constant term it is nonzero on the cylinder $\langle T_{\rm cyl}(w)\rangle = -\pi^2 c/6R^2$. This can be understood in terms of a **Casimir energy** arising as response of the system to the introduction of periodic boundary conditions on the cylinder. In particular, this amounts to a shift of the Hamiltonian on the cylinder which after integration of the energy density reads

$$H_{\rm cyl} = \frac{2\pi}{R}(L_0 + \bar{L}_0 - c/12) \ . \tag{4.28}$$

Notice that the central charge can therefore be recovered from the energy spectrum. This observation will turn out to be crucial in context of the thermodynamic Bethe ansatz which we are going to study in the next section.

There are more general scenarios which elucidate further the role of the central charge as response to the introduction of macroscopic length scales. For example, it was shown by Polyakov that in the context of curved manifolds the following vacuum expectation value is in general non-zero, $\langle T^\mu_{\ \mu}\rangle = c/24\pi\,\mathcal{R}$, where $\mathcal{R}$ is the scalar curvature [86]. Since classically the trace of the energy-momentum tensor ought to vanish, one refers to the latter relation as **trace anomaly.** Additional examples also include manifolds with boundaries as discussed in [87].

## 4.2 The thermodynamic Bethe ansatz

The TBA-approach allows to extract various types of informations from a massive integrable quantum field theory once its scattering matrix is known. Most easily one obtains the central charge $c$ of the Virasoro algebra of the underlying ultraviolet conformal field theory, the conformal dimension $d_\Phi$ and the factor of proportionality of the perturbing operator $\Phi$ in (4.1), the vacuum expectation value of the energy-momentum tensor $\langle T^\mu_{\ \mu}\rangle$ and other interesting quantities. In particular, the TBA provides a test laboratory in which certain conjectured scattering matrices may be probed for consistency.

Moreover, the TBA is useful since it provides quantities which may be employed in other contexts, like the computation of correlation functions. For instance,

the constant of proportionality, the dimension of the perturbing field and $\langle T^{\mu}_{\mu} \rangle$ may be applied in a perturbative approach around the operator product expansion of a two point function within the conformal field theory [88]. On the massive side, the vacuum expectation value $\langle T^{\mu}_{\mu} \rangle$ may also be used as an initial value for the recursive system between different $n$-particle form factors [12] when calculating the correlation functions in the perturbed theory. Thus, the TBA plays not only a key role in linking conformal and integrable field theories but also serves as complementary approach to other techniques. The different aspects of the TBA are shown in form of a diagram in Figure 4.1.

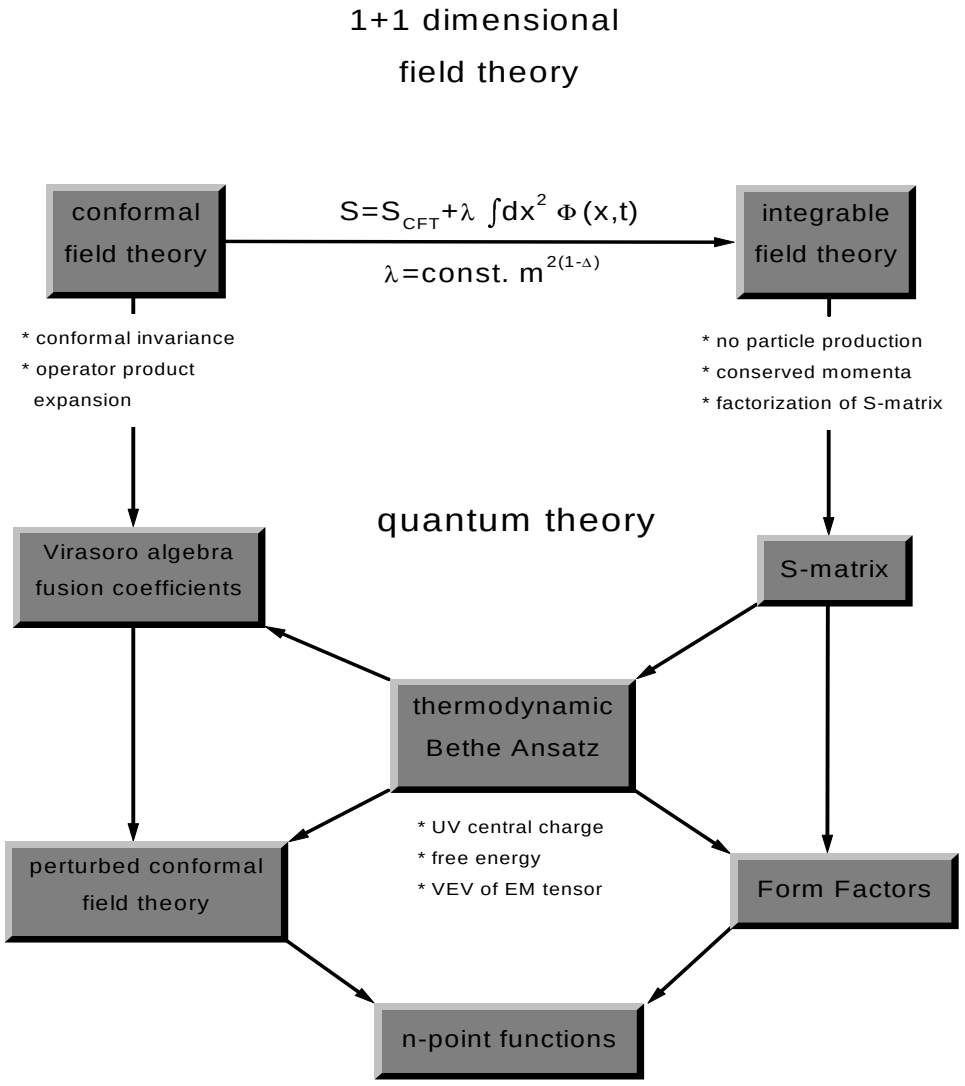


Figure 4.1: The role of the TBA in 1+1 dimensional field theory.

### *4.2.1 Quantum field theory on a torus*

As a preliminary step to the discussion of the TBA we present a simple argument for the partition function of a Euclidean quantum field theory with periodic boundary conditions.

Suppose first that we are dealing with a relativistic massive quantum field theory in Minkowski space. Imposing periodic boundary conditions amounts to a definition of the theory on a torus, see Figure 4.2. By performing a Wick rotation we might change to Euclidean metric and one of the periods, say $R$, which specified the time direction before is now identified as inverse temperature. The other period of the torus, say $L$, must then be the space direction or so-called quantization axis of the system. However, due to the Euclidean signature the choice of the quantization axis is arbitrary and both periods play a symmetric role, whence we can write the associated partition function in two different ways,

$$Z(R,L) = \mathrm{Tr}\, e^{-LH_R} \quad \text{and} \quad Z(R,L) = \mathrm{Tr}\, e^{-RH_L} \,. \tag{4.29}$$

Here $H_R$ and $H_L$ denote the Hamiltonians obtained when quantizing the system along the $R$-axis and the $L$-axis, respectively. Later on in the derivation we will perform the thermodynamic limit sending one of the periods to infinity, $L \to \infty$, which in geometric terms implies that the torus becomes an infinitely long cylinder. At the same time the two expressions for the partition function in (4.29) approach

$$Z(R,L) \approx e^{-LE_0(R)} \qquad \text{and} \qquad Z(R,L) \approx e^{-LR\,f(R)} \,, \tag{4.30}$$

where $E_0(R)$ denotes the non-degenerate ground state energy of $H_R$ and $f(R)$ is the bulk free energy per unit length at temperature $T = 1/R$. Comparing both equations gives the relation

$$E_0(R) \approx R f(R) \,. \tag{4.31}$$

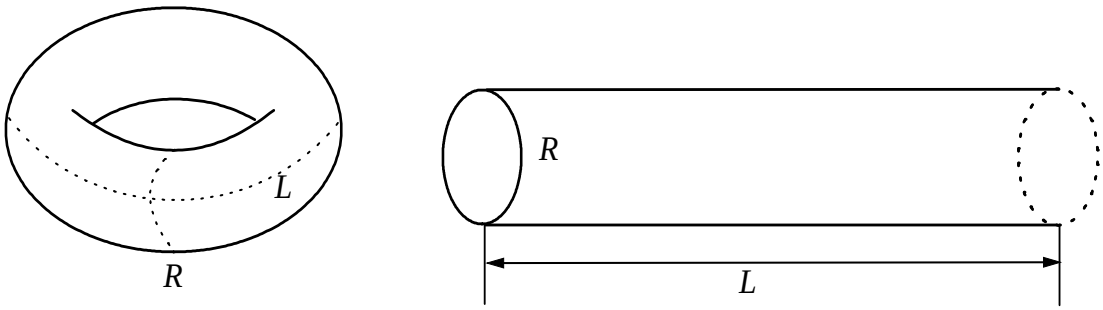


Figure 4.2: From the torus to the cylinder.

This simple observation will turn out to be crucial for the whole approach. For large temperatures $T = 1/R$ compared to the overall mass scale $m$ the system will approach the UV limit $r := mR \to 0$, where the theory becomes scale and therefore conformally invariant. Using now the expression (4.28) for the Hamiltonian of a CFT on a cylinder the above relation (4.31) specializes to

$$r \to 0: \qquad R f_{\mathrm{CFT}}(R) \approx \frac{2\pi}{R}(\Delta_0 + \bar{\Delta}_0) - \frac{\pi}{6R} c =: -\frac{\pi}{6R}\, c_{\mathrm{eff}} \,. \tag{4.32}$$

Here we have set the vacuum energy density in the plane to zero and used that in the $L \to \infty$ limit only the lowest conformal weights $(\Delta_0, \bar{\Delta}_0)$ contribute to the partition function. The quantity $c_{\text{eff}} = c - 12d_0$ with $d_0 = \Delta_0 + \bar{\Delta}_0$ being the lowest scaling dimension is called **effective central charge**. In the case of a unitary CFT it coincides with the ordinary central charge defined in (4.10) since the lowest scaling dimension is then given by the vacuum, $d_0 = 0$. The above result (4.32) for the free energy of a conformal model was derived independently by Affleck and Bloethe et al. [89].

Thus, provided we are able to calculate the free energy of the massive quantum field theory and to perform the high-energy limit we can recover the central charge of the underlying UV conformal field theory. We will now show how to achieve this in context of integrable models by means of the thermodynamic Bethe ansatz.

### *4.2.2 The thermodynamic Bethe ansatz equations*

In reference to the above geometry consider an integrable QFT on a circle of circumference $L$, which we will take to infinity in due course. For simplicity and to unburden formulas assume for the moment that there is only one particle species of mass $m$. The latter determines the correlation length of the system, $\xi = 1/m$. Integrability ensures that the number of particles and their individual momenta are conserved. Thus, the physical state space decomposes into superselection sectors with fixed particle number $N$. Restricting ourselves to one sector we can associate to each state an asymptotic wave-function which is assumed to have similar properties as known from the Bethe ansatz.

#### The Bethe ansatz equations

Intuitively the argumentation goes as follows [23, 100, 96, 90]. Choose a configuration of particle positions $\{x_1, \ldots, x_N\}$ in real space such that $|x_i - x_{i+1}| \gg \xi\,,\ i = 1, ..., N-1$. (Note that this is always possible, since the limit $L \to \infty$ will eventually be taken.) One therefore might neglect off-shell contributions and the asymptotic wave function should be the one of free particles in this region. Exchanging now two-particle positions, say $x_k$ and $x_l$, maps the original configuration to another satisfying the same requirement. The corresponding asymptotic wave-function in the new region is assumed to differ from the original one by the two-particle scattering amplitude $S(\theta_k - \theta_l)$. Hence, when translating the $k^{\text{th}}$ particle by the period $L$ the wave function collects all the scattering amplitudes with the other particles in the system. At the same time we have imposed periodic boundary conditions by defining the system on a circle, whence this contribution must cancel against the factor acquired from translation leading to the following restriction on the rapidities,

$$e^{iLm\sinh\theta_k} \prod_{l\neq k}^{N} S(\theta_k - \theta_l) = 1\ . \tag{4.33}$$

This set of constraints is known as Bethe Ansatz equations and is believed to be tightly linked to the integrable structure of the quantum field theory under consideration. Taking the logarithm (4.33) can be cast into the equivalent form

$$Lm\sinh\theta_k + \sum\nolimits_{l\neq k}^{N} \delta(\theta_k - \theta_l) = 2\pi n_k\ , \quad n_k \in \mathbb{Z}\,,$$

where $\delta = -i \ln S$ is the scattering phase. It is common in the literature to call the allowed rapidities $\theta_k$ *roots*. Notice that for free particles $S = 1$ we obtain the familiar quantization conditions for non-interacting particles in a finite interval. Thus, the general case can be interpreted as treating the system as a dilute quantum gas. The total energy and momentum of the system can be deduced from (4.33) to be given by the formulas

$$E = m \sum_{k=1}^{N} \cosh \theta_k \quad \text{and} \quad P = m \sum_{k=1}^{N} \sinh \theta_k = \frac{2\pi}{L} \sum_{k=1}^{N} n_k$$

showing that the integers $n_k$ can be interpreted as pseudo-momenta. For a typical factorizable S-matrix of an integrable model the Bethe ansatz equations form a complicated system of transcendental equations, which in general can not be solved directly. One therefore turns to the thermodynamic limit, i.e. the period $L$ and the particle number $N$ tend to infinity such that the density $N/L$ remains finite.

**The thermodynamic limit**

From (4.33) one can deduce that the spacing between the rapidities $\theta_k$ is of order $1/L$ whence it is legitimate to introduce continuous rapidity densities defined by

$$\begin{aligned} L\varrho_p(\theta)d\theta &= \text{number of particles in } [\theta, \theta + d\theta] \,, \\ L\varrho_h(\theta)d\theta &= \text{number of holes in } [\theta, \theta + d\theta] \,, \end{aligned} \tag{4.34}$$

where the terminology of a 'hole' refers to a state which is allowed by the Bethe ansatz equations but is not occupied. Notice that the rapidity densities are assumed to be macroscopic variables, while the microscopic structure is described by the solutions of (4.33). Now the Bethe ansatz equations can be re-written in terms of densities,

$$m \sinh \theta_k + \int_{-\infty}^{\infty} \delta(\theta_k - \theta) \varrho_p(\theta) d\theta = \frac{2\pi}{L} n_k \,. \tag{4.35}$$

An analogue of the above equation was first derived in case of the one-dimensional Bose gas [91]. Assuming the **Pauli exclusion principle** to hold for the solutions the l.h.s. in (4.35) defines for arbitrary rapidities $\theta$ a monotonic increasing function which upon differentiation w.r.t. $\theta$ gives the total density $\varrho = \varrho_p + \varrho_h$ of allowed states,

$$\varrho(\theta) = \frac{m}{2\pi} \cosh \theta + \varphi * \varrho_p(\theta), \qquad \varphi = -i \frac{d}{d\theta} \ln S(\theta) \,, \tag{4.36}$$

where the symbol $*$ stands for the convolution of two functions,

$$f * g(\theta) := \int \frac{d\theta'}{2\pi} f(\theta - \theta') g(\theta') \,. \tag{4.37}$$

This integral equation is still not easy to solve. Instead, one discusses the system in its thermal equilibrium, where the free energy is minimized. This requires the notion of entropy first.

Since at finite temperature there should exist holes one obtains different possibilities to arrange the particles leading to microscopic states of approximately equal energy. Using the defining relation (4.34) and exploiting again the exclusion principle the number of possibilities in an infinitesimal rapidity interval is given by

$$\exp d\mathcal{S} = \frac{(L\varrho(\theta)d\theta)!}{\big(L\varrho_p(\theta)d\theta\big)!\,(L\varrho_h(\theta)d\theta)!} \ ,$$

whence the entropy per unit length $s = \mathcal{S}/L$ after integration equals for large particle numbers

$$s[\varrho,\varrho_p] \approx \int d\theta \left(\varrho \ln \varrho - \varrho_p \ln \varrho_p - \varrho_h \ln \varrho_h\right) \ .$$

Notice that we used Stirling's formula $\ln k! \approx k \ln k,\ k \gg 1$ to derive the above identity. The free energy of our QFT at temperature $T = 1/R$ is then given by

$$f[\varrho,\varrho_p] = e[\varrho_p] - 1/R\ s[\varrho,\varrho_p] \ ,$$

where $e[\varrho_p] = \int d\theta\ m\cosh\theta\ \varrho_p(\theta)$ is the internal energy of the system per unit length. Recall that $R$ is the other period in the toroidal geometry used in Section 4.2.1. Minimizing the free energy w.r.t. the densities $\varrho, \varrho_p$ by exploiting the constraint (4.36) we obtain the properties of the system in thermal equilibrium. Explicitly, the extremum condition $\delta f = 0$ reads

$$\ln \frac{\varrho_h}{\varrho_p} + \varphi * \ln\left(1 + \frac{\varrho_p}{\varrho_h}\right) = R\, m \cosh\theta \ . \tag{4.38}$$

The above constraint is known as thermodynamic Bethe ansatz equation. The single quantity to be determined is the ratio of the densities $\varrho_p/\varrho_h$ and the only input required is the logarithmic derivative of the scattering matrix $\varphi = -i\frac{d}{d\theta}\ln S(\theta)$. Since the Pauli exclusion principle was assumed to hold in the derivation one usually rewrites the density ratio in form of a Fermi distribution

$$\frac{\varrho_p}{\varrho_p + \varrho_h} = \frac{1}{e^{\varepsilon} + 1} \tag{4.39}$$

where the function $\varepsilon = \varepsilon(\theta)$ defined by the above equation is referred to as **pseudo-energy** for obvious reasons. However, there is a certain arbitrariness in introducing the distribution (4.39) and the pseudo-energy $\varepsilon$ on which is discussed below. The equilibrium condition may now be expressed in terms of the new variable as

$$\varepsilon + \varphi * L(\theta) = R\, m \cosh\theta \ , \quad L := \ln\left(1 + e^{-\varepsilon}\right) \ . \tag{4.40}$$

This form of the TBA equations will turn out to be most convenient for numerical purposes as will become apparent in the next section. Once this integral equation is solved one is in the position to calculate the free energy per unit length

$$f(R) = -\frac{m}{2\pi R}\int d\theta\ \cosh\theta\, L(\theta)$$

from which any further thermodynamic quantity can be derived. Now in view of formula (4.32) we introduce a normalized free energy which yields in the UV regime directly the effective central charge, the so-called scaling function

$$c(r) = \frac{3\,r}{\pi^2}\int d\theta\,\cosh\theta\,L(\theta)\;. \tag{4.41}$$

Here $r = mR = R/\xi$ is the scale parameter controlling the high energy limit. Letting the latter tend to zero gives

$$\lim_{r\to 0} c(r) = c_{\text{eff}} = c - 12d_0\;. \tag{4.42}$$

Note that besides the explicit $r$ dependence of the scaling function there is an additional hidden one entering through the solutions of the TBA equations (4.38). With regard to our discussion in context of conformal field theory concerning the physical meaning of the central charge we might interpret the scaling function as off-critical measure of the Casimir energy.

It is now straightforward to extend the discussion to the general case when $n$ particle species are present in the theory. Let the mass spectrum be $\{m_1, ..., m_n\}$ and assume that the particle content is non-degenerate, i.e. the scattering matrix $S_{ij}(\theta)$ is diagonal. Then instead of a single non-linear integral equation we now obtain a system of $n$ coupled TBA equations

$$\varepsilon_i(\theta) = r\,m_i\cosh\theta - \sum_{j=1}^{n}\varphi_{ij} * L_j(\theta), \quad L_i = \ln\left(1+e^{-\varepsilon_i}\right) \tag{4.43}$$

where $i = 1, ..., n$ and the pseudo-energies $\varepsilon_i$ are defined analogous as in (4.39) with $\varrho_h, \varrho_p \to \varrho_h^{(i)}, \varrho_p^{(i)}$ being the densities belonging to the particle species $i$. Analogously one obtains for the scaling function

$$c(r) = \frac{3}{\pi^2}\sum_{i=1}^{n} m_i'\,r\int d\theta\,\cosh\theta\,L_i(\theta) \tag{4.44}$$

where the scale parameter is now defined as $r = m_1 R$ with $m_1$ being the lightest mass in the spectrum and $m_i' := m_i/m_1$. However, henceforth this re-scaling of the mass spectrum is automatically implied without changing the notation. Before we now start to discuss the solutions of the TBA equations there is a different aspect which needs to be discussed in more detail, statistics and the introduction of the pseudo-energies.

### Statistical ambiguities

When performing the thermodynamic limit and introducing the particle densities we changed from microscopic to macroscopic variables (infinite particle numbers). The thermodynamic analysis then followed the usual classical procedure assuming the exclusion principle to hold when setting $\varrho = \varrho_p + \varrho_h$. On the microscopic level this should be reflected by Fermi statistics which motivated the definition (4.39) of

the pseudo-energies. Alternatively, it might also occur that Bose statistics governs the solutions of the TBA equations in which case the density of holes just equals the density of all possible states, i.e. $\varrho = \varrho_h$. Following the analogous steps in the thermodynamic analysis it would now be natural to define the pseudo-energies by $\varrho_p/\varrho = 1/(e^{\tilde{\varepsilon}} - 1)$ leading to a TBA equation of the form

$$\tilde{\varepsilon}(\theta) + \varphi * \tilde{L}(\theta) = R\, m \cosh\theta \;, \quad \tilde{L} := -\ln(1 - e^{-\tilde{\varepsilon}}) \;. \tag{4.45}$$

Inside the TBA approach the decision for either Fermi (4.40) or Bose statistics (4.45) is usually motivated by the symmetry property of the asymptotic wave-function under an exchange of two identical particles [23]. The latter is assumed to be anti-symmetric for $S(0) = -1$ and symmetric for $S(0) = 1$ describing Fermi and Bose statistics, respectively. However, this argument is rather ad hoc and should be viewed as a working hypothesis.

An important observation in this context is that one might change from the fermionic to the bosonic description by altering the S-matrix by a phase of the following kind

$$S(\theta) \to S'(\theta) = e^{-2\pi i\, \Theta(\mathrm{Re}\,\theta)} S(\theta) \;. \tag{4.46}$$

Here $\Theta$ denotes the Heavyside step function with $\Theta(0) = 1/2$. Notice that the phase factor leaves the bootstrap properties unchanged and hence can be interpreted in terms of a CDD ambiguity [92]. In terms of the TBA-kernel this amounts to the replacement

$$\varphi(\theta) \to \varphi'(\theta) = \varphi(\theta) - 2\pi\delta(\theta) \tag{4.47}$$

in the TBA equation (4.40). Upon identifying $\tilde{\varepsilon} = \varepsilon + \ln(1 + e^{-\varepsilon})$ one then obtains (4.45). Thus, we might always fix a different choice of statistics in terms of the pseudo-energies by a re-definition of the TBA kernel. This important observation that the TBA equations stay invariant under a simultaneous change of the phase of the S-matrix and the introduction of a different statistics was made in [92]. Therein the more general case of Haldane statistics [93] was also discussed.

*When considering the S-matrices constructed in Chapter 3 below we will always assume Fermi statistics to hold for the solutions of the TBA equations* due to the fact that they satisfy $S_{ii}(0) = S_{ii}^{aa}(0) = -1$ (compare Chapter 3 for the notation) and that no other analytical and numerical solutions with different statistics are known. Although the integrable models under consideration, affine Toda field theories, are defined in terms of bosonic fields via the action functional (3.20) the introduction of Fermi statistics at the TBA level does not lead to a contradiction. For example we will recover Bose statistics from the solutions of the TBA equations in certain limits, like the weak coupling in affine Toda theory or the semiclassical limit in the homogeneous Sine-Gordon models. *Indeed, the statistics of the TBA solutions is not necessarily the same as the statistics of the fields in which the classical action functional is defined.* Recall in particular that the concept of bosons and fermions is equivalent in 1+1 dimensions, i.e. bosonic fields might be expressed in terms of fermionic ones and vice versa (see e.g. [94]).

**The central charge calculation and Roger's dilogarithm**

The most important quantity we are interested in the TBA analysis is the effective central charge of the underlying UV conformal field theory. While in general the TBA equations (4.43) cannot be solved analytically for finite temperatures due to their non-linear nature and therefore also the explicit form of the off-critical scaling function remains undetermined, the situation improves in the UV regime, $r \to 0$. Following the standard procedure developed in [23] we demonstrate how the central charge might be extracted by analytical means specializing for simplicity again to the case that only one particle species is present. The first step is to set up a set of so-called "massless" TBA equations in the rapidity range $\ln\frac{r}{2} \ll \theta \ll \ln\frac{2}{r}$ with $r \ll 1$. The nomenclature "massless" originates in the following approximative replacement of the on-shell energies when performing the shift $\theta \to \theta - \ln\frac{r}{2}$

$$r\,\cosh(\theta - \ln\tfrac{r}{2}) \approx e^{\theta}\ .$$

Here we have assumed that $\theta \gg 2\ln\frac{r}{2}$ and neglected terms of order $r^2$. Upon introducing the functions $\hat{\varepsilon}(\theta) = \varepsilon(\theta - \ln\frac{r}{2}), \hat{L}(\theta) = L(\theta - \ln\frac{r}{2})$ the TBA equations (4.43) in the above mentioned rapidity range are approximately given by

$$r \ll 1: \quad e^{\theta} \approx \hat{\varepsilon}(\theta) + \varphi * \hat{L}(\theta)\ . \tag{4.48}$$

Notice that the explicit dependence on the scale parameter $r$ has vanished. We might now proceed similarly and perform also the shift $\theta \to \theta - \ln\frac{2}{r}$ and obtain an analogous equation involving on-shell energies of the kind $e^{-\theta}$ in the appropriate range for the rapidity variable. However, at this point we make the simplifying assumption that our theory is invariant under a parity transformation, $\theta \to -\theta$, i.e. the solutions of the original TBA equations are assumed to be symmetric. Then it is sufficient to consider only the equation (4.48) and the expression for the scaling function simplifies to

$$r \ll 1: \quad c(r) = \frac{6}{\pi^2}\int_0^{\infty} d\theta\ L(\theta)\,\cosh\theta \approx \frac{6}{\pi^2}\int_{\ln\frac{r}{2}}^{\infty} d\theta\ \hat{L}(\theta)\,e^{\theta}\ , \tag{4.49}$$

where we have again discarded terms of order $r^2$ as in the derivation of the approximate TBA equation (4.48) in the UV regime. Now, the crucial trick is to differentiate the latter and to replace the exponential term in (4.49) by the r.h.s. which yields

$$\begin{aligned} c(r) &\approx \frac{6}{\pi^2}\int_{\hat{\varepsilon}(\ln\frac{r}{2})}^{\hat{\varepsilon}(\infty)} d\varepsilon\ \ln(1+e^{-\varepsilon}) + \frac{6}{\pi^2}\int_{\ln\frac{r}{2}}^{\infty} d\theta\ \hat{L}(\theta)\,\varphi * \frac{d\hat{L}(\theta)}{d\theta} \\ &\approx \frac{6}{\pi^2}\int_{\hat{\varepsilon}(\ln\frac{r}{2})}^{\hat{\varepsilon}(\infty)} d\varepsilon\ \ln(1+e^{-\varepsilon}) + \frac{6}{\pi^2}\int_{\ln\frac{r}{2}}^{\infty} d\theta\ \frac{d\hat{L}(\theta)}{d\theta}\,\varphi * \hat{L}(\theta)\ . \end{aligned}$$

The interchange of the two integrations in the second step ought to be exact in the extreme UV limit $r \to 0$. Exploiting again the equation (4.48) in replacing the

convolution term of the second integral and a subsequent partial integration gives the final result

$$\begin{aligned}\lim_{r\to 0} c(r) &= \frac{3}{\pi^2}\int_{\varepsilon(0)}^{\varepsilon(\infty)} d\varepsilon\ \left[\ln(1+e^{-\varepsilon})+\frac{\varepsilon}{1+e^{\varepsilon}}\right] \\ &= \frac{6}{\pi^2}\mathcal{L}\left(\frac{1}{1+e^{\varepsilon(0)}}\right)-\frac{6}{\pi^2}\mathcal{L}\left(\frac{1}{1+e^{\varepsilon(\infty)}}\right)\ .\end{aligned} \tag{4.50}$$

Here we have used the integral representation of Roger's dilogarithm function [113]

$$\mathcal{L}(x) := \sum_{k=1}^{\infty}\frac{x^k}{k^2}+\frac{1}{2}\ln x\ln(1-x) = -\frac{1}{2}\int_0^x dy\ \left[\frac{\ln(1-y)}{y}+\frac{\ln y}{1-y}\right] \tag{4.51}$$

and employed the substitution $y = (1+e^{\varepsilon})^{-1}$. From the above formula we infer that only the values of the TBA solutions $L(\theta)$ at the origin and at infinity are required to compute the central charge. The latter can be deduced to $\lim_{\theta\to\infty} L(\theta) = 0$ on physical grounds. At large rapidities the on-shell energies in (4.43) become dominant and the system becomes approximately free, i.e. $\varepsilon(\theta) \approx r\cosh\theta$ for small but finite scale parameter. Thus, the second term in (4.50) does not contribute. It is straightforward to generalize this result to the general case with $n$ particle species present, giving the compact formula

$$c_{\text{eff}} = \frac{6}{\pi^2}\sum_{i=1}^{n}\mathcal{L}\left(\frac{1}{1+e^{\varepsilon_i(0)}}\right) = \frac{6}{\pi^2}\sum_{i=1}^{n}\mathcal{L}\left(1-e^{-L_i(0)}\right)\ . \tag{4.52}$$

This formula is central in the TBA analysis and will be frequently used in the following whence its derivation has been presented here in some detail. To close the analytical calculation it remains to determine the value of the TBA solutions at the origin as $r\to 0$. For the case when a dynamical interaction between the particles is absent this is easily achieved. As example consider systems with Fermi and Bose statistics. In the first case we infer directly from (4.40) that the solution to the TBA equation reads $L(\theta) = \ln(1+e^{-r\cosh\theta})$, whence we infer from the general formula (4.52) that $c_{\text{eff}} = \frac{6}{\pi^2}\mathcal{L}(\frac{1}{2}) = 1/2$. In accordance with the well known central charge of the free fermion theory. For Bose statistics we must keep in mind that the derivation of (4.52) was performed in context of Fermi statistics. However, exploiting the statistical ambiguity explained in the previous subsection we saw that (4.45) is equivalent to (4.40) under the transformation (4.47), whence we easily derive $L(\theta) = -\ln(1-e^{-r\cosh\theta})$ and the effective central charge takes the expected value $c_{\text{eff}} = \frac{6}{\pi^2}\mathcal{L}(1) = 1$.

The general case with a dynamical interaction present is more involved and there exists various schemes which allow to determine the solution at the origin. However, these depend crucially on the form of the TBA solution, whence one refers usually to the outcome of numerical calculations before one turns to analytical considerations. The numerical procedure applied to solve (4.43) is described in the next section together with the question whether the TBA equations admit more than one solution.

*4.2.3 Existence, uniqueness and the numerical procedure*

In this section we are going to investigate the existence and uniqueness properties of the solutions of the TBA equations [43]. The main physical motivation for this considerations is to clarify whether it is possible to obtain different effective central charges for a fixed dynamical interaction due to the existence of several different solutions. As a side product we obtain useful estimates on the error and the rate of convergence when solving the TBA equations numerically. Precise estimates of this kind were not obtained previously in this context and convergence is simply presumed. The procedure we are going to employ is the **contraction principle** (or **Banach fixed point theorem**), see e.g. [95]. For the case of the non-relativistic one-dimensional Bose gas the uniqueness question was already addressed by Yang and Yang [22], albeit with a different method.

In order to keep the notation simple we commence our discussion for a system with one particle only which is of fermionic type. Thereafter, we discuss the straightforward generalization. The standard numerical procedure to solve integral equations of the type (4.40) consists in evaluating the original function at discrete points and a subsequent iteration. Introducing the scale parameter $r = mR$, this means we consider (4.40) as recursive equation

$$\varepsilon_{n+1}(\theta) := r\cosh\theta - \varphi * \ln(1+e^{-\varepsilon_n})(\theta) \tag{4.53}$$

and perform the iteration starting with $\varepsilon_0(\theta) = r\cosh\theta$. The exact solution is then thought to be the limit $\varepsilon = \lim_{n\to\infty}\varepsilon_n$. However, a priori it is not clear whether this limit exists at all and how it depends on the initial value $\varepsilon_0$. In particular, different initial values might lead to different solutions.

The natural mathematical setup for this type of problem is to rewrite the TBA-equation (4.40) as

$$(A\xi)(\theta) := \varphi * \ln(1+e^{\xi(\theta)-r\cosh\theta}) = \xi(\theta), \tag{4.54}$$

and treat it as a fixed point problem for the operator $A$ with $\xi(\theta) = r\cosh\theta - \varepsilon(\theta)$.

In order to give meaning to the limit $\lim_{n\to\infty}\varepsilon_n$ we have to specify a norm. Of course, it is natural to assume that $\xi$ as function of $\theta$ is measurable, continuous and essentially bounded on the whole real line. The latter assumption is supported by all known numerical results. In fact, assuming on physical grounds that $\varphi \sim e^{-|\theta|}$ for large rapidities, since the particles become then approximately non-interacting, it follows from (4.54), that possible solutions $\xi$ vanish at infinity. This means possible solutions of (4.54) constitute a Banach space with respect to the norm

$$\|f\|_\infty = \operatorname{ess\,sup}|f(\theta)|\,, \tag{4.55}$$

i.e. $L_\infty(\mathbb{R})$. In principle we are now in a position to apply the Banach fixed point theorem[‡], which states the following:

[‡]One may of course apply different types of fixed point theorems exploiting different properties of the operator $A$. For instance if $A$ is shown to be compact one can employ the Leray-Schauder fixed point theorem. In the second refence of [96] it is claimed that the problem at hand was treated in this manner, albeit a proof was not provided.

*Let $D \subset L_\infty$ be a non-empty set in a Banach space and let $A$ be an operator which maps $D$ $q$-contractively into itself, i.e. for all $f, g \in D$ and some fixed $q$, $0 \leq q < 1$*

$$\|A(f) - A(g)\|_\infty \leq q\|f - g\|_\infty. \tag{4.56}$$

*Then the following statements hold:*

i) *There exists a unique fixed point $\xi$ in $D$, i.e. equation (4.54) has exactly one solution.*

ii) *The sequence constructed in (4.53) by iteration converges to the solution of (4.54).*

iii) *The error of the iterative procedure may be estimated by*

$$\|\xi - \xi_n\|_\infty \leq \frac{q^n}{1-q}\|\xi_1 - \xi_0\|_\infty \quad \text{and} \quad \left\|\xi - \xi_{n+1}\right\|_\infty \leq \frac{q}{1-q}\left\|\xi_{n+1} - \xi_n\right\|_\infty .$$

iv) *The rate of convergence is determined by*

$$\left\|\xi - \xi_{n+1}\right\|_\infty \leq q\left\|\xi - \xi_n\right\|_\infty .$$

In order to be able to apply the theorem we first have to choose a suitable set in the Banach space. We choose some $q \in [0, 1)$ such that $e^{-r} \leq q$ and take $D$ to be the convex[§] set $D_{q,r} := \left\{f : \ \|f\|_\infty \leq \ln \frac{q}{1-q} + r\right\}$. We may now apply the following estimate for the convolution operator $\varphi*$ (which is a special case of Young's inequality)

$$\|\varphi * f\|_\infty \leq \|\varphi\|_1 \|f\|_\infty. \tag{4.57}$$

In the following we assume that $\|\varphi\|_1 \leq 1$. In fact, for the concrete one-particle theory we will consider below, the Sinh-Gordon model, we have $\|\varphi\|_1 := \int \frac{d\theta}{2\pi}|\varphi(\theta)| = 1$. Interpreting the function $L(\theta) = \ln(1 + e^{f(\theta) - r\cosh\theta})$ in (4.54) as operator acting on $f \in D$ we have the estimate

$$L(f) \leq \ln\left[1 + \exp\left(\|f\|_\infty - r\right)\right] \leq \ln\frac{1}{1-q} \leq \ln\frac{q}{1-q} + r \ .$$

The last inequality follows from our special choice of $q$. Thus, $A$ maps $D_{q,r}$ into itself.

In the final step we show that the contraction property (4.56) is fulfilled on $D_{q,r}$ . It suffices to prove this for the map $L$, because of (4.57) and the fact that

[§]For $f, g \in D_{q,r}$ also $tf + (1-t)g \in D_{q,r}$, with $0 \leq t \leq 1$.

$\|\varphi\|_1 \leq 1$. We have

$$\begin{aligned}
\|L(f) - L(g)\|_\infty &= \left\| \int_0^1 dt \, \frac{d}{dt} L(g + t(f-g)) \right\|_\infty \\
&= \left\| \int_0^1 dt \, \frac{(f-g)}{1 + \exp(-g - t(f-g) + r\cosh\theta)} \right\|_\infty \\
&\leq \max_{0\leq t\leq 1} \left| \frac{1}{1 + \exp(-g - t(f-g) + r)} \right| \|f-g\|_\infty \\
&\leq \max_{0\leq t\leq 1} \left| \frac{1}{1 + \exp\left(-\|g - t(f-g)\|_\infty + r\right)} \right| \|f-g\|_\infty \\
&\leq q \, \|f-g\|_\infty \ .
\end{aligned}$$

In the last inequality we used the fact that $D_{q,r}$ is a convex set.

We may now safely apply the fixed point theorem. First of all we conclude from i) and ii) that a solution of (4.54) not only exists, but it is also unique. In addition we can use iii) and iv) as a criterium for error estimates. From our special choice of the closed set $D_{q,r}$ one sees that the rate of convergence depends crucially on the parameter $r$, the smaller $r$ the greater $q$ is, whence the sequence $(\xi_n)$ converges slower.

One could be mathematically more pedantic at this point and think about different requirements on the function $\xi$. For instance one might allow functions which are not bounded (there is no known example except when $r = 0$ exactly) and then pursue similar arguments as before on $L_p$ rather than $L_\infty$.

The generalization of the presented arguments to a situation involving $n$ different types of particles may be carried out by the same arguments even though it turns out to be more involved due to the coupling of the equations belonging to different particle species.

### *4.2.4 Approximate analytical solutions*

Having established how the TBA equations can be solved numerically by means of the contraction principle we now turn to analytical considerations, see [43, 44]. The motivation is twofold. On the one hand the numerical problem becomes quite complex when one increases the number of particle species, on the other hand and more importantly one would like to gain a deeper structural insight into the solutions of (4.43). Due to the nonlinear nature of the TBA equations only few analytical solutions are known. Nonetheless, one may obtain approximate analytical solutions when $r$ tends to zero, i.e. in the UV limit. These approximations depend on the form of the solutions which vary dependent on the model.

In this section we shall assume that the particle densities become large in the high energy regime, i.e. the solutions $L_i(\theta)$ of (4.43) should be much larger than one inside a rapidity range specified below. This kind of behaviour will be found for all of the affine Toda field theories.

Nevertheless, most of the approximation scheme can be discussed in complete generality and only in the last step when comparing against numerical data one needs to specify a particular model. Therefore, we present the derivation of the approximate

formulas separately and justify the assumptions made about the particular form of the solutions in retrospective when discussing the concrete examples of affine Toda field theory.

We shall now generalize the method of [58] which can be separated into three distinct steps:

1. Instead of regarding the TBA-equation as an integral equation, one transforms it into an infinite order differential equation by means of the convolution theorem.

2. In the high-energy regime this infinite order differential equation can for large densities be approximated by a second order differential equation giving the leading contribution in the UV limit.

3. After solving the finite order differential equations the solution is used to compute an approximate scaling function.

In this approach certain constants of integration are left undetermined, whence in a second part we discuss further enhanced approximate solutions to the TBA equation and provide a simple matching condition which allows to fix the constants for a concrete model at hand.

**The TBA equation as infinite order differential equation**

The first step can be performed with the sole assumption that the Fourier transform of the TBA kernel $\varphi_{ij}(\theta) = -i\frac{d}{d\theta}\ln S_{ij}(\theta)$ can be expanded as a power series

$$\tilde{\varphi}_{ij}(t) - 2\pi\delta_{ij} := \int_{-\infty}^{\infty} d\theta\ \varphi_{ij}(\theta)e^{it\theta} - 2\pi\delta_{ij} = 2\pi\sum_{k=0}^{\infty}(-i)^k\eta_{ij}^{(k)}t^k \quad , \tag{4.58}$$

where for convenience we have subtracted a constant term which only effects the definition of the zeroth order coefficient $\eta_{ij}^{(0)}$. In view of the discussion in 4.2.2 this amounts to a reformulation of (4.43) in terms of Bose statistics, compare (4.47). The coefficient $\eta_{ij}^{(0)}$ will then turn out to vanish in context of ATFT and Fermi statistics. Now, it is a simple consequence of the convolution theorem[¶] that the integral equations (4.43) may also be written as a set of infinite order differential equations [58, 101, 43]

$$rm_i\cosh\theta + \ln\left(1 - e^{-L_i(\theta)}\right) = \sum_{j=1}^{n}\sum_{k=0}^{\infty}\eta_{ij}^{(k)}L_j^{(k)}(\theta) \quad . \tag{4.59}$$

Here we have expressed the pseudo-energies in terms of the $L$-function and introduced the abbreviation $L_i^{(k)}(\theta) = (d/d\theta)^k L_i(\theta)$. The whole dependence of the scattering matrix is now incorporated in the coefficients $\eta_{ij}^{(k)}$. This alternative formulation of the TBA-equations is most convenient for the analytical considerations to follow.

[¶] $(f * g)(\theta) = 1/(2\pi)^2 \int dk \widetilde{f}(k)\widetilde{g}(k)e^{-ik\theta}$

**The ultraviolet regime**

In the second step we shall now pass on to the ultraviolet limit, i.e. the scale parameter $r$ is going to zero. Similar to the general discussion of the central charge calculation in 4.2.2 we introduce the quantity $\hat{L}_i(\theta) := L_i(\theta - \ln\frac{r}{2})$ and perform the shift $\theta \to \theta - \ln\frac{r}{2}$. The TBA-equations (4.59) then acquire the form

$$m_i e^{\theta} + \ln\left(1 - e^{-\hat{L}_i(\theta)}\right) = \sum_{j=1}^{n}\sum_{k=0}^{\infty} \eta_{ij}^{(k)} \hat{L}_j^{(k)}(\theta) \ , \tag{4.60}$$

where we have neglected the terms proportional to $e^{2\ln(r/2)-\theta}$, under the assumption that $2\ln\frac{r}{2} \ll \theta$. Obviously the dependence on the scale parameter $r$ has vanished, such that the $\hat{L}_i(\theta)$ are $r$-independent. Analogous manipulations can be applied to the equation for the scaling function (4.44). Assuming parity invariance of the scattering matrix one easily verifies that the solutions of (4.43) must be symmetric in the rapidity variable. Thus, rewriting the integral such that the integration variable runs only over positive values one obtains after a similar shift as in the derivation of (4.60) the approximate expression (compare also 4.2.2),

$$r \to 0: \quad c(r) \approx \frac{6}{\pi^2} \sum_{i=1}^{n} m_i \int_{\ln\frac{r}{2}}^{\infty} d\theta \, \hat{L}_i(\theta) e^{\theta} \ . \tag{4.61}$$

Again terms proportional to $r^2$ have been neglected in the above expression.

**Assumptions on the solutions and leading order behaviour**

At this point we make now several assumptions on the coefficients in the series expansion (4.58) and the behaviour of the solutions $\hat{L}_i$ which will be justified in the next section for the concrete models at hand:

i) The functions $\hat{L}_i(\theta)$ obey the equations (4.60).

ii) In the power series expansion (4.58) the coefficients are symmetric in the particle type indices, i.e. $\eta_{ij}^{(k)} = \eta_{ji}^{(k)}$.

iii) All odd coefficients vanish in (4.58), i.e. $\eta_{ij}^{(2k+1)} = 0$.

iv) The asymptotic behaviour of the function $\hat{L}_i(\theta)$ and its derivatives read

$$\lim_{\theta\to\infty} \hat{L}_i^{(k)}(\theta) = 0 \qquad \text{for } k \geq 1\,, 1 \leq i \leq n \quad , \tag{4.62}$$

$$\lim_{\theta\to\infty} e^{\theta}\hat{L}_i(\theta) = 0 \qquad \text{for } 1 \leq i \leq n \quad . \tag{4.63}$$

Assumption ii) is guaranteed when the two-particle scattering matrix is parity invariant. The requirement iii) will turn out to be satisfied for Fermi statistics by all scattering matrices of interest to us. The asymptotic behaviour iv) will be verified

in retrospect, that is all known numerical solutions exhibit this kind of asymptotics. Noting that the conditions (4.62),(4.63) imply $\lim_{r,\theta\to 0} L_i^{(k)}(\theta) = 0$ such that (4.59) becomes a set of coupled equations for $n$ constants $L_i(0)$,

$$\ln(1 - e^{-L_i(0)}) = \sum_{j=1}^{n} \eta_{ij}^{(0)} L_j(0) \ .$$

Solving this equation allows to determine the effective central charge via the general formula (4.52). Later on we will see that in context of affine Toda theories $\eta_{ij}^{(0)} = 0$ for Fermi statistics whence the above equation implies via (4.52) that $c_{\text{eff}} = n$. However, our aim will be to go beyond the renormalization fixed point and calculate the leading order perturbation term in the off-critical scaling function.

In order to deduce the leading order behaviour in the ultraviolet limit we now proceed as follows: Under the assumption that the property $\hat{L}_i(\theta) = \hat{L}_i(2\ln\frac{r}{2} - \theta)$ originating in the symmetry of the non-shifted solutions $L_i(\theta)$ still holds at this point of the derivation, we may neglect in (4.60) also the term $e^{\theta}$. *Assuming that* $\hat{L}_i(\theta)$ *is large* and (4.62) holds, the TBA-equation in the ultraviolet limit may be approximated by

$$\sum_{j=1}^{n} (\eta_{ij}^{(2)} \hat{L}_j^{(2)}(\theta) + \eta_{ij}^{(0)} \hat{L}_j(\theta)) + e^{-\hat{L}_i(\theta)} = 0 \quad . \tag{4.64}$$

Unfortunately, this equation may not be solved analytically in its full generality. However, in all cases we shall be considering in the following $\eta_i^{(0)} = \sum_{j=1}^{n} \eta_{ij}^{(0)} = 0$ with fermionic type of statistics. For this case the solution of (4.64) reads

$$\hat{L}_i(\theta) = \ln\left(\frac{\sin^2\left(\kappa_i\left(\theta - \delta_i\right)\right)}{2\kappa_i^2 \eta_i^{(2)}}\right) + \ln\left(\frac{\cos^2\left(\tilde{\kappa}_i\left(\theta - \tilde{\delta}_i\right)\right)}{2\tilde{\kappa}_i^2 \eta_i^{(2)}}\right) \quad , \tag{4.65}$$

with $\kappa_i, \delta_i, \tilde{\kappa}_i, \tilde{\delta}_i$ being constants of integration and $\eta_i^{(2)} = \sum_{j=1}^{n} \eta_{ij}^{(2)}$. We will discard the second term in the following w.l.g. Invoking the property $\hat{L}_i(\theta) = \hat{L}_i(2\ln\frac{r}{2} - \theta)$ of the original function we obtain the following relation between the constants,

$$\kappa_i = \frac{\pi}{2(\delta_i - \ln\frac{r}{2})} \ . \tag{4.66}$$

Thus, we recovered the scale dependence of the solutions and only one constant of integration remains undetermined. Not surprisingly it will be characteristic for the specific model under consideration and we therefore postpone the discussion of further restrictions on $\kappa_i, \delta_i$. Now, removing the shift in the definition of the $\hat{L}_i$-functions we have as approximate solutions to the TBA equations,

$$L_i^0(\theta) = \ln\left(\frac{\cos^2\left(\kappa_i\theta\right)}{2\kappa_i^2\eta_i}\right) \qquad \text{for } |\theta| \leq \frac{\arccos(\kappa_i\sqrt{2\eta_i})}{\kappa_i}. \tag{4.67}$$

Here the upper index shall indicate that we are dealing with an approximate solution $L_i^0$ different form the exact one $L_i$. The restriction on the range of the rapidity stems

from the physical requirement $L_i \geq 0$. In order to demonstrate consistency of the approximate solution with regard to the assumption that the derivatives of $L_i(\theta)$ with respect to $\theta$ are negligible as $r \to 0$, i.e. equation (4.62), we report the following derivatives

$$\begin{aligned}
(L_i^0)^{(1)}(\theta) &= -2\kappa_i \tan(\kappa_i\theta) && (4.68)\\
(L_i^0)^{(2)}(\theta) &= -2\kappa_i^2/\cos^2(\kappa_i\theta) && (4.69)\\
(L_i^0)^{(3)}(\theta) &= -4\kappa_i^3 \tan(\kappa_i\theta)/\cos^2(\kappa_i\theta) && (4.70)\\
(L_i^0)^{(k)}(\theta) &\sim \kappa_i^k \quad . && (4.71)
\end{aligned}$$

Using the fact that $\kappa_i$ tends to zero for small $r$, the equations (4.68)-(4.71) are compatible with the assumption. Closer inspection shows that for given $r$ the series build from the $L_i^0(\theta)$ starts to diverge at a certain value of $k$. Since (4.67) is not exact this does not pose any problem, but one should be aware of it.

### The scaling function to leading order

We now turn to the main quantity of interest in the TBA approach, the scaling function. In order to apply the above approximation to its computation one considers the so-called "truncated scaling function"[58],

$$\hat{c}(r,r') = \frac{6}{\pi^2}\sum_{i=1}^{n} m_i \int_{r'}^{\infty} d\theta\, \hat{L}_i(\theta) e^{\theta} \quad , \tag{4.72}$$

which obviously coincides with (4.61) for $r' = \ln\frac{r}{2}$. Recall that $\hat{L}_i$ are the solutions of (4.60). The reason of introducing the dummy variable $r'$ is that we might derive now a differential equation for the truncated version of the scaling function,

$$\frac{\partial \hat{c}(r,r')}{\partial r'} = -\frac{6}{\pi^2} e^{r'} \sum_{i=1}^{n} m_i \hat{L}_i(r') \quad . \tag{4.73}$$

Using this differential equation together with the boundary condition $\hat{c}(r,\infty) = 0$ one may now verify by direct substitution that under the assumptions i) – iv) on the solutions $\hat{L}_i$ the truncated scaling function may also be written as

$$\begin{aligned}
\hat{c}(r,r') &= \frac{3}{\pi^2}\sum_{i,j=1}^{n}\left(\sum_{k=1}^{\infty}\eta_{ij}^{(2k)}\sum_{l=1}^{2k-1}(-1)^{l+1}\hat{L}_i^{(l)}(r')\hat{L}_j^{(2k-l)}(r') + \eta_{ij}^{(0)}\hat{L}_i(r')\hat{L}_j(r')\right)\\
&\quad -\frac{6}{\pi^2}\sum_{i=1}^{n}\left(\mathcal{L}(1-e^{-\hat{L}_i(r')}) + \frac{\hat{L}_i(r')}{2}\ln(1-e^{-\hat{L}_i(r')}) + m_i e^{r'}\hat{L}_i(r')\right) \qquad (4.74)
\end{aligned}$$

Here $\mathcal{L}(x)$ denotes Rogers dilogarithm (4.51)[‖]. Proceeding now with the same assumptions which lead to the derivation of (4.64) and (4.67) the leading order expres-

[‖]The identity $\int_0^x dy \ln(1-e^{-y}) = \mathcal{L}(1-e^{-x}) + x/2\ln(1-e^{-x})$ is useful in this context.

sion for the truncated scaling function (4.74) becomes

$$\hat{c}(r,r') = n + \frac{3}{\pi^2}\sum_{i=1}^{n}\left(\eta_i^{(2)}\left(d\hat{L}_i^0/d\theta(r')\right)^2 - 2e^{-\hat{L}_i^0(r')}\right) \quad . \tag{4.75}$$

Substitution of the solution (4.65) into (4.75) yields

$$\hat{c}(r,r') = n - \frac{12}{\pi^2}\sum_{i=1}^{n}\eta_i^{(2)}\kappa_i^2 \quad . \tag{4.76}$$

Notice that this expression for the truncated effective central charge is independent of the dummy variable $r'$. We can use the latter property to argue that in fact the r.h.s. of (4.76) corresponds to the scaling function (4.61) which upon exploiting (4.66) becomes in this approximation

$$c(r) = n - \ 3\ \sum_{i=1}^{n}\frac{\eta_i^{(2)}}{(\delta_i - \ln\frac{r}{2})^2} + ... \tag{4.77}$$

where the whole dependence on the S-matrix is now reduced to the coefficient $\eta_i^{(2)} = \sum_{j=1}^{n}\eta_{ij}^{(2)}$ of the power series expansion (4.58). Additional information on the model under investigation is encoded in the constant $\delta_i$. Hence, the remaining step is now to deduce further restrictions on the constants of integration besides (4.66). This, can be done by going beyond the rapidity region where the large density approximation (4.67) is valid.

**Enhanced approximate solutions and Y-systems**

The restriction on the range for the rapidities in (4.67), for which the large density approximation $L_i^0(\theta)$ ceases to be valid, makes it desirable to develop also an approximation outside the given interval. For large rapidities we naturally expect that the solution will tend to the one of a free theory and approaches small density values. Solving (4.43) for vanishing kernel yields the free on-shell solution

$$L_i^f(\theta) = \ln\left(1 + e^{-rm_i\cosh\theta}\right) \ . \tag{4.78}$$

Ideally we would like to have expressions for both regions which match at some distinct rapidity value, say $\theta_i^m$, to be specified below. At this point one can then determine the constant of integration $\delta_i$. Since $L_i^0(\theta)$ and $L_i^f(\theta)$ become relatively poor approximations in the transition region between large and small densities, we first seek for improved analytical expressions. This is easily achieved by expanding (4.43) around the "zero order" small density approximations. In this case we obtain the integral representation

$$L_i^s(\theta) = \exp\left(-rm_i\cosh\theta + \sum\nolimits_{j=1}^{n}(\varphi_{ij} * L_j^f)(\theta)\right) \ . \tag{4.79}$$

For vanishing $\varphi_{ij}$ we may check for consistency and observe that the functions $L_i^s(\theta)$ become the first term of the expansion in (4.78). One could try to proceed similarly

for the large density regime and develop around $L_i^0$ instead of $L_i^f$. However, there is an immediate problem resulting from the restriction on the range of rapidities for the validity of $L_i^0$, which makes it problematic to compute the convolution. We shall therefore proceed in a different manner for the large density regime and employ so-called $Y$-systems for this purpose.

In many cases the TBA-equations may be expressed equivalently as a set of functional relations referred to as $Y$-systems in the literature [50]. Introducing the quantities $Y_i = \exp(-\varepsilon_i)$, the determining equations can always be cast into the general form

$$Y_i(\theta + i\pi\omega_i)Y_i(\theta - i\pi\omega_i) = \exp(g_i(\theta)) \tag{4.80}$$

with $\omega_i$ being some real number and $g_i(\theta)$ being a function whose precise form depends on the particular model. Below when treating concrete examples we will see how these functional relations can be explicitly derived from (4.43). We can formally solve the equation (4.80) by Fourier transformation

$$Y_i(\theta) = \exp\left[(\Omega_i * g_i)(\theta)\right] , \qquad \Omega_i(\theta) := \left[2\omega_i \cosh\tfrac{\theta}{2\omega_i}\right]^{-1} \tag{4.81}$$

i.e. substituting (4.81) into the l.h.s. of (4.80) yields $\exp(g_i(\theta))$. Of course this identification is not completely compelling and we could have chosen also a different combination of $Y$'s. However, in order to be able to evaluate the $g_i(\theta)$ we require a concrete functional input for the function $Y_i(\theta)$ in form of an approximated function. Choosing here the large density approximation $L_i^0$ makes the choice for $g_i(\theta)$ with hindsight somewhat canonical, since other combinations lead generally to non-physical answers.

We replace now inside the defining relation of $g_i(\theta)$ the $Y$'s by $Y_i(\theta) \to \exp(L_i^0(\theta)) - 1$. Analogously to the approximating approach described in the previous subsection, we can replace the convolution by an infinite series of differentials

$$\varepsilon_i(\theta) = -(g_i * \Omega_i)(\theta) = -\sum_{m=0}^{\infty} \nu_i^{(m)} \frac{d^m}{d\theta^m} g_i(\theta) \ , \tag{4.82}$$

where the $\nu$'s are defined by the power series expansion

$$\int_{-\infty}^{\infty} d\theta\, \Omega_i(\theta)\, e^{it\theta} = 2\pi \sum_{m=0}^{\infty} (-i)^m \nu_i^{(m)} t^m = \pi \sum_{m=0}^{\infty} \frac{E_{2m}}{(2m)!} (\pi\omega_i)^{2m}\, t^{2m} \ . \tag{4.83}$$

The $E_m$ denote the Euler numbers, which enter through the expansion $1/\cosh x = \sum_{m=0}^{\infty} x^{2m} E_{2m}/(2m)!$. In accordance with the assumptions of our previous approximations for the solutions of the TBA-equations in the large density regime, we can neglect all higher order derivatives of the $L_i^0(\theta)$. Thus we only keep the zeroth order in (4.82). From (4.83) we read off the coefficient $\nu_i^{(0)} = 1/2$, such that we obtain a simple expression for an improved large density approximation [44]

$$L_i^l(\theta) = \ln[1 + Y_i^l(\theta)] = \ln[1 + \exp(g_i(\theta)/2)] \, . \tag{4.84}$$

In principle we could proceed similarly for the small density approximation and replace now $Y_i(\theta) \to \exp(L_i^s(\theta)) - 1$ in the defining relations for the $g_i$'s. However, in this situation we can not neglect the higher order derivatives of the $L_i^s$ such that we have to keep the convolution in (4.82) and end up with an integral representation instead.

### The constant of integration and a matching condition

We now wish to match $L_i^s$ and $L_i^l$ in the transition region between the small and large density regimes at some distinct value of the rapidity, say $\theta_i^m$. We select this point to be the value when the following function proportional to the integrand in the scaling function (4.44)

$$f_i(\theta) = (6/\pi^2) r m_i L_i(\theta) \cosh\theta \ , \tag{4.85}$$

has its maximum in the small density approximation [44]

$$\frac{d}{d\theta} f_i^s(\theta)\Big|_{\theta_i^m} = 0 \ . \tag{4.86}$$

In regard to the quantity we wish to compute, the scaling function, this is the point in which we would like to have the highest degree of agreement between the exact and approximated solution, since this will optimize the outcome for $c(r)$. Having specified the $\theta_i^m$, the matching condition provides a simple rational to fix the constant $\delta_i$ [44],

$$L_i^l(\theta_i^m) = L_i^s(\theta_i^m) \qquad \Rightarrow \quad \delta_i^m \ . \tag{4.87}$$

In general, we can not solve these equations analytically, but it is a trivial numerical problem, which is by no means comparable with the one of solving (4.43). Needless to say that the outcome of (4.87) is not to be considered as exact, but as our examples below demonstrate it will lead to rather good approximations. One of the reasons why this procedure is successful is that $L_i^s(\theta_i^m)$ is still very close to the precise solution, despite the fact that is at its worst in comparison with the remaining rapidity range.

Combining the improved large and small density approximation we have the following approximated analytical $L$-functions for the entire range of the rapidity [44]

$$L_i^a(\theta) = \begin{cases} L_i^l(\theta) & \text{for } |\theta| \le \theta_i^m \\ L_i^s(\theta) & \text{for } |\theta| > \theta_i^m \end{cases} \ , \tag{4.88}$$

such that the scaling function becomes well approximated by

$$c(r) \simeq \sum_{i=1}^{n} \int_0^\infty d\theta \ f_i^a(\theta) = \frac{6r}{\pi^2} \sum_{i=1}^{n} m_i \int_0^\infty d\theta \, L_i^a(\theta) \cosh\theta \ . \tag{4.89}$$

To develop matters further and report on the quality of $L^0$, $L^f$, $L^s$, $L^l$ we have to specify a particular theory at this point.

### 4.3 The TBA analysis for affine Toda theory

This section is concerned with the TBA analysis of affine Toda field theories discussed in Chapter 3. In order to make contact with the general considerations mentioned at the beginning of this chapter we re-write the classical action functional (3.20) of ATFT as the sum of two terms

$$S_{\mathrm{ATFT}}(\mathfrak{g}) = S_{\mathrm{TFT}}(\mathfrak{g}) - \frac{m^2}{\beta^2}\int e^{\beta\langle\alpha_0,\phi\rangle}d^2x\ . \tag{4.90}$$

The implicitly defined action $S_{\mathrm{TFT}}(\mathfrak{g})$ describes Toda field theory (TFT) which are known to be conformally invariant [41]. They differ in its definition from the affine theories by the above term involving the affine or highest root $\alpha_0 = -\theta$, compare Section 2.1.2. Thus, in accordance with the general picture of linking integrability to broken conformal symmetry we might interpret ATFT as perturbed conformally invariant Toda models.

To motivate the conformal invariance property of TFT at the classical level we consider the equations of motion following from $S_{\mathrm{TFT}}(\mathfrak{g})$. The latter coincide with the ones of ATFT when omitting the affine contribution of the potential term in (3.19). (Keep in mind that we are dealing now with Euclidean geometry). Under a conformal coordinate transformation the derivative term in (3.19) changes according to

$$\partial_z\partial_{\bar z}\phi \to \partial_w\partial_{\bar w}\phi = \frac{\partial z}{\partial w}\frac{\partial\bar z}{\partial\bar w}\partial_z\partial_{\bar z}\phi$$

where we have introduced as usual complex coordinates. Thus, the equations of motion stay invariant if the potential term scales in an analogous manner. This leads to the following requirement on the transformation behaviour of the fields

$$\phi(z,\bar z) \to \phi'(w,\bar w) = \phi(z,\bar z) + \frac{\rho^\vee}{\beta}\ln\left|\frac{\partial z}{\partial w}\right|^2\ ,$$

where $\rho^\vee$ is the dual Weyl vector (2.11) satisfying $\langle\rho^\vee,\alpha_i\rangle = 1$ for all simple roots $i = 1,...,n$. One immediately verifies that this invariance is spoiled as soon as the affine term is taken into account, since $\langle\rho^\vee,\alpha_0\rangle = 1-h$. Alternatively, one might also calculate the energy-momentum tensor from $S_{\mathrm{TFT}}(\mathfrak{g})$ and show that it can be made traceless, see e.g. [64, 41]. This classical conformal invariance of TFT was shown to survive quantization [41] and therein the conformal anomaly for the $ADE$ series was determined to

$$ADE: \quad c(\beta) = n + 48\pi|\rho|^2\left(\frac{\beta}{4\pi}+\frac{1}{\beta}\right)^2\ . \tag{4.91}$$

Notice that the central charge is coupling dependent and exhibits the same self-duality behaviour w.r.t. the transformation $\beta \to 4\pi/\beta$ as observed for simply-laced ATFT (compare Section 3.2.2). However, much of the quantum structure of TFT still remains to be understood. Even for the best known and simplest example, Liouville field theory with $\mathfrak{g} = A_1$, operator algebra and structure constants are still subject to investigations [97, 42]. As mentioned in the survey of CFT in Section 4.1 the properties of conformal field theories with central charge $c \geq 1$ are much less

understood than those of the minimal models with $c < 1$, see e.g. [83] for further details. For the case at hand (4.91) we realize by using the Freudenthal-de Vries strange formula $|\rho|^2 = h^\vee/12 \dim X_n$ (see e.g. [63]) and (2.40) that

$$c(\beta) \geq n(1 + 4\,h(h+1)) \geq 25\,.$$

Hence, Toda models belong to the class of conformal field theories for which even unitarity can not be established, compare Subsection 4.1.3. (Note that for Liouville theory the lower bound is just assumed at the self-dual point $\beta^2 = 4\pi$.)

Recent advances in exploring the structure of the three and four point functions in Liouville theory include the introduction of so-called reflection amplitudes [42]. However, the origin of these reflection amplitudes has not been rigorously derived so far [42, 98], whence semi-classical methods in connection with the thermodynamic Bethe ansatz were used to provide consistency checks. Perturbing the conformal field theory the scaling function for the Sinh-Gordon model was approximately computed by considering only the zero mode dynamics which lead to a re-formulation of the problem in the setting of quantum mechanics with the reflection amplitude as crucial input [42, 99]. This procedure was extended to all simply-laced ATFT in [45] and just recently to the non simply-laced case in [46] resulting in a perturbative expansion of the scaling function of the kind

$$c(r) = n + \frac{a_1}{(\delta - \ln\frac{r}{2})^2} + \frac{a_2}{(\delta - \ln\frac{r}{2})^5} + \frac{a_3}{(\delta - \ln\frac{r}{2})^7} + ...$$

The leading order term in this expansion matches the result found in [43, 44] as described below. By direct comparison this allows now to fix the constants of integration. However, one should keep in mind that the semi-classical analysis based on reflection amplitudes in [42] and [45, 46] relies on extra input information as for instance the precise relationship between the coupling constant and the masses [102] obtained by Bethe Ansatz methods. Therefore, it is certainly desirable to determine the constant and the scaling function solely within the TBA approach which uses the S-matrix as only input information. We already saw how to derive the leading order behaviour in the previous subsection and we will now provide in the context of ATFT a rigorous argument which establishes that the constants of integration (4.66) do not depend on the particle type, such that we may replace $\kappa_i \to \kappa$ and $\delta_i \to \delta$. In addition, we determine them approximately from within the TBA analysis by matching the large and small density regimes. This allows then to compare against the semi-classical approach [42, 45] and the agreement we find will provide an additional consistency check for the ATFT S-matrix.

### *4.3.1 The universal TBA-kernel*

Recall from our previous discussion that at the quantum level to each of the affine Toda models a pair of dual affine Lie algebras $(X_n^{(1)}, \hat{X}_{\hat{n}}^{(\ell)})$ is associated which describe the Lie algebraic structure in the weak and strong coupling regime, respectively. As explained in Chapter 2 $\hat{X}_{\hat{n}}^{(\ell)}$ denotes a twisted affine Lie algebra w.r.t. a Dynkin diagram automorphism of order $\ell$, while $X_n^{(1)}$ is a non-twisted algebra of rank $n$. For $X_n^{(1)}$ simply-laced both algebras coincide, i.e. $X_n^{(1)} \cong \hat{X}^{(\ell)}$, $\ell = 1$, which is reflected

in the quantum theory by a strong-weak self-duality in the coupling constant. In the following we will now exploit the associated Lie algebraic structure to derive generic expressions for the TBA analysis.

From the universal integral representation (3.82), we immediately derive the Fourier transformed TBA-kernel (4.58) for ATFT. However, when taking the logarithmic derivative one has to be careful about interchanging the derivative with the integral, since these two operations do not commute. Comparison with the block representation of the S-matrix (3.55) yields

$$\varphi_{ij}(\theta) = \frac{1}{2\pi}\int_{-\infty}^{\infty} dt\ \left[2\delta_{ij} - \phi_{ij}(t)\right]\ \exp\frac{t\theta}{i\pi}, \tag{4.92}$$

such that the Fourier transformed universal TBA-kernel (4.58) acquires the form

$$\begin{aligned}\widetilde{\varphi}_{ij}(t) &= 2\pi\delta_{ij} - \pi\phi_{ij}(\pi t)\\ &= 2\pi\delta_{ij} - 8\pi\sinh t\pi\vartheta_h \sinh t_j\pi\vartheta_H\ A(e^{t\pi\vartheta_h}, e^{t\pi\vartheta_H})^{-1}_{ij}\quad .\end{aligned} \tag{4.93}$$

Recall that $A(q,\hat{q})$ is the $q$-deformed Cartan matrix (2.67) of the non-twisted Lie algebra and that the integers $t_i = \ell\alpha_i^2/2$ are the entries of the symmetrizer of the Cartan matrix, compare (2.55) in Chapter 2. The deformation parameters inside the integral representation are chosen in terms of the angles $\vartheta_h := \frac{2-B}{2h}$ and $\vartheta_H := \frac{B}{2H}$, previously defined in (3.41) of Chapter 3 together with the effective coupling constant $0 \leq B \leq 2$. Remember further the definition of the Coxeter numbers $h$, $\hat{h}$ and the dual Coxeter numbers $h^\vee$, $\hat{h}^\vee$ of $X_n^{(1)}$ and $\hat{X}^{(\ell)}$, respectively, as well as the $\ell^{\text{th}}$ Coxeter number $H = \ell\hat{h}$ of $\hat{X}^{(\ell)}$ in Chapter 2.

### The weak coupling limit

Notice that the appearance of the extra term $\delta_{ij}$ in (4.92) is of particular importance in the weak or strong coupling limit, where the particles become free, i.e. $S_{ij} = 1$. Sending $\beta \to 0, \infty$ or equivalently $B \to 0, 2$ we infer from (4.93) that the TBA kernel approaches the $\delta$-function times the unit matrix, whence the TBA equations (4.43) decouple and can be solved exactly,

$$B = 0: \quad L_i(\theta) = -\ln\left(1 - e^{-rm_i\cosh\theta}\right)\ . \tag{4.94}$$

The above density distribution corresponds to the one of a free relativistic Bose gas despite the fact that we used Fermi statistics in the formulation of the TBA equations (4.43). This shows the statistical ambiguity in the formulation of the TBA mentioned before, compare Section 4.2.2. Now, in accordance with the physical picture suggested by the action functional (3.20) that the theory consists of $n$ free bosons at $\beta = 0$, the effective central charge deduced from (4.94) in the extreme UV limit is $c_{\text{eff}} = \lim_{r\to 0} c(r) = n$. The order in which the weak coupling limit is to be performed, before or after taking the logarithmic derivative $-i\frac{d}{d\theta}\ln S_{ij}(\theta)$, is crucial here, since in the former case the result would be a gas of $n$ free *fermions* with central charge $c = n/2$. After this preliminary discussion of vanishing coupling constant we now turn to the general case $B \neq 0$.

**Series expansion and the second order coefficient**

Based on the compact expression (4.93) the discussion of the previous section about approximate solutions can now be applied to all affine Toda models at once. The only information we require to derive the leading order behaviour in the UV limit is the zeroth and second order coefficient $\eta_{ij}^{(2)}$ in the power series expansion (4.58). From (4.93) we read off directly $\eta_{ij}^{(0)} = 0$ (which is in accordance with the requirement imposed in 4.2.4) and

$$\eta_{ij}^{(2)} = \frac{\pi^2}{h\,H} B(2-B) A_{ij}^{-1}\, t_j = \frac{\pi^2}{h\,h^\vee} B(2-B)\ \langle \lambda_i, \lambda_j \rangle \quad . \tag{4.95}$$

In the latter equality we used the fact that the inverse of the Cartan matrix is related to the fundamental weights as $\lambda_i = \sum_j A_{ij}^{-1}\,\alpha_j$, $t_i = \ell\alpha_i^2/2$ and $H = \ell\,\hat{h} = \ell\,h^\vee$. This implies on the other hand that

$$\eta_i^{(2)} = \sum_{j=1}^{n} \eta_{ij}^{(2)} = \frac{\pi^2}{h\,h^\vee} B(2-B)\ \langle \lambda_i, \rho \rangle \tag{4.96}$$

with $\rho$ being the Weyl vector (2.11). Therefore,

$$\eta = \sum_{i=1}^{n} \eta_i^{(2)} = B(2-B)\frac{\pi^2|\rho|^2}{h\,h^\vee} = nB(2-B)\frac{\pi^2(h+1)}{12h}\ . \tag{4.97}$$

We used here again the Freudenthal-de Vries strange formula and $\dim X_n^{(1)} = n(h+1)$, compare (2.40). Notice that in terms of the quantities belonging to the untwisted Lie algebra $X_n^{(1)}$ the formula (4.97) is identical for the simply-laced and the non simply-laced case. Before we now use (4.96) and (4.97) to apply the approximation scheme of Section 4.2.4 we derive the set of functional equations or $Y$-systems needed to improve the leading order approximations.

*4.3.2 Universal TBA equations and Y-systems*

The universal expression for the kernel (4.93) can be exploited in order to derive universal TBA-equations for *all* ATFT, which may be expressed equivalently as a set of functional relations referred to as $Y$-systems. Fourier transforming (4.43) in a suitable manner and invoking the convolution theorem we can manipulate the TBA equations by using the expression (4.93). After Fourier transforming back we obtain

$$\varepsilon_i + \sum_{j=1}^{n} \Delta_{ij} * L_j = \sum_{j=1}^{n} \Gamma_{ij} * (\varepsilon_j + L_j)\,. \tag{4.98}$$

The universal TBA kernels $\Delta$ and $\Gamma$ are then given by

$$\Omega_i(\theta) = \Big(2(\vartheta_h + t_i\vartheta_H)\cosh\tfrac{\theta}{2(\vartheta_h+t_i\vartheta_H)}\Big)^{-1}, \tag{4.99}$$

$$\Gamma_{ij}(\theta) = \sum_{k=1}^{I_{ij}} \Omega_i(\theta + i(2k-1-I_{ij})\theta_H), \tag{4.100}$$

$$\Delta_{ij}(\theta) = [\Omega_i(\theta+\theta_h-t_i\theta_H) + \Omega_i(\theta-\theta_h+t_i\theta_H)]\,\delta_{ij}\,. \tag{4.101}$$

The key point here is that the entire mass dependence, which enters through the on-shell energies $m_i \cosh\theta$, has completely dropped out from the equations due to the identity (3.44) for the mass spectrum. Noting further that the identity

$$[\, I_{ij}]_{\hat{q}(i\pi)}\, m_j \cosh\theta \;=\sum_{k=1}^{I_{ij}} m_j \;\cosh\left[\theta + (2k-1-I_{ij})\theta_H\right] \tag{4.102}$$

can be employed to the l.h.s. of the mass formula, we have assembled all ingredients to derive functional relations for the quantities $Y_i = \exp(-\varepsilon_i)$. For this purpose we may either shift the TBA equations appropriately in the complex rapidity plane or use again Fourier transformations, see [43],

$$\begin{aligned} Y_i(\theta+\theta_h+t_i\theta_H)Y_i(\theta-\theta_h-t_i\theta_H) = \left[1+Y_i(\theta-\theta_h+t_i\theta_H)\right]\left[1+Y_i(\theta+\theta_h-t_i\theta_H)\right] \\ \times \prod_{j=1}^{n}\prod_{k=1}^{I_{ij}} \left[1+Y_j^{-1}(\theta+(2k-1-I_{ij})\theta_H)\right]^{-1} \;. \end{aligned} \tag{4.103}$$

These equations are of the general form (4.80) and specify concretely the quantities $\omega_i$ and $g_i(\theta)$. We recover various particular cases from (4.103). In case the associated Lie algebra is simply-laced, we have $\theta_h + t_i\theta_H \to i\pi/h, \quad \theta_h - t_i\theta_H \to i\pi/h(1-B)$ and $I_{ij} \to 0, 1$, such that we recover the relations derived in [43],

$$\begin{aligned} Y_i\left(\theta+\tfrac{i\pi}{h}\right) Y_i\left(\theta-\tfrac{i\pi}{h}\right) = \left[1+Y_i\left(\theta+\tfrac{i\pi}{h}(1-B)\right)\right]\left[1+Y_i\left(\theta-\tfrac{i\pi}{h}(1-B)\right)\right] \\ \times \prod_{j=1}^{n}\left[1+Y_j^{-1}\left(\theta\right)\right]^{-I_{ij}} \;. \end{aligned} \tag{4.104}$$

As stated therein we obtain the system for minimal ATFT [50] by taking the limit $B \to i\infty$.

The concrete formula for the approximated solution of the Y-systems in the large density regime, as defined in (4.84), reads

$$Y_i^l(\theta) = \tfrac{\cos(2\theta\beta_i)+\cos(2(\theta_h-t_i\theta_H)\beta_i)}{4\eta_i\beta_i^2} \prod_{j=1}^{n}\prod_{m=1}^{I_{ij}} \left(1-\tfrac{2\eta_j\beta_j^2}{\cos^2(\beta_j(\theta+(2m-1-I_{ij})\theta_H)}\right)^{\frac{1}{2}} \;. \tag{4.105}$$

Exploiting possible periodicities of the functional equations (4.103) they may be utilized in the process of obtaining approximated analytical solutions [100]. As we demonstrated they can also be employed to improve on approximated analytical solution in the large density regime. In the following subsection we supply a further application and use them to put constraints on the constant of integration $\delta_i$ in (4.66).

### *4.3.3 The constants of integration $\kappa$ and $\delta$*

There are various constraints we can put on the constants $\kappa_i$ and $\delta_i$ on general grounds, e.g. the lower bound already mentioned. Having the numerical data at hand we can use them to approximate the constant. In [43] this was done for the

$ADE$ series by matching $L_i^0$ with the numerical data at $\theta = 0$ and a simple analytical approximation was provided

$$\delta^{\text{num}} = \ln[B(2-B)2^{1+B(2-B)}] \; . \tag{4.106}$$

Of course the idea is to become entirely independent of the numerical analysis. For this reason the argument which led to the matching condition (4.87) was given. When we consider a concrete theory like ATFT, we can exploit its particular structure and put additional constraints on the constants from general properties. For instance, when we restrict ourselves to the simply-laced case it is obvious to demand that the constants respect also the strong-weak self-duality, i.e. $\kappa_i(B) = \kappa_i(2-B)$ and $\delta_i(B) = \delta_i(2-B)$.

Finally we present a brief argument which establishes that the constants $\kappa_i$ are in fact independent of the particle type $i$. We replace for this purpose in the functional relations (4.103) the $Y$-functions by $Y_i^0(\theta)$ belonging to the solution (4.67) and consider the equation at $\theta = 0$, such that

$$\frac{\cosh^2[\pi\kappa_i(\vartheta_h + t_i\vartheta_H)] - 2\kappa_i^2\eta_i^{(2)}}{\cosh^2[\pi\kappa_i(\vartheta_h + t_i\vartheta_H)]} = \prod_{j=1}^{n}\prod_{m=1}^{I_{ij}} \frac{(\cosh^2[\pi\kappa_i(2m-1-I_{ij})\vartheta_H] - 2\kappa_i^2\eta_i^{(2)})^{\frac{1}{2}}}{\cosh[\pi\kappa_i(2m-1-I_{ij})\vartheta_H]} \; . \tag{4.107}$$

Keeping in mind that $\kappa_i$ is a very small quantity in the ultraviolet regime, we expand (4.107) up to second order in $\kappa_i$, which yields after cancellation

$$4t_i\vartheta_h\vartheta_H = \frac{\alpha_i^2}{2}\frac{B(2-B)}{hh^\vee} = \sum_{j=1} A_{ij}\frac{\kappa_j^2}{\kappa_i^2}\frac{\eta_j^{(2)}}{\pi} = \frac{B(2-B)}{hh^\vee}\sum_{j=1} A_{ij}\frac{\kappa_j^2}{\kappa_i^2}\langle\lambda_j,\rho\rangle \; . \tag{4.108}$$

We substituted here the expression (4.96) for the constants $\eta_j$ in the last equality. Using once more the relation $\lambda_i = \sum_j A_{ij}^{-1}\alpha_j$, we can evaluate the inner product such that (4.108) reduces to

$$\alpha_i^2 = \sum_{j=1}^{n}\sum_{k=1}^{n} A_{ij}\left(\frac{\kappa_j^2}{\kappa_i^2}\right)A_{jk}^{-1}\alpha_k^2 \; . \tag{4.109}$$

Clearly this equation is satisfied if all the $\kappa_i$ are identical. From the uniqueness of the solution of the TBA-equations follows then immediately that we can always take $\kappa_i \to \kappa$. Since the uniqueness discussion has only been presented for the one-particle case, it is reassuring that we can obtain the same result also directly from (4.109). From the fact that the $\kappa_i$ are real numbers and all entries of the inverse Cartan matrix are positive follows that $\kappa_i^2 = \kappa_j^2$ for all $i$ and $j$. The ambiguity in the sign is irrelevant for the use in $L_i^0(\theta)$.

### *4.3.4 The scaling functions*

Exploiting the independence of $\kappa, \delta$ of the particle index and the relation (4.97) the leading order behaviour for the scaling function is now immediate to derive from the general expression (4.77),

$$c(r) \approx n - \frac{3\eta}{(\delta - \ln\frac{r}{2})^2} = n\left(1 - \frac{\pi^2(h+1)B(2-B)}{4h(\delta-\ln\frac{r}{2})^2}\right) \; . \tag{4.110}$$

From the universal expression (4.93) it follows in fact that this expression holds for *all* affine Toda field theories related to a dual pair of simple affine Lie algebras $(X_n^{(1)},\hat{X}^{(\ell)})$. However, strong-weak duality is only guaranteed for $\ell = 1$, i.e. the $ADE$ series, since the constant $\delta$ is in general coupling dependent.

Restricting ourselves to the simply-laced case, we can view the results of [42, 99, 45] obtained by means of a semi-classical treatment for the scaling function as complementary to the one obtained from the TBA analysis and compare directly with the expression (4.110). Translating the quantities in [42, 45] to our conventions, i.e. $R \to r$, $B \to B/2$, we observe that $c(r)$ becomes a power series expansion in $\kappa$. We also observe that the second order coefficients precisely coincide in their general form. Comparing the expressions, we may read off directly

$$\delta^{\text{semi}} = \ln\left(\frac{4\pi\Gamma\left(\frac{1}{h}\right)\left(\frac{2}{B}-1\right)^{\frac{B}{2}-1}}{\varkappa\,\Gamma\left(\frac{1}{h}-\frac{B}{2h}\right)\Gamma\left(1+\frac{B}{2h}\right)}\right) - \gamma_E \tag{4.111}$$

for all ATFT related to simply-laced Lie algebras**. Here $\gamma_E$ denotes Euler's constant and $\varkappa = (\prod_{i=1}^{n} n_i^{n_i})^{\frac{1}{2h}}$ is a constant which can be computed from the Kac labels $n_i$ of the related Lie algebra. Contrary to the statement made in [99], this identification can be carried out effortlessly without the need of higher order terms. Recalling the simple analytical expression (4.106) of [43] we may now compare. Figure 4.3 demonstrates impressively that this working hypothesis shows exactly the same qualitative behaviour as $\delta^{\text{semi}}$ and also quantitatively the difference is remarkably small.

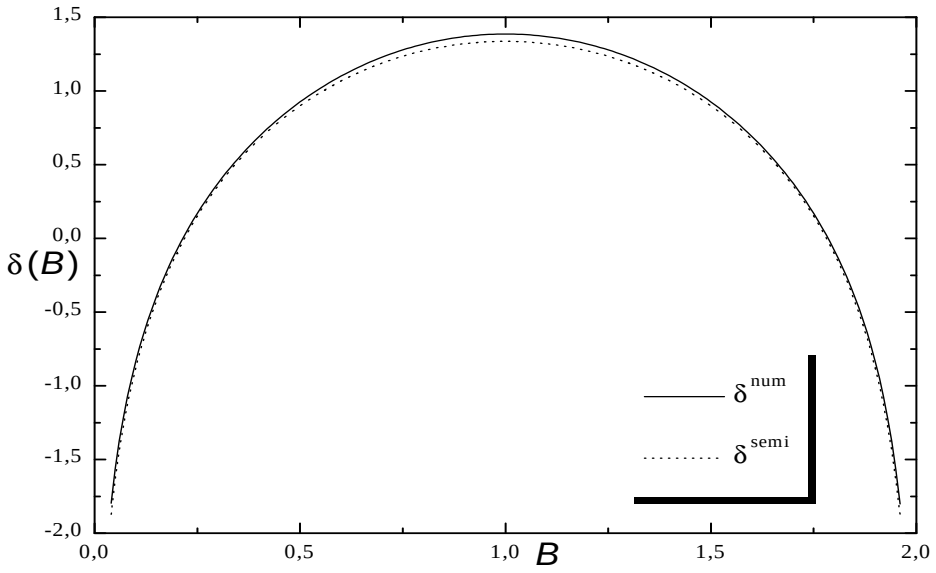


Figure 4.3: The semi-classical constant $\delta^{\text{semi}}$ in comparison to the numerical fit $\delta^{\text{num}}$.

To illustrate the quality of our approximate solutions to the TBA-equations, we shall now work out some explicit examples.

**The expressions in [42] and [45] only coincide if in the former case $m = 1$ and in the latter $m = 1/2$. In addition, we note a missing bracket in equation (6.20) of [42], which is needed for the identification. Replace $C \to -4QC$ therein.

### *4.3.5 Explicit examples*

To exhibit whether there are any qualitative differences between the simply-laced and the non simply-laced case we consider the first examples of these series.

#### The Sinh-Gordon Model

The Sinh-Gordon model is the easiest example in the simply-laced series and therefore ideally suited as testing ground. The Coxeter number is $h = 2$ in this case. An efficient way to approximate the L-functions to a very high accuracy is

$$L^a(\theta) = \begin{cases} \ln\left[1 + \frac{\cos(2\kappa\theta)+\cosh(\pi\kappa(1-B))}{4\eta\kappa^2}\right] & \text{for } |\theta| \leq \theta^m \\ \exp\left[-rm\cosh\theta + (\varphi * L^f)(\theta)\right] & \text{for } |\theta| > \theta^m \end{cases} \tag{4.112}$$

with

$$\varphi(\theta) = \frac{4\sin(\pi B/2)\cosh\theta}{\cosh 2\theta - \cos\pi B}, \qquad \eta = \frac{\pi^2 B(2-B)}{8}. \tag{4.113}$$

The determining equation for the matching point reads

$$\sinh\theta^m - rm/2\sinh(2\theta^m) + \cosh(\theta^m)(\varphi' * L^f)(\theta^m) = 0 \ . \tag{4.114}$$

For instance at $B = 0.4$ this equation yields $\theta^m = 11.9999$ such that the matching condition (4.87) gives $\delta^m = 0.4913$. Figure 4.4 (a) shows that the large and small density approximation $L^0$ and $L^f$ may be improved in a fairly easy way. In view of the simplicity of the expression $L^a$ the agreement with the numerical solution is quite remarkable. Figure 4.4(a) also illustrates that when using the constant $\delta^{\text{semi}}$ instead of $\delta^m$ the agreement with the numerical solutions appears slightly better for small rapidities. When we employ $\delta^{\text{num}}$ instead of $\delta^{\text{semi}}$ the difference between the two approximated solutions is beyond resolution. However, as may be deduced from Figure 4.4(b), with regard to the computation of the scaling function the difference between using $\delta^m$ instead of $\delta^{\text{semi}}$ is almost negligible. Whereas in the former case the resulting value for the scaling function is slightly below the correct value, it is slightly above by almost the same amount in the latter case. Finally we compute the scaling function (4.110) up to leading order and find [43]

$$c(r) = 1 - \frac{3\pi^2 B(2-B)}{8(\delta - \ln\frac{r}{2})^2} + ...$$

which is in agreement with the leading order behaviour found in [42].

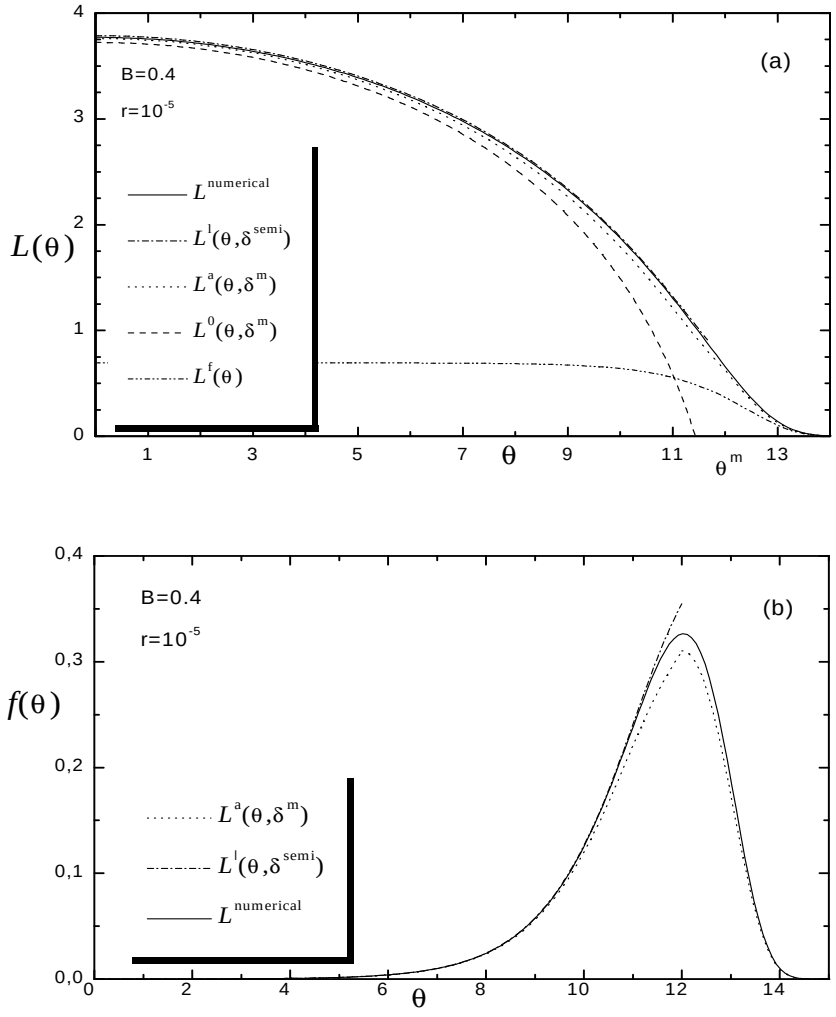


Figure 4.4: Numerical plots against the various analytical approximations for the Sinh-Gordon model. The Graph (a) depicts the solutions to the TBA equation, while (b) shows the free energy density (4.85).

### $(G_2^{(1)}, D_4^{(3)})$-ATFT

In this case we have $h = 6$ and $H = 12$ for the related Coxeter numbers. The two masses are $m_1 = m\sin(\pi(1/6 - B/24))$ and $m_2 = m\sin(\pi(1/3 - B/12))$. The L-functions are well approximated by

$$L_1^a(\theta) = \begin{cases} \ln[1 + \frac{\cos(2\kappa\theta)+\cosh(\pi\kappa(\frac{1}{3}-\frac{B}{4}))}{4\eta_1^{(2)}\kappa^2}\sqrt{1 - \frac{2\eta_2^{(2)}\kappa^2}{\cos^2(\kappa\theta)}}\ ] & \text{for } |\theta| \le \theta_1^m \\ \exp[-rm_1\cosh\theta + (\varphi_{11} * L_1^f + \varphi_{12} * L_2^f)(\theta)] & \text{for } |\theta| > \theta_1^m \end{cases}$$

$$L_2^a(\theta) = \begin{cases} \ln[1 + \frac{\cos(2\kappa\theta)+\cosh(\pi\kappa(\frac{1}{3}-\frac{5B}{24}))}{4\eta_2^{(2)}\kappa^2} \prod_{k=-1}^{1} \sqrt{1 - \frac{2\eta_1^{(2)}\kappa^2}{\cos^2(\kappa(\theta+\frac{kB}{12}))}}\,] & \text{for } |\theta| \leq \theta_2^m \\ \exp[-rm_2\cosh\theta + (\varphi_{21} * L_1^f + \varphi_{22} * L_2^f)(\theta)] & \text{for } |\theta| > \theta_2^m \end{cases},$$

with $\varphi$ given by (4.92) and

$$\eta_1^{(2)} = \frac{5\pi^2 B(2-B)}{72}, \quad \eta_2^{(2)} = \frac{\pi^2 B(2-B)}{8}, \quad \eta = \frac{7\pi^2 B(2-B)}{36}\,. \tag{4.115}$$

Using now the numerical data $L_1(0) = 4.2524$ and $L_2(0) = 3.67144$ as benchmarks, we compute by matching them with $L_1^a(0)$ and $L_2^a(0)$ the constant to $\delta = 1.1397$ in both cases. This confirms our general result of Section 4.3.3. Evaluating the equations (4.87) and (4.86) we obtain for $B = 0.5$ the matching values for the rapidities $\theta_1^m = 12.744$ and $\theta_2^m = 12.278$ such that $\delta_1^m = 1.9539$ and $\delta_2^m = 1.5572$. Figure 4.5(a) and 4.4(b) show a good agreement with the numerical outcome.

The approximated analytical expression for the scaling function reads

$$c(r) \simeq 2 - \frac{7\,\pi^2 B(2-B)}{12(\delta - \ln\frac{r}{2})^2}\,. \tag{4.116}$$

This expressions differs from the one quoted in [43], since in there the sign of some scattering matrices at zero rapidity was chosen differently.

In conclusion, we have demonstrated that it is possible to find simple analytical expressions which approximate the solutions of the TBA equations in the large and small density regime to high accuracy. We derived the $Y$-systems for all ATFT and besides demonstrating how they can be utilized to improve on the large density approximations we also showed how they can be used to put constraints on the constant of integration (4.66). By matching the two solutions of the different regimes at the point in which the particle density and the density of available states coincide, it is possible to fix the constant of integration, which originated in the approximation scheme of [58, 101, 43] described in Subsection 4.2.4. Moreover, the expression (4.77) for the scaling function has been proven valid for *all* ATFT which is in agreement with the leading order term in the alternative approach [42, 45, 46] using reflection amplitudes originating in conformal TFT. In particular, this yields sufficient evidence for the correctness of the universal ATFT S-matrix constructed via the bootstrap approach.

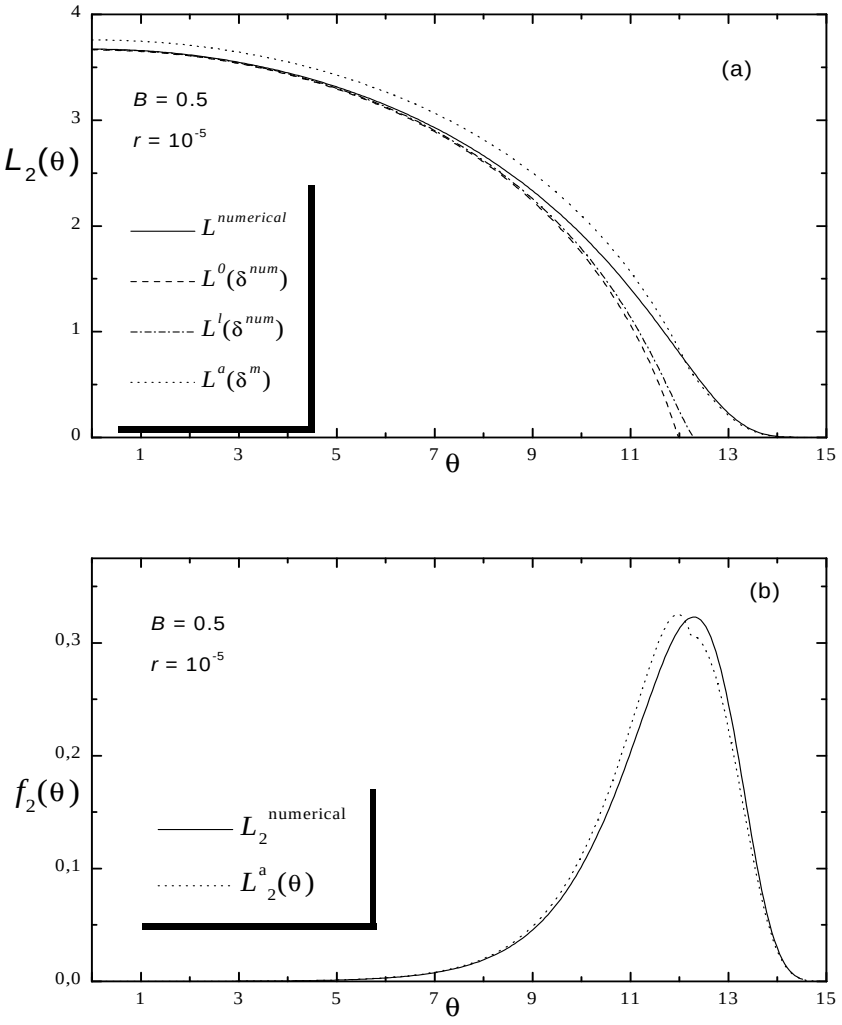


Figure 4.5: Numerical plots against the various analytical approximations for the $(G_2^{(1)},D_4^{(3)})$-theory. The Graph (a) depicts the solutions to the TBA equation, while (b) shows the free energy density (4.85).

## 4.4 TBA for the Homogeneous Sine-Gordon models

In this section we start with the analysis of the colour valued S-matrices or the $\mathfrak{g}|\tilde{\mathfrak{g}}$-theories as we called them in Chapter 3. Recall that both algebras are simply-laced and that one determines the main quantum number, while the other specifies colour degrees of freedom. First we start with a special subclass of these scattering matrices setting $\mathfrak{g} = A_n$ while keeping the colour structure $\tilde{\mathfrak{g}} = ADE$ generic. This class has recently been proposed [40] to describe integrable theories known as the **Homogeneous Sine-Gordon** (HSG) models [47, 103].

For these models one has an explicit Lagrangian at hand whence many informations of the field theory are accessible by a semi-classical analysis. This makes the TBA analysis particularly interesting since one might probe the different semi-classical predictions for consistency, as for example parity violation and the appearance of unstable bound states. The latter will be linked to resonance poles in the S-matrix leading to a "staircase pattern" in the scaling function, which has been observed previously for similar models [58, 59]. However, in comparison with the models studied so far, the HSG models are distinguished in two aspects. First they break parity invariance and second some of the resonance poles can be associated directly to unstable particles via a classical Lagrangian. We present in particular a detailed numerical analysis for the $su(3)$-HSG model [56], but expect that many of our findings for that case are generalizable to other Lie groups. Especially, one of the main outcomes of our TBA-analysis is that the suggested scattering matrix [40] leads indeed to the expected coset central charge [56] (see below), which gives strong support to the proposal. In addition, the detailed analysis of the HSG theories will serve as a preliminary step for the discussion of all $\mathfrak{g}|\tilde{\mathfrak{g}}$-theories.

### *4.4.1 Classical Lagrangian and perturbed WZNW cosets*

The HSG models have been constructed as integrable perturbations of WZNW-coset theories [48] of the form $\tilde{\mathfrak{g}}_k/u(1)^{\tilde{n}}$, where $\tilde{n} = \operatorname{rank}\tilde{\mathfrak{g}}$ and $k = n+1$ is an integer called the "level" with $n$ being the rank of $\mathfrak{g} = A_n$. The specific choice of the coset ensures that the perturbed theories possess a mass gap [54]. The defining action of the HSG models reads

$$S_{\mathrm{HSG}}[g] = S_{\mathrm{CFT}}[g] + \frac{m^2}{\pi\beta^2}\int d^2x\ \left\langle \Lambda_+, g(x,t)^{-1}\Lambda_- g(x,t)\right\rangle \quad . \tag{4.117}$$

Here $S_{\mathrm{CFT}}$ denotes the coset action, $\langle\ ,\ \rangle$ the Killing form of $\tilde{\mathfrak{g}}$ and $g(x,t)$ a bosonic scalar field taking values in the compact simple Lie group associated with $\tilde{\mathfrak{g}}$. $\Lambda_\pm$ are arbitrary semi-simple elements of the Cartan subalgebra, which have to be chosen such that they are not orthogonal to any root of $\tilde{\mathfrak{g}}$. They play the role of continuous vector coupling constants. The latter constraints do not restrict the parameter choice in the quantum case with regard to the proposed S-matrix which makes sense for every choice of $\Lambda_\pm$. They determine the mass ratios of the particle spectrum as well as the behaviour of the model under a parity transformation. The parameters $m$ and $\beta^2 = 1/k + O(1/k^2)$ are the bare mass scale and the coupling constant, respectively. The non-perturbative definition of the theory is achieved by identifying $\Phi(x,t) = \langle \Lambda_+, g(x,t)^{-1}\Lambda_- g(x,t)\rangle$ with a matrix element of the WZNW-field $g(x,t)$ taken in the adjoint representation, which is a spinless primary field of the coset-CFT and in addition exchanging $\beta^2$ by $1/k$ and $m$ by the renormalized mass [54]. The conformal data of $S_{\mathrm{CFT}}[g]$, which are of interest for the TBA analysis are the Virasoro central charge $c$ of the coset and the conformal dimensions $\Delta, \bar{\Delta}$ of the perturbing operator in the massless limit

$$c_{\tilde{\mathfrak{g}}_k} = \frac{k\ \dim\tilde{\mathfrak{g}}}{k+\tilde{h}} - \tilde{n} = \frac{k-1}{k+\tilde{h}}h\tilde{n}\,, \qquad \Delta = \bar{\Delta} = \frac{\tilde{h}}{k+\tilde{h}}\,. \tag{4.118}$$

Here $\tilde{n}$ denotes the rank of $\tilde{\mathfrak{g}}$ and $\tilde{h}$ its Coxeter number[††]. Since we have $\Delta < 1$ for all allowed values of $k$, the perturbation is always relevant in the sense of renormalization showing the Lagrangian to be of the general form (4.1).

The classical equations of motion following from (4.117) correspond to non-abelian affine Toda equations [47, 104], which are known to be classically integrable and admit soliton solutions. Identifying these solutions by a Noether charge allows for a semi-classical approach to the quantum theory by applying the Bohr-Sommerfeld quantization rule. In [55] the semi-classical mass for the soliton labelled by the quantum numbers $(i, a)$ was found to be

$$M_i^a = \frac{m_a}{\pi\beta^2} \sin\frac{\pi i}{k}\,, \qquad 1 \leq i \leq k-1,\ 1 \leq a \leq \tilde{n}, \tag{4.119}$$

where $\beta$ is a coupling constant and the $m_a$ are $\tilde{n}$ different mass scales. We used here the same convention as in the construction of the $\mathfrak{g}|\tilde{\mathfrak{g}}$-theories (compare 3.3.2), namely that the lower index $i$ refers to a vertex in the Dynkin diagram of $\mathfrak{g} = A_n$ determining the type of soliton solution while the upper index $a$ specifies a vertex in the Dynkin diagram of $\tilde{\mathfrak{g}}$ fixing the colour of the soliton. Thus, there are $\tilde{n} = \operatorname{rank}\tilde{\mathfrak{g}}$ towers containing $n = k-1$ solitons each of which describes the simplest example of a HSG theory, the complex Sine-Gordon model [103, 105, 106] associated with the coset $su(2)_k/u(1)$. Note that the semi-classical HSG mass spectrum matches the more general structure of the $\mathfrak{g}|\tilde{\mathfrak{g}}$-theories, see Chapter 3. In fact, the definition of the latter [38] was inspired by the analysis of the HSG-models [40, 56]. We postpone the discussion of further semi-classical formulas concerning the mass spectrum to the next subsection when introducing the S-matrix for the quantum theory.

In view of the discussion in Chapter 3 the latter should factorize. In fact, the integrability on the quantum level was established in [54] by the construction of higher spin conserved charges via the procedure of Zamolodchikov described at the beginning of this chapter. Based on the assumption that the semi-classical spectrum is exact, the S-matrix elements have then been determined in [40] by means of the bootstrap program for HSG-models related to simply-laced Lie algebras.

### *4.4.2 The Homogeneous Sine-Gordon S-matrix and resonances*

With regard to the choice $\mathfrak{g} = A_n$ the proposed scattering matrix consists partially of $\tilde{n}$ copies of minimal $A_n, k = n+1$ or equivalently $su(k)$-affine Toda field theories (ATFT) found by Köberle and Swieca [18], which describe the scattering of solitons with the same colour. As a consequence, the anti-particles are constructed in analogy to the ATFT, that is from the automorphism which leaves the $su(k)$-Dynkin diagram invariant, such that $\overline{(i,a)} = (k-i, a)$. The colour of a particle and its anti-particle is identical. The scattering between solitons belonging to different copies is described by an CDD factor which violates parity (compare 3.3.2 and 3.3.3). In the notation

[††]We slightly abuse here the notation and use $c_{\tilde{\mathfrak{g}}_k}$ instead of $c_{\tilde{\mathfrak{g}}_k/u(1)^{\tilde{n}}}$. Since we always encounter these type of coset in our discussion, we can avoid bulky expressions in this way.

of the $\mathfrak{g}|\tilde{\mathfrak{g}}$-theories the S-matrix then reads

$$S_{ij}^{ab}(\theta) = e^{i\pi\varepsilon_{ab}A^{-1}_{ij}} \exp \int \frac{dt}{t} \left(2\cosh\frac{\pi t}{k} - \tilde{I}\right)_{ab} \left(2\cosh\frac{\pi t}{k} - I^{su(k)}\right)^{-1}_{ij} e^{-it(\theta+\sigma_{ab})} \tag{4.120}$$

Here $I^{su(k)} = 2 - A^{su(k)}$ denotes the incidence matrix of the $su(k)$-Dynkin diagram and $\tilde{I} = 2 - \tilde{A}$ the one corresponding to the Dynkin diagram of $\tilde{\mathfrak{g}}$. A new feature in comparison with the definition (3.94) is the shift $\sigma_{ab}$ in the rapidity variable. Below we will see that these shifts are functions of the vector couplings in (4.117) and are anti-symmetric in the colour values $\sigma_{ab} = -\sigma_{ba}$. Thus, parity is broken not only by the phase factors $e^{i\pi\varepsilon_{ab}A^{-1}_{ij}}$ as discussed in Chapter 3 but also by the shifts $\sigma_{ab}$. Due to the fact that these shifts are real, the function $S_{ij}^{ab}(\theta)$ for $a \neq b$ will have poles beyond the imaginary axis such that the parameters $\sigma_{ab}$ characterize resonance poles.

Analyzing the above S-matrix in the associated block form (3.97) we have therefore have the following picture concerning the formation of bound states: Two solitons with the same colour value may form a bound state of the same colour, whilst solitons of different colour with $\tilde{A}_{ab} \neq 0, 2$, say $(i, a)$ and $(j, b)$, may only form an unstable state, say $(\tilde{k}, \tilde{c})$, whose lifetime and energy scale are characterized by the parameter $\sigma$ by means of the Breit-Wigner formula, see e.g. [110], in the form

$$\begin{aligned} (M_{\tilde{k}}^{\tilde{c}})^2 - \frac{(\Gamma_{\tilde{k}}^{\tilde{c}})^2}{4} &= (M_i^a)^2 + (M_j^b)^2 + 2M_i^a M_j^b \cosh\sigma_{ab}\cos\Theta \qquad (4.121) \\ M_{\tilde{k}}^{\tilde{c}}\Gamma_{\tilde{k}}^{\tilde{c}} &= 2M_i^a M_j^b \sinh|\sigma_{ab}|\sin\Theta\ , \qquad (4.122) \end{aligned}$$

where the resonance pole in $S_{ij}^{ab}(\theta)$ is situated at $\theta_R = \sigma_{ab} - i\Theta$ and $\Gamma_{\tilde{c}}^{\tilde{k}}$ denotes the decay width of the unstable particle with mass $M_{\tilde{k}}^{\tilde{c}}$. In the case $i = j$ these unstable states can be identified with solitons in the semi-classical limit [40, 55]. When $\sigma$ becomes zero, (4.122) shows that the unstable particles become stable, but are still not at the same footing as the other asymptotically stable particles. They become virtual states characterized by poles on the imaginary axis beyond the physical sheet.

How many free parameters do we have in our model? Computing mass shifts from renormalization, we only accumulate contributions from intermediate states having the same colour as the two scattering solitons. Thus, making use of the well known fact that the masses of the minimal $su(k)$-affine Toda theory all renormalize with an overall factor (3.30), i.e. for the solitons $(i, a)$ we have that $\delta M_i^a/M_i^a$ equals a constant for fixed colour value $a$ and all possible values of the main quantum number $i$, we acquire in principle $\tilde{n}$ different mass scales $m_1, \ldots, m_{\tilde{n}}$ in the HSG-model, see (4.119). In addition there are $\tilde{n} - 1$ independent parameters in the model in form of the possible rapidity shifts $\sigma_{ab} = -\sigma_{ba}$ for each $a, b$ such that $\tilde{A}_{ab} \neq 0, 2$. This means overall we have $2\tilde{n} - 1$ independent parameters in the quantum theory. There is a precise correspondence to the free parameters which one obtains from the classical point of view. In the latter case we have the $2\tilde{n}$ independent components of $\Lambda_\pm$ at our free disposal. This number is reduced by 1 as a result of the symmetry $\Lambda_+ \to s\Lambda_+$ and $\Lambda_- \to s^{-1}\Lambda_-$ which introduces an additional dependence as may be seen from

the explicit expressions for the classical mass ratios and the classical resonance shifts

$$\frac{m_a}{m_b} = \frac{M_i^a}{M_i^b} = \sqrt{\frac{\langle \alpha_a, \Lambda_+ \rangle \langle \alpha_a, \Lambda_- \rangle}{\langle \alpha_b, \Lambda_+ \rangle \langle \alpha_b, \Lambda_- \rangle}}, \qquad \sigma_{ab} = \ln \sqrt{\frac{\langle \alpha_a, \Lambda_+ \rangle \langle \alpha_b, \Lambda_- \rangle}{\langle \alpha_a, \Lambda_- \rangle \langle \alpha_b, \Lambda_+ \rangle}}\,. \tag{4.123}$$

Here the $\alpha_a$'s denote the simple roots of $\tilde{\mathfrak{g}}$. Note the anti-symmetry property $\sigma_{ab} = -\sigma_{ba}$ mentioned before. In [40] the parity violation to which this property gives rise was motivated by the following semi-classical observation. The unstable bound state formed by two solitons $(i,a)$ and $(i,b)$ is kinematically allowed to decay in two different ways which are linked to each other by a parity transformation. However, tree-level calculations in perturbation theory showed that only the decay amplitude of one of these decay processes is non-vanishing.

### *4.4.3 Ultraviolet central charge for the HSG model*

In this section we are going to determine the conformal field theory which governs the UV regime of the quantum field theory associated with the S-matrix elements (4.120). According to the defining relation (4.117) and the discussion of the previous section, we expect to recover the WZNW-coset theory with effective central charge (4.118) in the extreme ultraviolet limit. We start by stating the TBA-kernel $\varphi_{ij}^{ab}(\theta) = -i\frac{d}{d\theta} \ln S_{ij}^{ab}(\theta)$ for HSG theories belonging to simply-laced algebras. From the integral representation (4.120) it is calculated to

$$\varphi_{ij}^{ab}(\theta) = \int_{-\infty}^{\infty} dt \left[ \delta_{ab}\delta_{ij} - \left( 2\cosh\frac{\pi t}{h} - \tilde{I} \right)_{ab} \left( 2\cosh\frac{\pi t}{h} - I^{su(k)} \right)^{-1}_{ij} \right] e^{-it(\theta+\sigma_{ab})}\,, \tag{4.124}$$

where the extra term involving the two Kronecker $\delta$'s is due to the fact that integration and differentiation do not commute analogous to the discussion of affine Toda models. Careful comparison with the block representation (3.97) then yields the additional contribution. Different form the discussion of affine Toda models we are not going to apply the large density approximation since the numerical solution will show a different behaviour. In fact, instead of growing over all bounds as $r \to 0$ we will find that the solutions to the TBA equations (4.43) approach a finite constant value in the region $\ln\frac{r}{2} \ll \theta \ll \ln\frac{2}{r}$. Thus, we need not to consider the series expansion of the TBA-kernel as in Section 4.3.

**TBA with parity violation**

Since up to now the TBA analysis has only been carried out for parity invariant S-matrices, a few preliminary comments are due to implement parity violation. The starting point in the derivation of the key equations (4.43) are the Bethe ansatz equations (4.33), which are the outcome of dragging one soliton, say of type $A = (i,a)$, along the world line, compare 4.2.2. For the time being we do not need the distinction between the two quantum numbers. On this trip the formal wave-function of $A$ picks up the corresponding S-matrix element as a phase factor when meeting another soliton. Due to the parity violation it matters, whether the soliton is moved clockwise

or counter-clockwise along the world line, such that we end up with two different sets of Bethe Ansatz equations

$$e^{iLM_A \sinh\theta_A} \prod_{B\neq A} S_{AB}(\theta_A-\theta_B) = 1 \quad \text{and} \quad e^{-iLM_A \sinh\theta_A} \prod_{B\neq A} S_{BA}(\theta_B-\theta_A) = 1\,, \tag{4.125}$$

with $L$ denoting the length of the compactified space direction, compare 4.2.1 and 4.2.2. These two sets of equations are of course not entirely independent and may be obtained from each other by complex conjugation exploiting the Hermitian analyticity (3.9) of the scattering matrix. We may now carry out the thermodynamic limit of (4.125) as in 4.2.2 for the parity preserving case and obtain the following sets of non-linear integral equations

$$\epsilon_A^+(\theta) + \sum_B \varphi_{AB} * L_B^+(\theta) = r\, M_A \cosh\theta \tag{4.126}$$

$$\epsilon_A^-(\theta) + \sum_B \varphi_{BA} * L_B^-(\theta) = r\, M_A \cosh\theta\ . \tag{4.127}$$

Recall that '$*$' denotes the rapidity convolution of two functions and that $r = m_1 R$ is the inverse temperature times the overall mass scale $m_1$ of the lightest particle. We also re-defined the masses by $M_i^a \to M_i^a/m_1$ keeping, however, the same notation. As in the case of ATFT we have chosen Fermi statistics by introducing the so-called pseudo-energies $\epsilon_A^+(\theta) = \epsilon_A^-(-\theta)$ and the related functions $L_A^\pm(\theta) = \ln(1+e^{-\epsilon_A^\pm(\theta)})$. The TBA kernels $\varphi_{AB}$ in the integrals carry the information of the dynamical interaction of the system and are given by (4.124). Notice that (4.127) may be obtained from (4.126) simply by the parity transformation $\theta \to -\theta$ and the equality $\varphi_{AB}(\theta) = \varphi_{BA}(-\theta)$ following from Hermitian analyticity (3.9). The main difference of these equations in comparison with the parity invariant case is that we have lost the usual symmetry of the pseudo-energies as a function of the rapidities, such that we have now in general $\epsilon_A^+(\theta) \neq \epsilon_A^-(\theta)$. This symmetry may be recovered when restoring parity.

The scaling function (4.44) may be computed similar as in the usual way

$$c(r) = \frac{3\,r}{\pi^2} \sum_A M_A \int_0^\infty d\theta\, \cosh\theta\, (L_A^-(\theta) + L_A^+(\theta))\,, \tag{4.128}$$

once the equations (4.126) have been solved for the $\epsilon_A^\pm(\theta)$. Of special interest is the deep UV limit, i.e. $r \to 0$, in which one recovers the effective central charge $c_{\text{eff}} = c - 12(\Delta_0 + \bar\Delta_0)$. Recall that $c$ is the Virasoro central charge and $\Delta_0, \bar\Delta_0$ are the lowest conformal dimensions related to the two chiral sectors of the conformal model. Since the WZNW-coset is unitary, we expect that $\Delta_0, \bar\Delta_0 = 0$ and $c_{\text{eff}} = c$. This assumption will turn out to be consistent with the analytical and numerical results.

### The central charge calculation

In this section we follow the usual argumentation of the TBA-analysis which leads to the effective central charge, paying, however, attention to the parity violation. We

will recover indeed the value in (4.118) as the central charge of the HSG-models. Extending the general formula (4.52) to the case at hand we infer that only the value $\epsilon_A^{\pm}(0)$ of the solutions in the UV limit is required. Hence, we take the limits $r, \theta \to 0$ of (4.126) and (4.127). When we assume that the kernels $\varphi_{AB}(\theta)$ are strongly peaked[‖] at $\theta = 0$ and that the solutions develop characteristic plateaus of constant height in the region $\ln \frac{r}{2} \ll \theta \ll \ln \frac{2}{r}$ (as one observes for the scaling models of minimal ATFT [23, 96] for example), we can take out the $L$-functions from the integral in the equations (4.126), (4.127) and obtain the following determining equation

$$\epsilon_A^{\pm}(0) + \sum_B N_{AB} L_B^{\pm}(0) = 0 \qquad \text{with} \qquad N_{AB} = \frac{1}{2\pi} \int_{-\infty}^{\infty} d\theta \; \varphi_{AB}(\theta) \; . \tag{4.129}$$

The on-shell energies have been discarded since their contribution in the interval $\ln \frac{r}{2} \ll \theta \ll \ln \frac{2}{r}$ is minute. In particular, the above equation is assumed to become exact in the extreme limit. Having the resonance parameter $\sigma$ present in our theory we may also encounter a situation in which $\varphi_{AB}(\theta)$ is peaked at $\theta = \pm\sigma$ with $\sigma$ finite. This means in order for (4.129) to be valid, we have to assume $\epsilon_A^{\pm}(0) = \epsilon_A^{\pm}(\pm\sigma)$ in the limit $r \to 0$ in addition to accommodate that situation. *The last assumption as well as the characteristic plateau behaviour will be justified in retrospective for particular cases from the numerical results (see e.g. Figure 4.6).* Note that in (4.129) we have recovered the parity invariance.

For small values of $r$ we may approximate, in analogy to the parity invariant situation discussed in 4.2.2, $rM_A \cosh\theta$ by $\frac{r}{2} M_A \exp\theta$, such that taking the derivative of the relations (4.126) and (4.127) thereafter yields

$$\frac{\epsilon_A^{\pm}(\theta)}{d\theta} + \frac{1}{2\pi} \sum_B \int_{-\infty}^{\infty} d\theta' \frac{\varphi_{AB}(\pm\theta \mp \theta')}{1 + e^{\epsilon_B^{\pm}(\theta')}} \frac{d\epsilon_B^{\pm}(\theta')}{d\theta'} \approx \frac{r}{2} M_A \exp\theta \quad . \tag{4.130}$$

The scaling function acquires the form

$$c(r) \approx \frac{3\,r}{2\pi^2} \sum_A M_A \int_0^{\infty} d\theta \, e^{\theta} (L_A^-(\theta) + L_A^+(\theta)) \, , \qquad \text{for } r \approx 0 \tag{4.131}$$

in this approximation. Replacing in (4.131) the term $\frac{r}{2} M_A \exp\theta$ by the l.h.s. of (4.130) a few manipulations similar to those in Section 4.2.2 lead to

$$\lim_{r\to 0} c(r) \simeq \frac{3}{2\pi^2} \sum_{p=+,-} \sum_A \int_{\epsilon_A^p(0)}^{\epsilon_A^p(\infty)} d\epsilon_A^p \left[ \ln(1 + e^{-\epsilon_A^p}) + \frac{\epsilon_A^p}{1 + e^{-\epsilon_A^p}} \right] \quad . \tag{4.132}$$

[‖] That this assumption holds for the case at hand is most easily seen by noting that the logarithmic derivative of a basic building block of the S-matrix reads

$$-i \frac{d}{d\theta} \ln \frac{\sinh \frac{1}{2}(\theta + \frac{i\pi}{k})}{\sinh \frac{1}{2}(\theta + \frac{i\pi}{k})} = - \frac{\sin\left(\frac{\pi}{k}\, x\right)}{\cosh\theta - \cos\left(\frac{\pi}{k}\, x\right)} = -2 \sum_{n=1}^{\infty} \sin\left(\frac{\pi}{k}\, x\right) e^{-n|\theta|} \, .$$

From this we can read off directly the decay properties.

Upon the substitution $y_A^p = 1/(1+\exp(\epsilon_A^p))$ we obtain the well known expression (4.52) for the effective central charge

$$c_{\text{eff}} = \frac{6}{\pi^2}\sum_A \mathcal{L}\left(\frac{1}{1+e^{\epsilon_A^{\pm}(0)}}\right) \ . \tag{4.133}$$

Here we used the integral representation for Roger's dilogarithm function (4.51) and the facts that $\epsilon_A^+(0) = \epsilon_A^-(0)$, $y_A^+(\infty) = y_A^-(\infty) = 0$. This means we end up precisely with the same situation as in the parity invariant case for scaling models [23]: Determining at first the phases of the scattering matrices we have to solve the constant TBA-equation (4.129) and may compute the effective central charge in terms of Roger's dilogarithm thereafter. Notice that in the ultraviolet limit we have recovered the parity invariance and (4.133) holds for all finite values of the resonance parameter.

For the case at hand we read off from the integral representation (4.124) of the TBA kernel

$$N_{ij}^{ab} = \delta_{ij}\delta_{ab} - \tilde{A}_{ab}\,(A^{su(k)})^{-1}_{\ ij} \ . \tag{4.134}$$

With $N_{ij}^{ab}$ in the form (4.134) and the identifications $Q_i^a = \prod_{j=1}^{k-1}(1+e^{-\epsilon_j^a(0)})^{(A^{su(k)})^{-1}_{ij}}$ the constant TBA-equations are precisely the equations which occur in the context of the restricted solid-on-solid models [107, 111]. It was noted in there that (4.129) may be solved elegantly in terms of Weyl-characters and the reported effective central charge coincides indeed with the one for the HSG-models (4.118).

It should be stressed that we understand the $N$-matrix here as defined in (4.129) and not as the difference between the phases of the S-matrix. In the latter case we encounter contributions from the non-trivial constant phase factors in (4.120). Also in that case we may arrive at the same answer by compensating them with a choice of a non-standard statistical interaction as outlined in [92].

We would like to close this section with a comment which links our analysis to structures which may be observed directly inside the conformal field theory. When one carries out a saddle point analysis, see e.g. [112], on a Virasoro character (4.20) which can be written in the particular form

$$\chi(q) = \sum_{\vec{m}=0}^{\infty} \frac{q^{\frac{1}{2}\vec{m}(\mathbf{1}-N)\vec{m}^t+\vec{m}\cdot\vec{B}}}{(q)_1\ldots(q)_{(k-1)\tilde{n}}} \ , \tag{4.135}$$

with $(q)_m = \prod_{k=1}^m(1-q^k)$, one recovers the set of coupled equations as (4.129) and the corresponding effective central charge is expressible as a sum of Roger's dilogarithms as (4.194). Note that when we choose $\mathfrak{g} \equiv A_1$ the HSG-model reduces to the minimal ATFT and (4.135) reduces to the character formulae in [51].

*Thus, the equations (4.129) and (4.194) constitute an interface between massive and massless theories, since they may be obtained on one hand in the ultraviolet limit from a massive model and on the other hand from a limit inside the conformal field theory.*

This means we can guess a new form of the coset character, by substituting (4.134) into (4.135). However, since the specific form of the vector $\vec{B}$ does not enter in this analysis (it distinguishes the different highest weight representations) more

work needs to be done in order to make this more than a mere conjecture. This issue is left for future investigations.

*4.4.4 The su(3)$_k$-HSG model*

We shall now focus our discussion on $\tilde{\mathfrak{g}} = A_2 \equiv su(3)$ and explore the structure of the scaling function in more detail supplemented by a detailed numerical analysis at the end of this section. Special emphasis will be given to the role of the resonance parameters. Similar as for staircase models [58, 59] studied previously, they allow to describe the ultraviolet limit of the HSG-model alternatively as the flow between different conformal field theories in the ultraviolet and infrared regime. Below we will find the following massless flow [56]

$$\text{UV} \equiv su(3)_k/u(1)^2 \leftrightarrow su(2)/u(1) \otimes su(2)/u(1) \equiv \text{IR} \; . \tag{4.136}$$

We also observe the flow $(su(3)_k/u(1)^2)/(su(2)_k/u(1)) \to su(2)_k/u(1)$ as a subsystem inside the HSG-model. For $k = 2$ this subsystem describes the flow between the tricritical Ising and the Ising model previously studied in [57]. In terms of the HSG-model we will then obtain the following physical picture [56]: The resonance parameter characterizes the mass scale of the unstable particles (4.121). Approaching the extreme ultraviolet regime from the infrared we pass various regions: At first all solitons are too heavy to contribute to the off-critical central charge, then the two copies of the minimal ATFT will set in, leading to the central charge corresponding to IR in (4.136) and finally the unstable bound states will start to contribute such that we indeed obtain (4.118) as the ultraviolet central charge of the HSG-model in accordance with the result of the previous subsection.

First of all we need to establish how many free parameters we have at our disposal in the case $\tilde{\mathfrak{g}} = su(3)$. According to the discussion in Section 4.4.1 we can tune the resonance parameter and the mass ratio

$$\sigma := \sigma_{21} = -\sigma_{12} \quad \text{and} \quad m_1/m_2 \; . \tag{4.137}$$

It will also be useful to exploit a symmetry present in the TBA-equations related to $SU(3)_k$ by noting that the parity transformed equations (4.127) turn into the equations (4.126) when we exchange the masses of the different types of solitons. This means the system remains invariant under the simultaneous transformations

$$\theta \to -\theta \qquad \text{and} \qquad m_1/m_2 \to m_2/m_1 \; . \tag{4.138}$$

For the special case $m_1/m_2 = 1$ we deduce therefore that $\epsilon_a^{(1)}(\theta) = \epsilon_a^{(2)}(-\theta)$, meaning that a parity transformation then amounts to an interchange of the colours. Furthermore, we see from (4.127) and the defining relation $\sigma = \sigma_{21} = -\sigma_{12}$ that changing the sign of the rapidity variable is equivalent to $\sigma \to -\sigma$. Therefore, we can restrict ourselves to the choice $\sigma \geq 0$ without loss of generality.

**Staircase behaviour of the scaling function**

We will now come to the evaluation of the scaling function (4.128) for finite and small scale parameter $r$. To do this we have to solve first the TBA equations (4.126) for the

pseudo-energies, which due to the non-linear nature of the integral equations is hardly achieved analytically as pointed out before. We therefore pass on to the UV regime with $r \ll 1$ where we can set up approximate TBA equations involving formally massless particles** analogous to the general discussion in 4.2.1. Certain statements and approximation schemes we will use in order to extract the staircase behaviour of the scaling function depend on the general form of the $L$-functions. Since the latter is not known a priori, one may justify ones assumptions in retrospective by referring to the numerics at the end of this section, where we present numerical solutions for the equations (4.126) for various levels $k$. The latter show that the L-functions develop at most two (three if $m_1$ and $m_2$ are very different) plateaus in the range $\ln \frac{r}{2} \ll \theta \ll \ln \frac{2}{r}$ and then fall off rapidly (see Figure 4.6). This type of behaviour is similar to the one known from minimal ATFT [23, 96], and we can therefore adopt various arguments presented in that context. The main difficulty we have to deal with here is to find the appropriate "massless" TBA equations accommodating the dependence of the TBA equations on the resonance shifts $\sigma$.

We start by separating the kernel (4.124) into two parts

$$\phi_{ij}(\theta) = \Phi^{aa}_{ij}(\theta) = \int dt \, \left[\delta_{ij} - 2\cosh\tfrac{\pi t}{k}\left(2\cosh\tfrac{\pi t}{k} - I^{su(k)}\right)^{-1}_{ij}\right] e^{-it\theta} \,, \quad (4.139)$$

$$\psi_{ij}(\theta) = \Phi^{ab}_{ij}(\theta + \sigma_{ba}) = \int dt \, \left(2\cosh\tfrac{\pi t}{k} - I^{su(k)}\right)^{-1}_{ij} e^{-it\theta} \quad , \; a \neq b \,. \quad (4.140)$$

Here $\phi_{ij}(\theta)$ is just the TBA kernel of the $su(k)$-minimal ATFT and in the remaining kernels $\psi_{ij}(\theta)$ we have removed the resonance shift. Note that $\phi, \psi$ do not depend on the colour values $a, b$ which may therefore be dropped all together in the notation. Note that the integral representations for these kernels are generically valid for all values of the level $k$. The convolution term in (4.126) in terms of $\phi, \psi$ is then re-written as

$$\sum_{b=1}^{\tilde{n}} \sum_{j=1}^{k-1} \varphi^{ab}_{ij} * L^b_j(\theta) = \sum_{j=1}^{k-1} \phi_{ij} * L^a_j(\theta) + \sum_{\substack{b=1 \\ b\neq a}}^{\tilde{n}} \sum_{j=1}^{k-1} \psi_{ij} * L^b_j(\theta - \sigma_{ba}) \,. \quad (4.141)$$

These equations illustrate that whenever we are in a regime in which the second term in (4.141) is negligible we are left with $\tilde{n}$ non-interacting copies of the $su(k)$-minimal ATFT.

We will now specialize the discussion on the $su(3)_k$-case for which we can eliminate the dependence on $\sigma$ in the second convolution term by performing the shifts $\theta \to \theta \pm \sigma/2$ in the TBA equations. In the UV limit $r \to 0$ with $\sigma \gg 1$ the shifted functions can be approximated by the solutions of the following sets of integral

**The concept of massless scattering has been introduced originally in [57] as follows: The on-shell energy of a right and left moving particle is given by $E_\pm = M/2e^{\pm\theta}$ which is formally obtained from the on-shell energy of a massive particle $E = m\cosh\theta$ by the replacement $\theta \to \theta \pm \sigma/2$ and taking the limit $m \to 0, \sigma \to \infty$ while keeping the expression $M = me^{\theta+\sigma/2}$ finite. It are these on-shell energies we will encounter in our analysis.

equations

$$\varepsilon_i^{\pm}(\theta) + \sum_{j=1}^{k-1} \phi_{ij} * L_j^{\pm}(\theta) + \sum_{j=1}^{k-1} \psi_{ij} * L_j^{\mp}(\theta) = r' M_i^{\pm} e^{\pm\theta} \tag{4.142}$$

$$\hat{\varepsilon}_i^{\pm}(\theta) + \sum_{j=1}^{k-1} \phi_{ij} * \hat{L}_j^{\pm}(\theta) = r' M_i^{\mp} e^{\pm\theta}, \tag{4.143}$$

where we have introduced the parameter $r' = r\, e^{\frac{\sigma}{2}}/2$ familiar from the discussion of massless scattering and the masses $M_i^{+/-} = M_i^{(1)/(2)}$. The relationship between the solutions of the massless system (4.142), (4.143) and those of the original TBA-equations is given by

$$\epsilon_i^{(1)/(2)}(\theta) = \varepsilon^{+/-}(\theta \mp \sigma/2) \qquad \text{for} \quad \ln\tfrac{r}{2} \ll \pm\theta \ll \ln\tfrac{r}{2} + \sigma \tag{4.144}$$

$$\epsilon_i^{(1)/(2)}(\theta) = \hat{\varepsilon}^{-/+}(\theta \pm \sigma/2) \qquad \text{for} \quad \pm\theta \ll \min[\ln\tfrac{2}{r}, \ln\tfrac{r}{2} + \sigma] \tag{4.145}$$

where we have assumed $m_1 = m_2$. Similar equations may be written down for the generic case. To derive (4.145) we have neglected here the convolution terms $(\psi_{ij} * L_j^{(1)})(\theta + \sigma)$ and $(\psi_{ij} * L_j^{(2)})(\theta - \sigma)$ which appear in the TBA-equations for $\epsilon_i^{(2)}(\theta)$ and $\epsilon_i^{(1)}(\theta)$, respectively. This is justified by the following argument: For $|\theta| \gg \ln\frac{2}{r}$ the free on-shell energy term is dominant in the TBA equations, i.e. $\epsilon_i^a(\theta) \approx r\, M_i^a \cosh\theta$ and the functions $L_i^a(\theta)$ are almost zero. The kernels $\psi_{ij}$ are centered in a region around the origin $\theta = 0$ outside of which they exponentially decrease, see footnote in Subsection 4.4.3 for this. This means that the convolution terms in question can be neglected safely if $\theta \ll \ln\frac{r}{2} + \sigma$ and $\theta \gg \ln\frac{2}{r} - \sigma$, respectively. Note that the massless system provides a solution for the whole range of $\theta$ for the non-vanishing $L$-function only if the ranges of validity in (4.144) and (4.145) overlap, i.e. if $\ln\frac{r}{2} \ll \min[\ln\frac{2}{r}, \ln\frac{r}{2} + \sigma]$, which is always true in the limit $r \to 0$ when $\sigma \gg 0$. The solution is uniquely defined in the overlapping region. These observations are confirmed by our numerical analysis below.

The resulting equations (4.143) are therefore decoupled and we can determine $\hat{L}^+$ and $\hat{L}^-$ individually. In contrast, the equations (4.142) for $L_i^{\pm}$ are still coupled to each other due to the presence of the resonance shift. Formally, the on-shell energies for massive particles have been replaced by on-shell energies for massless particles in the sense of [57], such that if we interpret $r'$ as an independent new scale parameter the sets of equations (4.142) and (4.143) could be identified as massless TBA systems in their own right.

Introducing then the scaling function associated with the system (4.142) as

$$c_{\rm o}(r') = \frac{3\, r'}{\pi^2} \sum_{i=1}^{k-1} \int d\theta \, \left[ M_i^+ e^{\theta} L_i^+(\theta) + M_i^- e^{-\theta} L_i^-(\theta) \right] \tag{4.146}$$

and analogously the scaling function associated with (4.143) as

$$\hat{c}_{\rm o}(r') = \frac{3\, r'}{\pi^2} \sum_{i=1}^{k-1} \int d\theta \, \left[ M_i^+ e^{\theta} \hat{L}_i^+(\theta) + M_i^- e^{-\theta} \hat{L}_i^-(\theta) \right] \tag{4.147}$$

we can express the scaling function (4.128) of the HSG model in the parameter regime $r \to 0,\ \sigma \gg 1$ approximately by [56]

$$\begin{aligned} c(r,\sigma) &= \frac{3\, r\, e^{\frac{\sigma}{2}}}{2\pi^2} \sum_{a=1,2} \sum_{i=1}^{k-1} M_i^a \int d\theta \, \left[ e^{\theta} L_i^a(\theta - \tfrac{\sigma}{2}) + e^{-\theta} L_i^a(\theta + \tfrac{\sigma}{2}) \right] \\ &\approx c_{\mathrm{o}}\,(r') + \hat{c}_{\mathrm{o}}\,(r') \quad . \end{aligned} \tag{4.148}$$

**Remark**. *Notice, that we have formally decomposed the massive $su(3)_k$-HSG model in the UV regime into two massless TBA systems (4.142) and (4.143), reducing therefore the problem of calculating the scaling function of the HSG model in the UV limit $r \to 0$ to the problem of evaluating the scaling functions (4.146) and (4.147) for the scale parameter $r'$. The latter depends on the relative size of $\ln \frac{2}{r}$ and the resonance shift $\sigma/2$.*

Keeping now $\sigma \gg 0$ fixed, and letting $r$ vary from finite values to the deep UV regime, i.e. $r = 0$, the scale parameter $r'$ governing the massless TBA systems will pass different regions. For the regime $\ln \frac{2}{r} < \sigma/2$ we see that the scaling functions (4.146) and (4.147) are evaluated at $r' > 1$, whereas for $\ln \frac{2}{r} > \sigma/2$ they are taken at $r' < 1$. Thus, when performing the UV limit of the HSG model the massless TBA systems pass formally from the "infrared" to the "ultraviolet" regime with respect to the parameter $r'$. We emphasize that the scaling parameter $r'$ has only a formal meaning and that the physical relevant limit we consider is still the UV limit $r \to 0$ of the HSG model. However, proceeding this way has the advantage that we can treat the scaling function of the HSG model by the UV and IR central charges of the systems (4.142) and (4.143) as functions of $r'$ [56]

$$c(r,\sigma) \approx c_{\mathrm{o}}\,(r') + \hat{c}_{\mathrm{o}}\,(r') \approx \begin{cases} c_{IR} + \hat{c}_{IR}\,, & 0 \ll \ln \frac{2}{r} \ll \frac{\sigma}{2} \\ c_{UV} + \hat{c}_{UV}\,, & \frac{\sigma}{2} \ll \ln \frac{2}{r} \end{cases} \quad . \tag{4.149}$$

Here we defined the quantities $c_{IR} := \lim_{r' \to \infty} c_{\mathrm{o}}(r')$, $c_{UV} := \lim_{r' \to 0} c_{\mathrm{o}}(r')$ and $\hat{c}_{IR}, \hat{c}_{UV}$ analogously in terms of $\hat{c}_{\mathrm{o}}(r')$.

In the case of $c_{IR} + \hat{c}_{IR} \neq c_{UV} + \hat{c}_{UV}$, we infer from (4.149) that the scaling function develops at least two plateaus at different heights. A similar phenomenon was previously observed for theories discussed in [59], where infinitely many plateaus occurred which prompted to call them "staircase models". As a difference, however, the TBA equations related to these models do not break parity. In the next subsection we determine the central charges belonging to the different regimes in (4.149) by means of standard TBA central charge calculation, setting up the so-called constant TBA equations.

### Central charges from constant TBA equations

In this subsection we will perform the limits $r' \to 0$ and $r' \to \infty$ for the massless systems (4.142) and (4.143) referring to them formally as "UV-" and "IR-limit", respectively, keeping however in mind that both limits are still linked to the UV limit

of the HSG model in the scale parameter $r$ as discussed in the preceding subsection. We commence with the discussion of the "UV limit" $r' \to 0$ for the subsystem (4.142). We then have three different rapidity regions in which the pseudo-energies are approximately given by

$$\varepsilon_i^{\pm}(\theta) \approx \begin{cases} r' M_i^{\pm}\, e^{\pm\theta}, & \text{for } \pm\theta \gg -\ln r' \\ -\sum_j \phi_{ij} * L_j^{\pm}(\theta) - \sum_j \psi_{ij} * L_j^{\mp}(\theta), & \text{for } \ln r' \ll \theta \ll -\ln r' \\ -\sum_j \phi_{ij} * L_j^{\pm}(\theta), & \text{for } \pm\theta \ll \ln r' \end{cases} . \quad (4.150)$$

We have only kept here the dominant terms up to exponentially small corrections. We proceed analogously to the discussion as may be found in [23, 96]. We see that in the first region the particles become asymptotically free. For the other two regions the TBA equations can be solved by assuming the L-functions to be constant. Exploiting once more that the TBA kernels are centered at the origin and decay exponentially, we can similar as in Subsection 4.4.3 take the $L$-functions outside of the integrals and end up with the sets of equations

$$x_i^{\pm} = \prod_{j=1}^{k-1} (1 + x_j^{\pm})^{\hat{N}_{ij}} (1 + x_j^{\mp})^{N'_{ij}} \qquad \text{for } \ln r' \ll \theta \ll -\ln r' \quad (4.151)$$

$$\hat{x}_i = \prod_{j=1}^{k-1} (1 + \hat{x}_j)^{\hat{N}_{ij}} \qquad \text{for } \pm\theta \ll \ln r' \quad (4.152)$$

for the constants $x_i^{\pm} = e^{-\varepsilon_i^{\pm}(0)}$ and $\hat{x}_i = e^{-\varepsilon_i^{\pm}(\mp\infty)}$. The N-matrices can be read off directly from the integral representations (4.139) and (4.140)

$$\hat{N} := \frac{1}{2\pi} \int \phi = 1 - 2(A^{su(k)})^{-1} \qquad \text{and} \qquad N' := \frac{1}{2\pi} \int \psi = (A^{su(k)})^{-1} . \quad (4.153)$$

Since the set of equations (4.152) has already been stated in the context of minimal ATFT and its solutions may be found in [96], we only need to investigate the equations (4.151). These equations are simplified by the following observation. Sending $\theta$ to $-\theta$ the constant L-functions must obey the same constant TBA equation (4.151) but with the role of $L_i^+$ and $L_i^-$ interchanged. The difference in the masses $m_1, m_2$ has no effect as long as $m_1 \sim m_2$ since the on-shell energies are negligible in the central region $\ln r' \ll \theta \ll -\ln r'$. Thus, we deduce $x_i^+ = x_i^- =: x_i$ and (4.151) reduces to

$$x_i = \prod_{j=1}^{k-1} (1 + x_j)^{N_{ij}} \qquad \text{with} \quad N = 1 - (A^{su(k)})^{-1} . \quad (4.154)$$

Remarkably, also these set of equations may be found in the literature in the context of the restricted solid-on-solid models [111] as already has been pointed out in 4.4.3. Specializing some of the general Weyl-character formulae in [111] to the $su(3)_k$-case a straightforward calculation leads to

$$x_i = \frac{\sin\left(\frac{\pi\,(i+1)}{k+3}\right) \sin\left(\frac{\pi\,(i+2)}{k+3}\right)}{\sin\left(\frac{\pi\,i}{k+3}\right) \sin\left(\frac{\pi\,(i+3)}{k+3}\right)} - 1 \quad \text{and} \quad \hat{x}_i = \frac{\sin^2\left(\frac{\pi\,(i+1)}{k+2}\right)}{\sin\left(\frac{\pi\,i}{k+2}\right) \sin\left(\frac{\pi\,(i+2)}{k+2}\right)} - 1 . \quad (4.155)$$

Having determined the solutions of the constant TBA equations (4.151) and (4.154) one can proceed via the standard TBA calculation as presented in 4.2.2, see also [23, 57, 96], and compute the central charges from (4.146), (4.147) and express them in terms of Roger's dilogarithm function (4.51)

$$c_{UV} = \lim_{r'\to 0} c_{\rm o}(r') = \frac{6}{\pi^2}\sum_{i=1}^{k-1}\left[2\mathcal{L}\left(\frac{x_i}{1+x_i}\right) - \mathcal{L}\left(\frac{\hat{x}_i}{1+\hat{x}_i}\right)\right] , \tag{4.156}$$

$$\hat{c}_{UV} = \lim_{r'\to 0} \hat{c}_{\rm o}(r') = \frac{6}{\pi^2}\sum_{a=1}^{k-1}\mathcal{L}\left(\frac{\hat{x}_i}{1+\hat{x}_i}\right) . \tag{4.157}$$

Using the non-trivial identities

$$\frac{6}{\pi^2}\sum_{i=1}^{k-1}\mathcal{L}\left(\frac{x_i}{1+x_i}\right) = 3\,\frac{k-1}{k+3} \quad \text{and} \quad \frac{6}{\pi^2}\sum_{i=1}^{k-1}\mathcal{L}\left(\frac{\hat{x}_i}{1+\hat{x}_i}\right) = 2\,\frac{k-1}{k+2} \tag{4.158}$$

found in [113] and [107], we finally end up with [56]

$$c_{UV} = \frac{(k-1)\,(4k+6)}{(k+3)\,(k+2)} \qquad \text{and} \qquad \hat{c}_{UV} = 2\,\frac{k-1}{k+2} . \tag{4.159}$$

For the reasons mentioned above $\hat{c}_{UV}$ coincides with the effective central charge obtained from $su(k)$ minimal ATFT describing parafermions [48] in the conformal limit. Notice that $c_{UV}$ corresponds to the coset $(su(3)_k/u(1)^2)/(su(2)_k/u(1))$.

The discussion of the infrared limit may be carried out completely analogous to the one performed for the UV limit. The only difference is that in case of the system (4.142) the constant TBA equations (4.151) drop out because in the central region $-\ln r' \ll \theta \ll \ln r'$ the free energy terms becomes dominant when $r' \to \infty$. Thus, in the infrared regime the central charges of both systems coincide with $\hat{c}_{UV}$,

$$c_{IR} = \lim_{r'\to\infty} c_{\rm o}(r') = \hat{c}_{IR} = \lim_{r'\to\infty} \hat{c}_{\rm o}(r') = 2\,\frac{k-1}{k+2} . \tag{4.160}$$

In summary, collecting the results (4.159) and (4.160), we can express equation (4.149) explicitly in terms of the level $k$ [56],

$$c(r, M_{\tilde{k}}^{\tilde{c}}) \approx \begin{cases} 4\,\frac{k-1}{k+2} , & \text{for} \quad 1 \ll \frac{2}{r} \ll M_{\tilde{k}}^{\tilde{c}} \\ 6\,\frac{k-1}{k+3} , & \text{for} \quad M_{\tilde{k}}^{\tilde{c}} \ll \frac{2}{r} \end{cases} . \tag{4.161}$$

We have replaced the limits in (4.149) by mass scales in order to exhibit the underlying physical picture. Here $M_{\tilde{k}}^{\tilde{c}}$ is the smallest mass of an unstable bound state which may be formed in the process $(i,a)+(j,b) \to (\tilde{k},\tilde{c})$ for $\tilde{A}_{ab} \neq 0, 2$. We also used that the Breit-Wigner formula (4.121) implies that $M_{\tilde{k}}^{\tilde{c}} \sim e^{\sigma/2}$ for large positive $\sigma$.

First one should note that in the deep UV limit we obtain the same effective central charge as in Subsection 4.4.3 when discussing the general case, albeit in a quite different manner. On the mathematical side this implies some non-trivial identities

for Rogers dilogarithm and on the physical (4.161) exhibits a more detailed behaviour than the analysis in Subsection 4.4.3.

**Summary**. *In the first regime of (4.161) the lower limit indicates the onset of the lightest stable soliton in the two copies of complex sine-Gordon model. The unstable particles are on an energy scale much larger than the temperature of the system. Thus, the dynamical interaction between solitons of different colours is "frozen" and we end up with two copies of the* $su(2)_k/u(1)$ *coset which do not interact with each other. As soon as the parameter* $r$ *reaches the energy scale of the unstable solitons with mass* $M_{\tilde{k}}^{\tilde{c}}$*, the solitons of different colours start to interact, being now enabled to form bound states. This interaction breaks parity and forces the system to approach the* $su(3)_k/u(1)^2$ *coset model with central charge given by the formula in (4.118).*

The case when $\sigma$ tends to infinity is special, since then the energy scale on which unstable particles are formed is never reached. Therefore, one needs to pay attention to the order in which the limits in $r, \sigma$ are taken, we have [56]

$$4\,\frac{k-1}{k+2} = \lim_{r\to 0}\lim_{\sigma\to\infty} c(r,\sigma) \neq \lim_{\sigma\to\infty}\lim_{r\to 0} c(r,\sigma) = 6\,\frac{k-1}{k+3}\,. \tag{4.162}$$

One might enforce an additional step in the scaling function by exploiting the fact that the mass ratio $m_1/m_2$ is not fixed. So it may be chosen to be very large or very small. This amounts to decouple the TBA systems for solitons with different colour by shifting one system to the infrared with respect to the scale parameter $r$. The plateau then has an approximate width of $\sim \ln|m_1/m_2|$ (see Figure 4.7). However, as soon as $r$ becomes small enough the picture we discussed for $m_1 \sim m_2$ is recovered.

### Restoring parity and eliminating the resonances

In this subsection we are going to investigate the special limit $\sigma \to 0$, which is equivalent to choosing the vector couplings $\Lambda_\pm$ in (4.117) parallel or anti-parallel. For the classical theory it was pointed out in [47] that only then the equations of motion are parity invariant. Also the TBA-equations become parity invariant in the absence of the resonance shifts, albeit the S-matrix still violates it through the phase factors in (4.120). Since in the UV regime a small difference in the masses $m_1$ and $m_2$ does not effect the outcome of the analysis, we can restrict ourselves to the special situation $m_1 = m_2$, in which case we obtain two identical copies of the system

$$\epsilon_i(\theta) + \sum_{j=1}^{k-1}(\phi_{ij} + \psi_{ij}) * L_j(\theta) = r\,M_i\cosh\theta\,. \tag{4.163}$$

Then we have $\epsilon_i(\theta) = \epsilon_i^{(1)}(\theta) = \epsilon_i^{(2)}(\theta)$, $M_i = M_i^{(1)} = M_i^{(2)}$ and the scaling function is given by the expression

$$c(r,\sigma=0) = \frac{12\,r}{\pi^2}\sum_{i=1}^{k-1} M_i \int_0^\infty d\theta\; L_i(\theta)\cosh\theta\,. \tag{4.164}$$

The factor two in comparison with (4.128) takes the two copies for $a = 1, 2$ into account. The discussion of the high-energy limit follows now the standard arguments similar to the one of the preceding subsection and as in 4.2.2. Instead of shifting by the resonance parameter $\sigma$, one now shifts the TBA equations by $\ln \frac{r}{2}$. The constant TBA equation which determines the UV central charge then just coincides with (4.151). We therefore obtain [56]

$$\lim_{r\to 0}\lim_{\sigma\to 0} c(r,\sigma) = \frac{12}{\pi^2}\sum_{i=1}^{k-1}\mathcal{L}\left(\frac{x_i}{1+x_i}\right) = 6\,\frac{k-1}{k+3}\,. \tag{4.165}$$

Thus, again we recover the coset central charge (4.118) for $\tilde{\mathfrak{g}} = su(3)$, but this time without breaking parity in the TBA equations. This is in agreement with the results of Subsection 4.4.3, which showed that we can obtain this limit for any finite value of the resonance parameter $\sigma$.

### Universal TBA equations and Y-systems

Before we turn to the discussion of specific examples for definite values of the level $k$, we turn to the alternative formulation of the TBA equations (4.126) in terms of a single integral kernel and $Y$-systems analogous to the discussion of affine Toda models in Section 4.3.2. In the present context this variant of the TBA equations is of particular advantage when one wants to discuss properties of the model and keep the level $k$ generic. By means of the convolution theorem and the Fourier transforms of the TBA kernels $\phi$ and $\psi$, which can be read off directly from (4.139) and (4.140), one derives the set of integral equations [56]

$$\epsilon_i^a(\theta) + \Omega_k * L_i^b(\theta-\sigma_{ba}) = \sum_{j=1}^{k-1} I_{ij}^{su(k)}\,\Omega_k * (\epsilon_j^a + L_j^a)(\theta)\,, \quad a\neq b\,. \tag{4.166}$$

We recall that $I^{su(k)} = 2 - A^{su(k)}$ denotes the incidence matrix of $su(k)$ and the kernel $\Omega_k$ is found to be

$$\Omega_k(\theta) = \frac{k/2}{\cosh(k\theta/2)}\,. \tag{4.167}$$

The on-shell energies have dropped out because of the crucial relation

$$\sum_{j=1}^{k-1} I_{ij} M_j^a = 2\cos\tfrac{\pi}{k}\, M_i^a\,, \tag{4.168}$$

which is a property of the mass spectrum inherited from affine Toda field theory, compare (3.44) in Chapter 3. Even though the explicit dependence on the scale parameter has been lost, it is recovered from the asymptotic condition

$$\epsilon_i^a(\theta) \underset{\theta\to\pm\infty}{\longrightarrow} r M_i^a\, e^{\pm\theta}\,. \tag{4.169}$$

The integral kernel present in (4.166) has now a very simple form and the $k$ dependence is easily read off.

Closely related to the TBA equations in the form (4.166) are the functional relations also referred to as $Y$-systems which we already encountered in context of ATFT, compare in particular (4.104). Using complex continuation and defining the quantity $Y_i^a(\theta) = \exp(-\epsilon_i^a(\theta))$ the integral equations are replaced by [56]

$$Y_i^a(\theta + \tfrac{i\pi}{k}) Y_i^a(\theta - \tfrac{i\pi}{k}) = \big[1 + Y_i^b(\theta - \sigma_{ba})\big] \prod_{j=1}^{k-1} \big[1 + Y_j^a(\theta)^{-1}\big]^{-I_{ij}}, \quad a \neq b\,. \quad (4.170)$$

The $Y$-functions are assumed to be well defined on the whole complex rapidity plane where they give rise to entire functions [50]. As we already saw in Section 4.3 these systems are useful in many aspects, for instance they may be exploited in order to establish periodicities in the $Y$-functions, which in turn can be used to provide approximate analytical solutions of the TBA-equations. The scaling function can be expanded in integer multiples of the period which is directly linked to the dimension of the perturbing operator.

Noting that the asymptotic behaviour of the $Y$-functions is $\lim_{\theta\to\infty} Y_i^a(\theta) \sim e^{-rM_i^a \cosh\theta}$, we recover for $\sigma \to \infty$ the $Y$-systems of the $su(k)$-minimal ATFT derived originally in [50]. In this case the $Y$-systems were shown to have a period related to the dimension of the perturbing operator (see (4.191)). We found some explicit periods for generic values of the resonance parameter $\sigma$ as we discuss in the next section for some concrete examples.

### Explicit examples

In this section we support our analytical discussion with some numerical results and in particular justify various assumptions for which we have no rigorous analytical argument so far. We numerically iterate the TBA-equations (4.126) and have to choose specific values for the level $k$ for this purpose. As we pointed out in the introduction, quantum integrability has only been established for the choice $k > h$. Since the perturbation is relevant also for smaller values of $k$ and in addition the S-matrix makes remains well defined, it will be interesting to see whether the TBA-analysis in the case of $su(3)_k$ will exhibit any qualitative differences for $k \leq 3$ and $k > 3$. From our examples for the values $k = 2, 3, 4$ the answer to this question is that there is no apparent difference. For all cases we find the staircase pattern of the scaling function predicted in the preceding section as the values of $\sigma$ and $x$ sweep through the different regimes. Besides presenting numerical plots we also discuss some peculiarities of the systems at hand. We provide the massless TBA equations (4.142) with their UV and IR central charges and state the $Y$-systems together with their periodicities. Finally, we also comment on the classical or weak coupling limit $k \to \infty$.

**The su(3)$_2$-HSG model** This is the simplest model for the $su(3)_k$ case, since it contains only the two self-conjugate solitons (1,1) and (1,2). The formation of stable particles via fusing is not possible and the only non-trivial S-matrix elements are

those between particles of different colour

$$S_{11}^{11} = S_{11}^{22} = -1, \quad S_{11}^{12}(\theta - \sigma) = -S_{11}^{21}(\theta + \sigma) = \tanh \frac{1}{2}\left(\theta - i\frac{\pi}{2}\right) . \tag{4.171}$$

Here we have chosen $\varepsilon_{12} = -\varepsilon_{21} = 1$ in (4.120) and used that the inverse Cartan matrix of $su(2)$ is just $1/2$. This scattering matrix may be related to various matrices which occurred before in the literature. First of all when performing the limit $\sigma \to \infty$ the scattering involving different colours becomes trivial and the systems consists of two free fermions leading to the central charge $c = 1$. Taking instead the limit $\sigma \to 0$ the expressions in (4.171) coincide precisely with a matrix which describes the scattering of massless "Goldstone fermions (Goldstinos)" discussed in [57]. Apart from a phase factor $\sqrt{-1}$, the matrix $S_{11}^{21}(\theta)|_{\sigma=0}$ was also proposed to describe the scattering of a massive particle [115]. Having only one colour available one is not able to set up the usual crossing and unitarity equations and in [115] the authors therefore resorted to the concept of "anti-crossing". As our analysis shows this may be consistently overcome by breaking the parity invariance. The TBA-analysis is summarized as follows [56],

$$\begin{aligned} \text{unstable particle formation} \quad &: \qquad c_{su(3)_2} = \frac{6}{5} = c_{UV} + \hat{c}_{UV} = \frac{7}{10} + \frac{1}{2} \\ \text{no unstable particle formation} \quad &: \qquad 2c_{su(2)_2} = 1 = c_{IR} + \hat{c}_{IR} = \frac{1}{2} + \frac{1}{2} \ . \end{aligned}$$

It is interesting to note that the flow from the tricritical Ising to the Ising model which was investigated in [57], emerges as a subsystem in the HSG-model in the form $c_{UV} \to c_{IR}$. This suggests that we could alternatively also view the HSG-system as consisting out of a massive and a massless fermion, where the former is described by (4.146),(4.142) and the latter by (4.147),(4.143), respectively.

Our numerical investigations of the model match the analytical discussion and justify various assumptions in retrospect. Figure 4.6 exhibits various plots of the $L$-functions in the different regimes. We observe that for $\ln \frac{2}{r} < \sigma/2$, $\sigma \neq 0$ the solutions are symmetric in the rapidity variable, since the contribution of the $\psi$ kernels responsible for parity violation is negligible. The solution displayed is just the free fermion $L$-function, $L^a(\theta) = \ln(1 + e^{-rM^a \cosh\theta})$. Advancing further into the ultraviolet regime, we observe that the solutions $L^a$ cease to be symmetric signaling the violation of parity invariance and the formation of unstable bound states. The second plateau is then formed, which will extend beyond $\theta = 0$ for the deep ultraviolet (see Figure 4.6). The staircase pattern of the scaling function is displayed in Figure 4.6 for the different cases discussed in the previous section. We observe always the value $6/5$ in the deep ultraviolet regime, but depending on the value of the resonance parameter and the mass ratio it may be reached sooner or later. The plateau at 1 corresponds to the situation when the unstable particles can not be formed yet and we only have two copies of $su(3)_2$ which do not interact. Choosing the mass ratios in the two copies to be very different, we can also "switch them on" individually as the plateau at $1/2$ indicates.

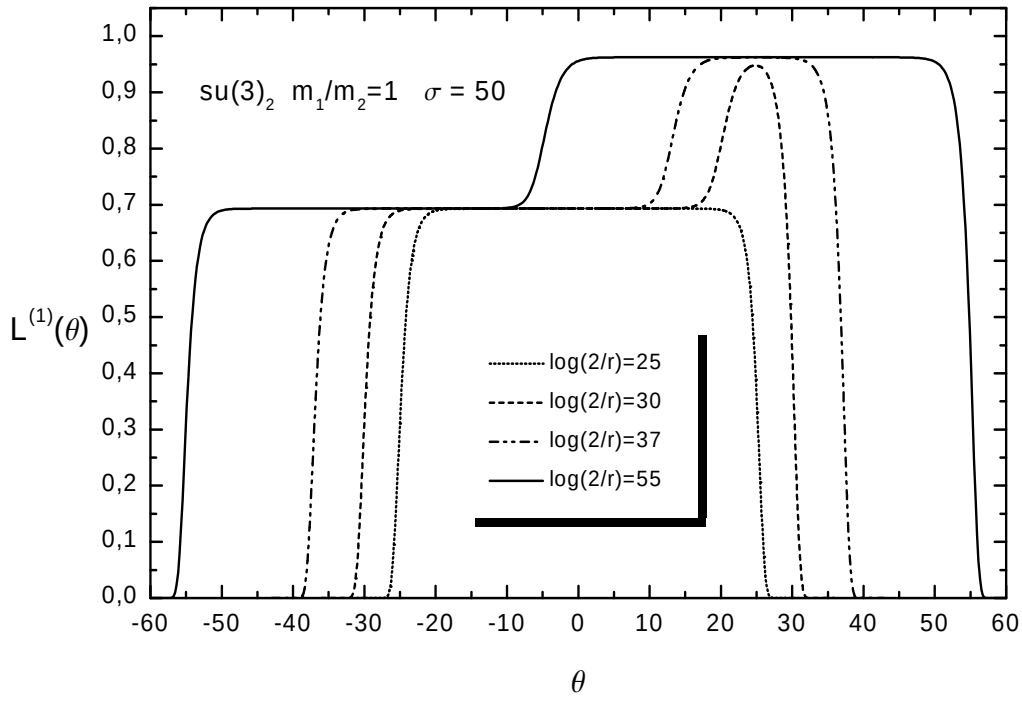


Figure 4.6: $L$-function for the $su(3)_2$ HSG model at various values of the scaling parameter $r$.

**The $\mathbf{su(3)_3}$-HSG model** This model consists of two pairs of solitons $\overline{(1,1)} = (2,1)$ and $\overline{(1,2)} = (2,2)$. When the soliton $(1,a)$ scatters with itself it may form $(2,a)$ for $a = 1,2$ as a bound state. The two-particle S-matrix elements in the general block representation (3.97) of Chapter 3 read

$$S^{ab}(\theta - \sigma_{ab}) = \begin{pmatrix} [1,\tilde{I}_{ab}]_{\theta,ab}^{\tilde{A}_{ab}} & [2,\tilde{I}_{ab}]_{\theta,ab}^{\tilde{A}_{ab}} \\ [2,\tilde{I}_{ab}]_{\theta,ab}^{\tilde{A}_{ab}} & [1,\tilde{I}_{ab}]_{\theta,ab}^{\tilde{A}_{ab}} \end{pmatrix} \quad \text{with} \quad \tilde{A} = \begin{pmatrix} 2 & -1 \\ -1 & 2 \end{pmatrix} . \tag{4.172}$$

Since soliton and anti-soliton of the same colour obey the same TBA equations we can exploit charge conjugation symmetry to identify $\epsilon^a(\theta) := \epsilon_1^a(\theta) = \epsilon_2^a(\theta)$ leading to the reduced set of equations

$$\epsilon^a(\theta) + \varphi * L^a(\theta) - \varphi * L^b(\theta - \sigma_{ba}) = rM^a \cosh\theta, \quad \varphi(\theta) = -\frac{4\sqrt{3}\cosh\theta}{1 + 2\cosh 2\theta} . \tag{4.173}$$

The corresponding scaling function therefore acquires a factor two,

$$c(r,\sigma) = \frac{6\,r}{\pi^2} \sum_{a=1,2} M^a \int d\theta \, \cosh\theta \, L^a(\theta) . \tag{4.174}$$

This system exhibits remarkable symmetry properties. We consider first the situation $\sigma = 0$ with $m_1 = m_2$ and note that the system becomes free in this case

$$M^{(1)} = M^{(2)} =: M \;\Rightarrow\; \epsilon^{(1)}(\theta) = \epsilon^{(2)}(\theta) = rM\cosh\theta . \tag{4.175}$$

meaning that the theory falls apart into four free fermions whose central charges add up to the expected coset central charge of $c = 2$. Also for unequal masses $m_1 \neq m_2$ the system develops towards the free fermion theory for high energies when the difference becomes negligible. This is also seen numerically.

For $\sigma \neq 0$ the two copies of the minimal $A_2$-ATFT or equivalently the scaling Potts model start to interact. The outcome of the TBA-analysis in that case is summarized as [56]

$$\begin{aligned} \text{unstable particle formation} \quad &: \qquad c_{su(3)_3} = 2 = c_{UV} + \hat{c}_{UV} = \frac{6}{5} + \frac{4}{5} \\ \text{no unstable particle formation} \quad &: \qquad 2c_{su(2)_3} = \frac{8}{5} = c_{IR} + \hat{c}_{IR} = \frac{4}{5} + \frac{4}{5} \ . \end{aligned}$$

As discussed in the previous case for $k = 2$ the $L$-functions develop an additional plateau after passing the point $\ln \frac{2}{r} = \sigma/2$. This plateau lies at $\ln 2$ which is the free fermion value signaling that the system contains a free fermion contribution in the UV limit as soon as the interaction between the solitons of different colours becomes relevant. Figure 4.7 exhibits the same behaviour as the previous case, we clearly observe the plateau at 8/5 corresponding to the two non-interacting copies of the minimal $A_2$-ATFT. As soon as the energy scale of the unstable particles is reached the scaling function approaches the correct value of $c_{su(3)_3} = 2$.

The Y-systems (4.170) for $k = 3$ read

$$Y^a_{1,2}\left(\theta + i\frac{\pi}{3}\right) Y^a_{1,2}\left(\theta - i\frac{\pi}{3}\right) = Y^a_{1,2}(\theta)\, \frac{1 + Y^b_{1,2}(\theta + \sigma_{ab})}{1 + Y^a_{1,2}(\theta)} \quad a, b = 1, 2,\ a \neq b\ . \quad (4.176)$$

Once again we may derive a periodicity

$$Y^a_{1,2}(\theta + 2\pi i + \sigma_{ba}) = Y^b_{1,2}(\theta) \quad (4.177)$$

by making the suitable shifts in (4.176) and subsequent iteration.

**The su(3)$_4$-HSG model** This model involves 6 solitons, two of which are self-conjugate $\overline{(2,1)} = (2,1)$, $\overline{(2,2)} = (2,2)$ and two conjugate pairs $\overline{(1,1)} = (3,1)$, $\overline{(1,2)} = (3,2)$. The corresponding two-particle S-matrix elements are obtained from the general formulae (3.97)

$$S^{ab}(\theta - \sigma_{ba}) = \begin{pmatrix} [1, \tilde{I}_{ab}]^{\tilde{A}_{ab}}_{\theta,ab} & [2, \tilde{I}_{ab}]^{\tilde{A}_{ab}}_{\theta,ab} & [3, \tilde{I}_{ab}]^{\tilde{A}_{ab}}_{\theta,ab} \\ [2, \tilde{I}_{ab}]^{\tilde{A}_{ab}}_{\theta,ab} & [3, \tilde{I}_{ab}]^{\tilde{A}_{ab}}_{\theta,ab} [1, \tilde{I}_{ab}]^{\tilde{A}_{ab}}_{\theta,ab} & [2, \tilde{I}_{ab}]^{\tilde{A}_{ab}}_{\theta,ab} \\ [3, \tilde{I}_{ab}]^{\tilde{A}_{ab}}_{\theta,ab} & [2, \tilde{I}_{ab}]^{\tilde{A}_{ab}}_{\theta,ab} & [1, \tilde{I}_{ab}]^{\tilde{A}_{ab}}_{\theta,ab} \end{pmatrix} \quad (4.178)$$

In this case the numerics becomes more involved but for the special case $m_1 = m_2$ one can reduce the set of six coupled integral equations to only two by exploiting the symmetry $L^{(1)}_i(\theta) = L^{(2)}_i(-\theta)$ and using charge conjugation symmetry, $L^a_1(\theta) = L^a_3(\theta)$. The numerical outcomes, shown in Figure 4.7 again match, with the analytic

expectations (4.161) and yield for $\ln \frac{2}{r} > \sigma/2$ the coset central charge of 18/7. In summary we obtain [56]

$$\begin{aligned} \text{unstable particle formation} \quad &: \qquad c_{su(3)_4} = \frac{18}{7} = c_{UV} + \hat{c}_{UV} = \frac{11}{7} + 1 \\ \text{no unstable particle formation} \quad &: \qquad 2c_{su(2)_4} = 2 = c_{IR} + \hat{c}_{IR} = 1 + 1 \ , \end{aligned}$$

which matches precisely the numerical outcome in Figure 4.7, with the same physical interpretation as already provided in the previous two examples.

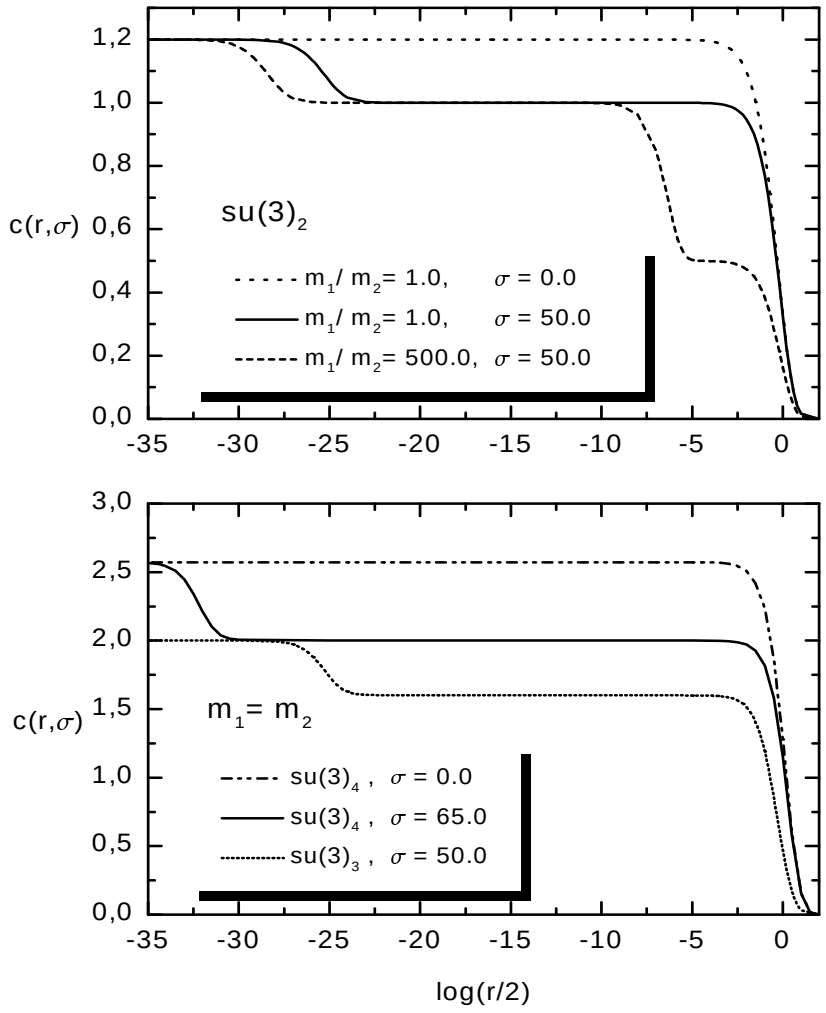


Figure 4.7: Scaling function for the $su(3)_k$ HSG models at level $k = 2, 3, 4$ with various choices of the parameters.

**The semi-classical limit** $k \to \infty$ As last example we carry out the limit $k \to \infty$, which is of special physical interest, since it may be identified with the weak coupling

or equivalently the classical limit, as is seen from the relation $\hbar\beta^2 = 1/k + O(1/k^2)$. To illustrate this equivalence we have temporarily re-introduced Planck's constant. It is clear from the TBA-equations that this limit may not be taken in a straightforward manner. However, we can take it in two steps, first for the on-shell energies and the kernels and finally for the sum over all particle contributions. The on-shell energies are easily computed by noting that the mass spectrum becomes equally spaced for $k \to \infty$

$$M_i^a = M_{k-i}^a = \frac{m_a}{\pi\beta^2} \sin\frac{\pi\, i}{k} \approx i\, m_a \qquad , \quad i < \frac{k}{2}\,. \tag{4.179}$$

For the TBA-kernels the limit may also be taken easily from their integral representations

$$\phi_{ij}(\theta) \underset{k\to\infty}{\longrightarrow} 2\pi\,\delta(\theta)\,\left(\delta_{ij} - 2\left(A_{ij}^{su(k)}\right)^{-1}\right) \quad \text{and} \quad \psi_{ij}(\theta) \underset{k\to\infty}{\longrightarrow} 2\pi\,\delta(\theta)\,\left(A_{ij}^{su(k)}\right)^{-1}, \tag{4.180}$$

when employing the usual integral representation of the delta-function. Inserting these quantities into the TBA-equations yields

$$\epsilon_i^a(\theta) \approx r\, i\, m_a \cosh\theta - \sum_{j=1}^{k-1}\left(\delta_{ij} - 2\left(A_{ij}^{su(k)}\right)^{-1}\right) L_j^a(\theta) - \sum_{j=1}^{k-1}\left(A_{ij}^{su(k)}\right)^{-1} L_j^b(\theta-\sigma)\,. \tag{4.181}$$

We now have to solve these equations for the pseudo-energies. In principle, we could proceed in the same way as in the case for finite $k$ by doing the appropriate shifts in the rapidity. However, we will be content here to discuss the cases $\sigma \to 0$ and $\sigma \to \infty$, which as follows from our previous discussion correspond to the situation of restored parity invariance and two non-interacting copies of the minimal ATFT, respectively. The related constant TBA-equations (4.152) and (4.154) become

$$\sigma \to \infty:\ \hat{x}_j \underset{k\to\infty}{\longrightarrow} \frac{(j+1)^2}{j(j+2)} - 1 \quad \text{and} \quad \sigma \to 0:\ x_j \underset{k\to\infty}{\longrightarrow} \frac{(j+1)(j+2)}{j(j+3)} - 1\,. \tag{4.182}$$

The other information we may exploit about the solutions of (4.181) is that for large rapidities they tend asymptotically to the free solution, meaning that

$$\sigma \to 0, \infty\ :\qquad L_j^a(\theta) \underset{\theta\to\pm\infty}{\longrightarrow} \ln(1 + e^{-r\, j\, m_a \cosh\theta})\,. \tag{4.183}$$

We are left with the task to seek functions which interpolate between the properties (4.182) and (4.183). Inspired by the analysis in [114] we take these functions to be

$$\sigma \ \to\ \infty: \quad L_j^a(\theta) = \ln\left[\frac{\sinh^2\left(\frac{j+1}{2}\, r m_a \cosh\theta\right)}{\sinh\left(\frac{j}{2}\, r m_a \cosh\theta\right)\sinh\left(\frac{j+2}{2}\, r m_a \cosh\theta\right)}\right] \tag{4.184}$$

$$\sigma \ \to\ 0: \quad L_j^a(\theta) = \ln\left[\frac{\sinh\left(\frac{j+1}{2}\, r m_a \cosh\theta\right)\sinh\left(\frac{j+2}{2}\, r m_a \cosh\theta\right)}{\sinh\left(\frac{j}{2}\, r m_a \cosh\theta\right)\sinh\left(\frac{j+3}{2}\, r m_a \cosh\theta\right)}\right]. \tag{4.185}$$

The expression (4.184) coincides with the expressions discussed in the context of the breather spectrum of the sine-Gordon model [114] and (4.185) is constructed in

analogy. We are now equipped to compute the scaling function in the limit $k \to \infty$,

$$c(r,\sigma) = \lim_{k\to\infty} \frac{3\,r}{\pi^2} \sum_{a=1}^{2} \int d\theta\, \cosh\theta \sum_{i=1}^{k-1} M_i^a\, L_i^a(\theta)\ . \tag{4.186}$$

Using (4.179), (4.184) and (4.185) the sum over the main quantum number may be computed directly by expanding the logarithm. We obtain for $k \to \infty$ [56]

$$c(r)|_{\sigma=\infty} \;=\; \frac{-6r}{\pi^2} \sum_{a=1}^{2} \int d\theta\, m_a \cosh\theta \ln\left(1 - e^{-r\, m_a \cosh\theta}\right) \tag{4.187}$$

$$c(r)|_{\sigma=0} \;=\; \frac{-6\,r}{\pi^2} \sum_{a=1}^{2} \int d\theta\ m_a \cosh\theta [\ln\left(1-e^{-r\, m_a \cosh\theta}\right) + \ln(1-e^{-r\, 2m_a \cosh\theta})] \tag{4.188}$$

Here we have acquired an additional factor of 2, resulting from the identification of particles and anti-particles which is needed when one linearizes the masses in (4.179). Taking now the limit $r \to 0$ we obtain [56]

$$\text{no unstable particle formation} \;:\quad 2\, c_{su(2)_\infty} = 4 \tag{4.189}$$

$$\text{unstable particle formation} \;:\quad c_{su(3)_\infty} = 6\ . \tag{4.190}$$

The results (4.187), (4.189) and (4.188), (4.190) allow a nice physical interpretation. We notice that for the case $\sigma \to \infty$ we obtain four times the scaling function of a free boson. This means in the classical limit we obtain twice the contribution of the non-interacting copies of $SU(2)_\infty/U(1)$, whose particle content reduces to two free bosons each of them contributing 1 to the effective central charge which is in agreement with (4.118). For the case $\sigma \to 0$ we obtain the same contribution, but in addition the one from the unstable particles, which are two free bosons of mass $2m_a$. This is also in agreement with (4.118).

Finally it is interesting to observe that when taking the resonance poles to be $\theta_R = \sigma - i\pi/k$ the semi-classical limit taken in the Breit-Wigner formula (4.121) leads to $m_{\tilde{c}}^2 = (m_a + m_b)^2$. On the other hand (4.188) seems to suggest that $m_{\tilde{c}} = 2m_a$, which implies that the mass scales should be the same. However, since our analysis is mainly based on exploiting the asymptotics we have to be cautious about this conclusion.

We can summarize that the main outcome of our the TBA-analysis indeed confirms the consistency of the scattering matrix proposed in [40]. In the deep ultraviolet limit we recover the $\tilde{\mathfrak{g}}_k/u(1)^{\tilde{n}}$-coset central charge for any value of the $2\tilde{n}-1$ free parameters entering the S-matrix, including the choice when the resonance parameters vanish and parity invariance is restored on the level of the TBA-equations. This is in contrast to the properties of the S-matrix, which is still not parity invariant due to the occurrence of the phase factors, which are required to close the bootstrap equations, compare Section 3.3. However, they do not contribute to our TBA-analysis, which means that so far we can not make any definite statement concerning the necessity of the parity breaking in the quantum theory of HSG theories

(4.117), since the same value for the central charge is recovered irrespective of the value of the $\sigma$'s. The underlying physical behaviour is, however, quite different as our numerical analysis demonstrates. For vanishing resonance parameter the deep ultraviolet coset central charge is reached straight away, whereas for non-trivial resonance parameter one passes the different regions in the energy scale. Also the choice of different mass scales leads to a theory with a different physical content, but still possessing the same central charge.

To settle this issue, it would therefore be highly desirable to carry out the series expansion of the scaling function in $r$ analogous to the discussion in [23] and determine the dimension $d_\Phi$ of the perturbing operator. It will be useful for this to know the periodicities of the Y-functions. We conjecture that they will be [56]

$$Y_i^a\left(\theta + i\pi(1-d_\Phi)^{-1} + \sigma_{ba}\right) = Y_{\bar{\imath}}^b(\theta), \tag{4.191}$$

which is confirmed by our $su(3)$-examples for various levels. For vanishing resonance parameter and the choice $k = 2$, this behaviour coincides with the one obtained in [50]. This means the form in (4.191) is of a very universal nature beyond the models discussed here.

We also observe from our $su(3)$-example that the different regions, i.e. $k > \tilde{h}$ and $k \leq \tilde{h}$, for which quantum integrability was shown and for which not, respectively, do not show up in our analysis. It would be very interesting to extend the case-by-case analysis to other algebras. The first challenge in these cases is to incorporate the different resonance parameters.

## 4.5 The central charge calculation for $\mathfrak{g}|\tilde{\mathfrak{g}}$ theories

This section is devoted to an extension of the previous TBA analysis for the HSG models to all $\mathfrak{g}|\tilde{\mathfrak{g}}$-theories as defined in Chapter 3. This means, the two algebras involved are now arbitrary but simply-laced. Since this gives a total of $ADE \times ADE$ possibilities we restrict ourselves to the central charge calculation analogous to the one performed for HSG models in Section 4.4.3 but without resonance poles, i.e. we set $\sigma = 0$. Emphasis in the following considerations will be given to the powerful Lie algebraic structure behind these theories. The latter will lead to a generic formula for the central charge and suggests an intimate relation between the models $\mathfrak{g}|\tilde{\mathfrak{g}}$ and $\tilde{\mathfrak{g}}|\mathfrak{g}$ in the UV regime via the constant TBA equations encountered before.

Similar to the discussion of the previous section TBA-equations with Fermi statistics and absence of resonances read

$$rm_i^a \cosh\theta = \varepsilon_i^a(\theta) + \sum_{b=1}^{\tilde{n}} \sum_{j=1}^{n} \int_{-\infty}^{\infty} d\theta' \varphi_{ij}^{ab}(\theta-\theta') \ln\left(1 + e^{-\varepsilon_b^j(\theta')}\right) \tag{4.192}$$

where $r$ is again the scale parameter, $m_i^a$ the mass of the particle $(i,a)$, $\varepsilon_i^a(\theta)$ the pseudo-energies and kernels are obtained from (3.94)

$$\varphi_{ij}^{ab}(\theta) = \int_{-\infty}^{\infty} dt \left[\delta_{ab}\delta_{ij} - \left(2\cosh\frac{\pi t}{h} - \tilde{I}\right)_{ab} \left(2\cosh\frac{\pi t}{h} - I\right)_{ij}^{-1}\right] e^{-it\theta} \ . \tag{4.193}$$

Note that in contrast to the HSG models both incidence matrices may now belong to arbitrary simply-laced algebras. The effective central charge $c_{\text{eff}} = c - 24\Delta_0$ of the underlying ultraviolet conformal field theory will now be calculated by the standard procedure (compare 4.2.2) under the assumption that the solutions of the TBA-equations develop the same "plateau behaviour" as we encountered for the HSG models. Notice that also for the class of scaling or minimal ATFT models [23] this behaviour holds true and that the latter are obtained by setting $\tilde{\mathfrak{g}} = A_1$. Thus, one may again approximate $\varepsilon_i^a(\theta) = \varepsilon_i^a = const$ in the large region $\ln \frac{r}{2} \ll \theta \ll \ln \frac{2}{r}$ when $r$ is small. By the same standard TBA arguments used also in the discussion of the previous section it follows that the effective central charge is expressible as

$$c_{\text{eff}} = \frac{6}{\pi^2} \sum_{a=1}^{\tilde{n}} \sum_{i=1}^{n} \mathcal{L}\left(\frac{x_i^a}{1+x_i^a}\right) \tag{4.194}$$

with $\mathcal{L}(x)$ denoting Rogers dilogarithm and where the $x_i^a = \exp(-\varepsilon_i^a)$ are obtained as solutions from the constant TBA-equations in the form

$$x_i^a = \prod_{j=1}^{n} \prod_{b=1}^{\tilde{n}} (1 + x_j^b)^{N_{ij}^{ab}} \ . \tag{4.195}$$

The matrix $N_{ij}^{ab}$ is defined analogously to (4.134) via the asymptotic behaviour of the scattering matrix which for the more general case at hand reads [38]

$$N_{ij}^{ab} = \frac{1}{2\pi} \int_{-\infty}^{\infty} d\theta \ \varphi_{ij}^{ab}(\theta) = \ \delta_{ab}\delta_{ij} - A_{ij}^{-1} \tilde{A}_{ab} \, . \tag{4.196}$$

In regard to finding explicit solutions for the set of coupled equations (4.195) and to exhibit the Lie algebraic structure present, it turns out to be convenient to introduce new variables because they may be related to Weyl characters of the Lie algebra $\mathfrak{g}$ or $\tilde{\mathfrak{g}}$. Following [108, 109] we define

$$Q_i^a = \prod_{j=1}^{n} (1 + x_j^a)^{A_{ij}^{-1}} \qquad \Leftrightarrow \qquad x_i^a = \prod_{j=1}^{n} \left(Q_j^a\right)^{A_{ij}} - 1 \tag{4.197}$$

such that the constant TBA-equations (4.195) acquire the more symmetric form

$$\prod_{j=1}^{n} \left(Q_j^a\right)^{I_{ij}} + \prod_{b=1}^{\tilde{n}} \left(Q_i^b\right)^{\tilde{I}_{ab}} = \left(Q_i^a\right)^2 \tag{4.198}$$

exhibiting a "dual" relation between the two algebras. The effective central charge (4.194) is then expressible in various equivalent ways [38]

$$c_{\text{eff}}^{\mathfrak{g}|\tilde{\mathfrak{g}}} = \tfrac{6}{\pi^2} \sum_{i=1}^{n} \sum_{a=1}^{\tilde{n}} \mathcal{L}\left(1 - \prod_{j=1}^{n} \left(Q_j^a\right)^{-A_{ij}}\right) = n\tilde{n} - \tfrac{6}{\pi^2} \sum_{i=1}^{n} \sum_{a=1}^{\tilde{n}} \mathcal{L}\left(\prod_{b=1}^{\tilde{n}} \left(Q_i^b\right)^{-\tilde{A}_{ab}}\right) \tag{4.199}$$

$$= n\tilde{n} - \tfrac{6}{\pi^2} \sum_{i=1}^{n} \sum_{a=1}^{\tilde{n}} \mathcal{L}\left(\prod_{j=1}^{n} \left(Q_j^a\right)^{-A_{ij}}\right) = \tfrac{6}{\pi^2} \sum_{a=1}^{\tilde{n}} \sum_{i=1}^{n} \mathcal{L}\left(1 - \prod_{b=1}^{\tilde{n}} \left(Q_i^b\right)^{-\tilde{A}_{ab}}\right) \tag{4.200}$$

where we used the well-known identity $\mathcal{L}(x) + \mathcal{L}(1-x) = \pi^2/6$, see e.g. [113]. It is also clear that having solved the equations (4.198) for the case $\mathfrak{g}|\tilde{\mathfrak{g}}$ we have exploiting the symmetry present immediately a solution for the case $\tilde{\mathfrak{g}}|\mathfrak{g}$ simply by interchanging the roles of the two algebras, i.e. interchanging main quantum numbers and colour degrees of freedom. Supposing now that $c_{\text{eff}}^{\mathfrak{g}|\tilde{\mathfrak{g}}} = \lambda\, c_{\text{eff}}^{\tilde{\mathfrak{g}}|\mathfrak{g}}$ for some unknown constant $\lambda$, it follows directly from (4.199) and (4.200) that $c_{\text{eff}}^{\mathfrak{g}|\tilde{\mathfrak{g}}} = \lambda n\tilde{n}/(1+\lambda)$. We conjecture now this constant to be $\lambda = \tilde{h}/h$ such that [38]

$$c_{\text{eff}}^{\mathfrak{g}|\tilde{\mathfrak{g}}} = \frac{n\tilde{n}\,\tilde{h}}{h+\tilde{h}}\ . \tag{4.201}$$

As expected from the identification of the scattering matrices for several special cases we must recover the results of the already known cases when we fix the algebras appropriately. For instance we obtain $c_{\text{eff}}^{\mathfrak{g}|A_1} = 2n/(h+2)$ which is the well known formula for the effective central charge of the minimal affine Toda theories. Furthermore, we recover the effective central charge of the Homogeneous sine-Gordon models $c_{\text{eff}}^{A_n|\tilde{\mathfrak{g}}} = n\tilde{n}\tilde{h}/(n+1+\tilde{h})$, compare (4.118). It should be noted that this is independent of whether a resonance parameter is present or not despite the fact that the TBA-equation are not parity invariant in that case, see our discussion of the previous section. Numerically we also solved (4.198) explicitly for numerous examples with $\mathfrak{g} \neq A_n$ and confirmed (4.201).

The knowledge of the ultraviolet central charge (4.201) will certainly be useful in identifying the Lagrangian corresponding to the $\mathfrak{g}|\tilde{\mathfrak{g}}$-theories, since it provides the renormalization fixed point. As we know from the Homogeneous Sine-Gordon models the $A_n|\tilde{\mathfrak{g}}$–theory may be viewed as perturbed $\tilde{\mathfrak{g}}_{n+1}/u(1)^{\otimes\tilde{n}}$-coset WZNW theories. In analogy, we could view for instance the "dual" theory of this, i.e. the $\tilde{\mathfrak{g}}|A_n$–theory, formally as perturbed $\tilde{\mathfrak{g}}_1^{\otimes(n+1)}/\tilde{\mathfrak{g}}_{n+1}$-coset WZNW theory as one infers from the above table [38]. Besides the identification of the fixed point theory for the situation in which $\mathfrak{g} \neq A_n$, it remains open to find the precise form of the perturbing operators. Also the Lie algebraic structure present in the constant TBA equations (4.198) deserves further investigations, since these provide an additional link to the conformal models and their spectra as mentioned in 4.4.3.

| $\mathfrak{g}\|\tilde{\mathfrak{g}}$ | $A_m$ | $D_m$ | $E_6$ | $E_7$ | $E_8$ |
|---|---|---|---|---|---|
| $A_n$ | $\frac{nm\,(m+1)}{n+m+2}$ | $\frac{nm\,(2m-2)}{n+2m-1}$ | $\frac{72\,n}{n+13}$ | $\frac{126\,n}{n+19}$ | $\frac{240\,n}{n+31}$ |
| $D_n$ | $\frac{nm\,(m+1)}{2n+m-1}$ | $\frac{nm\,(m-1)}{n+m-2}$ | $\frac{36\,n}{n+5}$ | $\frac{63\,n}{n+8}$ | $\frac{120\,n}{n+14}$ |
| $E_6$ | $\frac{6\,m\,(m+1)}{m+13}$ | $\frac{6\,m\,(m-1)}{m+5}$ | 18 | $\frac{126}{5}$ | $\frac{240}{7}$ |
| $E_7$ | $\frac{7\,m\,(m+1)}{m+19}$ | $\frac{7\,m\,(m-1)}{m+8}$ | $\frac{84}{5}$ | $\frac{49}{2}$ | 35 |
| $E_8$ | $\frac{8\,m\,(m+1)}{m+31}$ | $\frac{8\,m\,(m-1)}{m+14}$ | $\frac{96}{7}$ | 21 | 32 |

Table 4.1: Effective central charges $c_{\text{eff}}^{\mathfrak{g}|\tilde{\mathfrak{g}}}$ of the $\mathfrak{g}|\tilde{\mathfrak{g}}$-theories.

### *4.5.1 An explicit example: $D_4|D_4$*

In order to illustrate the working of our general formulae beyond the already treated case it is instructive to evaluate them for a concrete model with $\mathfrak{g} \neq A_n$ and $\tilde{\mathfrak{g}} \neq A_1$.

We chose the $D_4|D_4$-model which is an example for a theory hitherto unknown. The model contains 16 different particles labeled by $(i,a)$ with $1 \leq a,i \leq 4$. The Coxeter number is $h = \tilde{h} = 6$ for $D_4$. Naming the central particle in the $D_4$–Dynkin diagram by 1 the S-matrix elements according to (3.97) are computed to [38]

$$\begin{aligned}
&S_{22}^{aa}(\theta) = S_{33}^{aa}(\theta) = S_{44}^{aa}(\theta) = [1,0]^2_{\theta,aa}[5,0]^2_{\theta,aa} && \text{for } a = 1,2,3,4,\\
&S_{12}^{aa}(\theta) = S_{13}^{aa}(\theta) = S_{14}^{aa}(\theta) = [2,0]^2_{\theta,aa}[4,0]^2_{\theta,aa} && \text{for } a = 1,2,3,4,\\
&S_{23}^{aa}(\theta) = S_{24}^{aa}(\theta) = S_{34}^{aa}(\theta) = [3,0]^2_{\theta,aa} && \text{for } a = 1,2,3,4,\\
&S_{11}^{aa}(\theta) = [1,0]^2_{\theta,aa}[3,0]^4_{\theta,aa}[5,0]^2_{\theta,aa} && \text{for } a = 1,2,3,4,\\
&S_{22}^{1b}(\theta) = S_{33}^{1b}(\theta) = S_{44}^{1b}(\theta) = [1,1]^{-1}_{\theta,1b}[5,1]^{-1}_{\theta,1b} && \text{for } b = 2,3,4,\\
&S_{12}^{2b}(\theta) = S_{23}^{2b}(\theta) = S_{24}^{2b}(\theta) = [2,1]^{-1}_{\theta,2b}[4,1]^{-1}_{\theta,2b} && \text{for } b = 2,3,4,\\
&S_{23}^{1b}(\theta) = S_{24}^{1b}(\theta) = S_{34}^{1b}(\theta) = [3,1]^{-1}_{\theta,1b} && \text{for } b = 2,3,4,\\
&S_{11}^{1b}(\theta) = [1,1]^{-1}_{\theta,1b}[3,1]^{-2}_{\theta,1b}[5,1]^{-1}_{\theta,1b} && \text{for } b = 2,3,4,\\
&S_{ij}^{ab}(\theta) = 1 && \text{for } i,j = 1,2,3,4;\ a \neq b;\ a,b \neq 1\,.
\end{aligned}$$

The solutions to the constant TBA-equations (4.195) read [38]

$$x_1^1 = x_3^2 = x_4^2 = x_2^3 = x_2^4 = x_3^3 = x_3^4 = x_4^3 = x_4^4 = x_2^2 = 1 \tag{4.202}$$

$$x_1^2 = x_1^3 = x_1^4 = x_1^1 = 1/2 \tag{4.203}$$

$$x_2^1 = x_3^1 = x_4^1 = 2 \tag{4.204}$$

such that the effective central charge according to (4.194) is

$$c_{\text{eff}} = \frac{6}{\pi^2}\left(10\mathcal{L}\left(\frac{1}{2}\right) + 3\mathcal{L}\left(\frac{2}{3}\right) + 3\mathcal{L}\left(\frac{1}{3}\right)\right) = 8\,. \tag{4.205}$$

This result confirms the general formula (4.201).